UNIVERSITÀ DEGLI STUDI DI ROMA "TOR VERGATA"

FACOLTA' DI SCIENZE MATEMATICHE, FISICHE E NATURALI

DOTTORATO DI RICERCA IN BIOLOGIA CELLULARE E MOLECOLARE
XXI CICLO

Inhibition of Telomerase and Hypoxia-Inducible Factor-1 in Human Glioblastoma Multiforme

Maria Patrizia Mongiardi

A.A. 2008/2009

Docente Guida/Tutor: Dott. Andrea Levi

Coordinatore: Prof. Gianni Cesareni

Table of Contents

Abbreviations

ALT: *Alternative Lengthening of Telomeres*
ARNT: *Aryl Hydrocarbon Nuclear Translocator*
bHLH: *basic Helix-Loop-Helix*
bHLH-PAS: *basic-Helix-Loop-Helix-Per-ARNT-Sim*
CAIX: *Carbonic Anidrase 9*
DFX: *Deferoxamine*
DN-TERT: *Dominant Negative TERT*
EPAS: *Endothelial Per-ARNT-Sim protein*
GAPDH: *Gliceraldeide 3-Fosfato Deidrogenasi*
GBM: *Glioblastoma Multiforme*
GLUT1: *Glucose Transporter 1*
TERT: *Telomerase Reverse Transcriptase*
HIF-1: *Hypoxia Inducible Factor 1*
HRE: *Hypoxia Response Element*
HUVEC: *Human Vein Endothelial Cells*
ODDD: *Oxygen-Dependent Degradation Domain*
PGK1: *Phosphoglycerate Kinase 1*
PHD: *Prolyl Hydroxylase Domain*
pVHL: *von Hippel-Lindau protein*
shRNA: *short hairpin* RNA
TBP: *TATA Binding Protein*
TERT: *Telomerase Reverse Trascriptase*
TRAP: *Telomere Repeat Amplification Protocol*
VEGF: *Vascular Endothelial Growth Factor*

ABSTRACT

Glioblastoma Multiforme (GBM) is the most common and the most aggressive glial tumor. It is composed by a heterogeneous tumor cell population, poorly differentiated. GBM (WHO grade IV) develop from low grade astrocytoma (WHO grade I or II) or anaplastic astrocytoma (WHO grade III), but more frequently they arise *de novo*.

GBM tumors are paradigmatic in their ability to induce neo-angiogenesis, a fundamental process in the growth of solid tumors. Of note, endothelial cells of GBM have the peculiarity to reactivate telomerase, the enzyme necessary to maintain telomere length. Telomerase reactivation is a characteristic feature of tumor endothelial cells, since it was not observed in endothelial cells proliferating in non neoplastic contexts.

One of the most important regulators of angiogenic processes is the transcriptional factor HIF-1, which orchestrates cellular response to hypoxia. Although HIF-1 is universally recognized as a key factor in inducing neo-angiogenesis as a response to reduced oxygen levels, the consequences of HIF-1 inhibition on the growth of solid tumors are not fully elucidated.

The aim of my PhD studies was to explore the consequences of targeting angiogenesis on the development of human GBM. To address this purpose, I selected two parallel strategies: inhibition of telomerase expression in tumor endothelial cells and inhibition of HIF-1 in glial tumor cells.

We developed a controlled *in vivo* assay of tumor angiogenesis in which primary human umbilical vascular endothelial cells (HUVECs) were subcutaneously grafted with or without human GBM cells in immunocompromised mice as Matrigel implants. We found that primary HUVECs did not survive in Matrigel implants, and that telomerase up regulation had little effect on HUVEC survival. In the presence of GBM cells, however, the grafted HUVECs not only survived in Matrigel implants but developed tubule structures that integrated with murine microvessels. Telomerase up regulation in HUVECs enhanced such effect. More importantly, inhibition of telomerase in

HUVECs completely abolished tubule formation and greatly reduced survival of these cells in the tumor xenografts.

In the second part of this study, we investigated the consequence of downregulating HIF-1 function in a human GBM cell line on cell proliferation *in vitro* and tumor growth *in vivo*. RNA interference targeting the O_2-regulated HIF-1α subunit efficiently reduced HIF-1α expression and transcriptional induction of HIF-1α responsive genes. *In vitro* proliferation rate of HIF-1 α - inhibited cells was not altered. Conversely long term co-cultures of wild type and HIF-1 α - inhibited GBM cells resulted in the overgrowth of the wild type cells. Subcutaneous grafting in nude mice of wild type and HIF-1 α - inhibited GBM cells lead to comparable tumor formation and growth. Surprisingly, co-grafting of HIF-1-positive and HIF1-negative GBM cells resulted in more aggressive tumors, both in terms of tumor appearance and tumor growth. This suggests that heterogeneity of the cellular populations in their ability to mount a response to hypoxia may promote tumor aggressiveness.

RIASSUNTO

Il glioblastoma multiforme (GBM), il più comune e aggressivo dei tumori gliali, è composto da una popolazione eterogenea di cellule tumorali astrocitarie scarsamente differenziate. Questi tumori possono svilupparsi dall'evoluzione maligna di un astrocitoma di più basso grado (grado WHO I o II) o da un astrocitoma anaplastico (grado WHO III), ma più frequentemente si manifestano *de novo*, senza alcuna evidenza di una neoplasia precedente.

Il GBM è un tumore paradigmatico nella capacità di indurre neo-angiogenesi, processo necessario per la crescita dei tumori solidi. Le cellule endoteliali del GBM hanno la peculiarità di riattivare la telomerasi, enzima deputato al mantenimento dei telomeri. Questa riattivazione della telomerasi da parte delle cellule endoteliali è una caratteristica esclusiva delle cellule endoteliali tumorali: l'attività telomerasica, infatti, non è stata mai osservata in cellule endoteliali che proliferano in contesti di neoangiogenesi non neoplastica.

Uno dei regolatori piu' importanti dei processi angiogenetici è il fattore di trascrizione HIF-1, che coordina la risposta cellulare all'ipossia. Sebbene HIF-1 sia universalmente riconosciuto come un fattore chiave nell'induzione della neo-angiogenesi come risposta all'ipossia, le conseguenze di una sua inibizione nello sviluppo dei tumori solidi non sono ancora del tutto chiare.

Lo scopo dei miei studi di dottorato è stato quello di esplorare le conseguenze dell'inibizione dell'angiogenesi sullo sviluppo del GBM umano. A tale scopo, ho deciso di seguire due strategie parallele: l'inibizione della telomerasi nelle cellule endoteliali del tumore e l'inibizione di HIF-1 nelle cellule tumorali gliali.

Tramite un modello di angiogenesi neoplastica *in vivo*, messo a punto nel nostro laboratorio, siamo stati in grado di dimostrare che le cellule endoteliali umane primarie HUVEC,

indipendentemente dall'espressione di attività telomerasica, non crescono e non sopravvivono se iniettate nel sottocute murino. Al contrario, se le stesse cellule sono coiniettate insieme al GBM nel sottocute del topo, si evidenzia un significativo aumento della loro sopravvivenza. Inoltre, in questo modello sperimentale, le HUVEC collaborano con le cellule endoteliali dell'ospite per formare i neovasi associati al tumore. Questo effetto è amplificato nel caso in cui le cellule HUVEC esprimono alti livelli di telomerasi. Al contrario, cellule HUVEC in cui, tramite RNAi, è impedita la riattivazione dell'espressione della telomerasi non sopravvivono nemmeno se co-iniettate insieme al GBM.

Tramite l'utilizzo della tecnica dell'RNAi siamo andati poi ad inibire il *pathway* di HIF nelle cellule di GBM umano. *In vitro*, mediante curve di crescita e saggi di proliferazione, abbiamo dimostrato che il tasso proliferativo delle cellule in cui HIF-1 è inibito non si presenta alterato. Invece in co-coltura, dopo molte replicazioni cellulari, il numero delle cellule *wild type* è maggiore rispetto alla controparte con l'espressione di HIF-1 inibita. In modelli di tumorigenesi *in vivo* in topi nudi, mediante iniezione nel sottocute murino, abbiamo poi dimostrato che la tumorigenicità dei due gruppi è comparabile. Al contrario, inaspettatamente, co-iniettando le due popolazioni cellulari si ottenevano tumori misti con caratteristiche di aggressività accresciute, sia in termini di percentuale di attecchimento dello xenotrapianto, sia in termini di dimensioni raggiunte dal tumore. Questo dato suggerisce che l'eterogeneità della popolazione cellulare nella capacità di rispondere all'ipossia può promuovere l'aggressività tumorale.

INTRODUCTION

The incidence of primary brain tumors worldwide is approximately seven per 100,000 individuals per year, accounting for ~ 2% of primary tumors and 7% of the years of life lost from cancer before the age of 70. The common gliomas affecting the cerebral hemispheres of adults are termed "diffuse" gliomas due to their propensity to infiltrate, early and extensively, throughout the brain parenchyma. These gliomas are classified histologically, immunohistochemically, and/or ultrastructurally as astrocytomas, oligodendrogliomas, or tumors with morphological features of both astrocytes and oligodendrocytes, termed oligoastrocytomas. Tumors are then graded on a WHO consensus-derived scale of I to IV according to their degree of malignancy as judged by various histological features accompanied by genetic alterations (Louis et al., 2007). Grade I tumors are biologically benign and can be cured if they can be surgically resected; grade II tumors are low-grade malignancies that may follow long clinical courses, but early diffuse infiltration of the surrounding brain renders them incurable by surgery; grade III tumors exhibit increased anaplasia and proliferation over grade II tumors and are more rapidly fatal; grade IV tumors exhibit more advanced features of malignancy, including vascular proliferation and necrosis, and as they are recalcitrant to radio/chemotherapy they are generally lethal within 12 months.

My PhD studies are focused on grade IV astrocytomas, i.e. glioblastoma multiforme (GBM).

Glioblastoma Multiforme (GBM)

On the basis of clinical presentation, GBMs have been further subdivided into the primary or secondary GBM subtypes. Primary GBMs account for the great majority of GBM cases in older patients, while secondary GBMs are quite rare and tend to occur in patients below the age of 45 years. Primary GBM presents in an acute *de novo* manner with no evidence of a prior symptoms or antecedent lower grade pathology. In contrast, secondary GBM derives consistently from the progressive transformation of lower grade astrocytomas, with ~70% of grade II gliomas transforming into grade III/IV disease within 5–10 years of diagnosis. Remarkably, despite their distinct clinical histories, primary and secondary GBMs are morphologically and clinically indistinguishable as reflected by an equally poor prognosis when adjusted for patient age. However, although these GBM subtypes achieve a common phenotypic endpoint, recent genomic profiles have revealed strikingly different transcriptional patterns and recurrent DNA copy number aberrations between primary and secondary GBM as well as new disease subclasses within each category (Maher et al., 2006). These molecular distinctions make obvious the need to change the current standardized clinical management of these diseases toward one of rational application of targeted therapies to appropriate molecular subclasses.

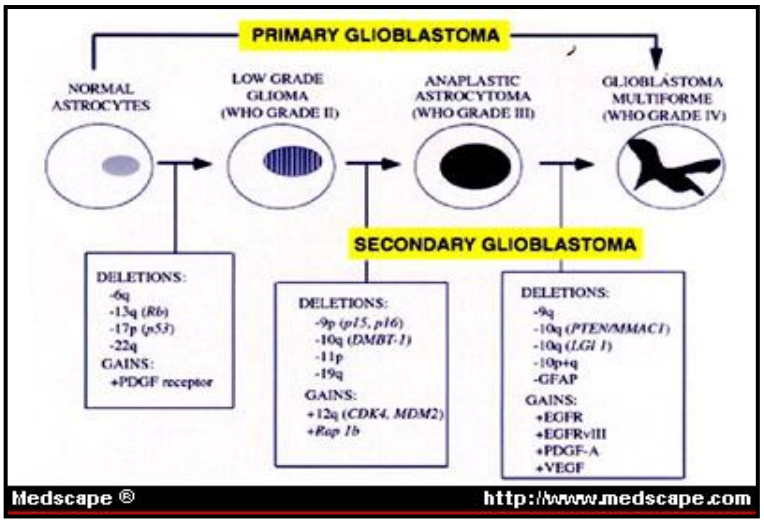

Figure 1. Diagram illustrating the speculated molecular aberrations in the development of human astrocytomas, involving loss of tumor suppressor genes and gain of tumor promoting genes. At least two molecular pathways have been postulated for GBMs: secondary GBM involving progression from a low- to high-grade astrocytoma and primary GBM involving de novo development of a GBM. WHO = World Health Organization

Molecular markers

Immunohistochemical markers are important and rapidly evolving tools in the classification and neuropathological diagnosis of malignant gliomas. Currently, the most clinically useful and specific of these markers for classification of gliomas are GFAP and OLIG2. GFAP is universally expressed in astrocytic and ependymal tumors and only rarely in oligodendroglial lineage tumors. OLIG2, a more recently discovered stem/progenitor and oligodendroglial marker, is CNS specific and is universally and abundantly expressed in all diffuse gliomas, but is rarely expressed at such high levels in other types of gliomas and CNS malignancies (Ligon et al., 2004). These markers thus serve as effective tools for unequivocal identification of gliomas and their distinction from

non-CNS tumors while aiding the pathologist in distinction of different glioma classes. A recently expanded collection of novel markers has emerged from numerous avenues of research and holds potential to be deployed to improve classification and inform the potential clinical course of glioma patients. Of particular interest are newly discovered stem and progenitor cell markers that, once clinically validated, may aid in the differential diagnosis of these tumors as well as monitoring their responses to therapy. Intensive research efforts are attempting to uncover agents that may target subpopulations of these cells with high tumorigenic potential and increased resistance to current therapies. Along these lines, the cell surface marker, CD133, and other markers of stem cells, such as Nestin and Musashi, have been shown to negatively correlate with outcome parameters. These newly discovered markers suggest that pathologists will soon have at their disposal highly useful tools for improved clinical diagnosis and classification of gliomas. Futhermore, as observed and published by our group, telomerase, a ribonucleoprotein which maintains chromosome length, can be considered another molecular marker for these tumors. Interestingly, expression levels of telomerase correlate with hystological grade of the tumor: in grade I and II gliomas, 30% of cases show telomerase activity, in grade III more than 80% of cases, and 100% in GBM, although the levels of this expression vary among different cells within the same tumor (Falchetti et al., 1999; Falchetti et al., 2000). Indeed, telomerase confers an extended proliferation rate to low-grade tumors by maintainment of telomere length. So the cells that undergo to repeated cell divisions accumulate genetic lesions that allow to anaplastic astrocytomas (AA) or GBM. Moreover, telomerase expression in GBM cells, which show long telomeres (Falchetti et al., 2000), suggests that telomerase may exhibit non-canonical functions.

With the wealth of accumulating profiling and genomic data, an increase in confidence is merited that useful diagnostic, prognostic, and drug response biomarkers will be incorporated into routine clinical management of GBM in the near future.

Angiogenesis

GBMs are among the most highly vascularized of all solid tumors. Microvascular hyperplasia, the defining histopathological phenotype of both primary and secondary GBM, consists of proliferating endothelial cells that emerge from normal parent microvessels as tufted microaggregates (glomeruloid bodies) accompanied by stromal elements, including pericytes and basal lamina (Stiver et al., 2004). Microvascular density, a measure of microvascular proliferation, is an independent prognostic factor for adult gliomas (Leon et al., 1996; Birlik et al., 2006). The idea that angiogenesis is rate limiting for tumor growth, and therefore a rational therapeutic target, is strongly supported by animal studies that have shown that angiogenesis is vital for macroscopic solid tumor growth (Folkman, 2007). One common feature in the transition from low-grade or anaplastic astrocytomas to secondary GBM is a dramatic increase in microvascular proliferation. An equivalently robust microvasculature proliferation phenotype is observed in primary GBM. Since there are marked genomic differences between primary and secondary GBM (Maher et al., 2006), it is likely that different genetic programs converge on a final common angiogenesis pathway involving Hypoxia-Inducible Factor (HIF)-dependent and non-HIF-dependent downstream effectors that include positive (VEGF, PDGF, bFGF,IL-8, SDF-1) and negative (thrombospondin1, thrombospondin2, endostatin, tumstatin, interferons) regulators of this process. A comprehensive understanding of the molecular mechanisms driving angiogenesis in GBM will be necessary for the rational development and deployment of anti-angiogenesis therapies. Interestingly, it is becoming evident that tumor-associated angiogenesis is not simply a physiological adaptation to hypoxia as a result of an increasing tumor cell mass. Rather it appears to be the result of critical genetic mutations that activate a transcriptional program for angiogenesis with local tumor oxygen status further modifying this response. The relative contributions of these two mechanisms are not yet fully

defined, but it is likely that both may operate to different extents in different tumors or even in different regions of the same tumor. Recently, a number of experimental studies have shown that key glioma-relevant mutations—including those in the *PTEN, EGFR* and *CMYC* genes—may act as an "angiogenic switch" by stabilizing HIF-1α or one of its downstream targets, VEGF (Watnick et al., 2003; Blum et al., 2005; Phung et al., 2006; Shchors et al., 2006). The distinction between microvascular proliferation being an adaptive response to hypoxia or it being an epiphenomenon of critical genetic mutations that also activate a cascade of proangiogenesis pathways has clinical and therapeutic importance.

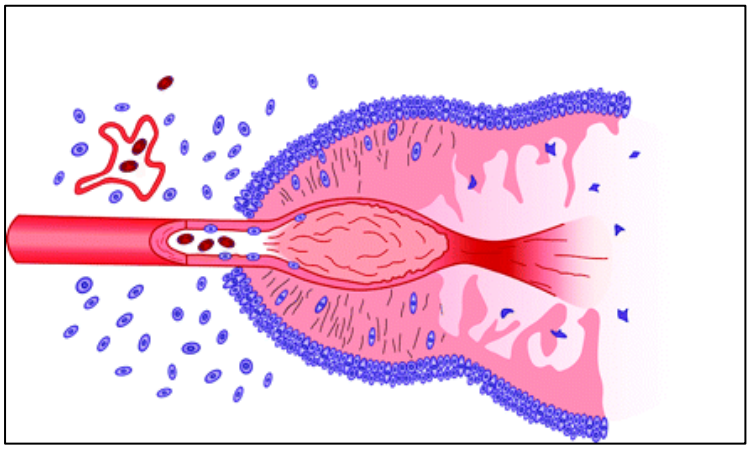

Figure 2. Schematic representation of the formation of a pseudopalisade. Growth of the glioblastoma stimulates neo-angiogenesis. Prominent secretion of angiogenic factors causes endothelial damage, which, in turn, produces vascular occlusion and hypoxia. Cells unable to survive the hypoxia succumb and form the nidus of coagulation necrosis. Other cells, however, migrate to the periphery of the hypoxic field in waves forming pseudopalisades. The migrating hypoxic cells secrete VEGF, proteases, and other factors that cause further microvascular proliferation and enhanced invasiveness in regions ringing the hypoxic field. These latter effects prompt further aggressive outward expansion of the glioblastoma cells.

Another issue is the functional consequences of tumor angiogenesis, with respect to tissue perfusion (Vogel et al., 2004). Tumor microvessels are highly tortuous with sluggish flow and diminished gradient for oxygen delivery and increasing susceptibility to thrombosis and microhemorrhages (Kaur et al., 2004). Thus, the GBM microvasculature proliferation may provide little support in oxygen/nutrient delivery but rather paradoxically contribute to further exacerbating a metabolic mismatch between the "supply and demand," leading to progressive hypoxia and eventually necrosis. This scenario is supported by the recent experience with anti-angiogenesis drugs, where their limited clinical benefit seems to be the result of "pruning" immature vessel growth and allowing "normalization" of the pre-existing vasculature (Horsman and Siemann, 2006). In addition to the poor vascular architecture, endothelial cells associated with the tumor vasculature fail to form tight junctions and have few associated pericytes or astrocytic foot processes leaving the integrity of the BBB compromised, resulting in increased interstitial edema. Interstitial edema may further compromise regional blood flow and exacerbate tumor hypoxia leading to areas of necrosis. In addition to these maladapted biophysical properties of GBM microvasculature, specific genetic mutations in GBM likely contribute to compromised tumor bioenergetics, specifically the shift in energy reduction from oxidative phosphorylation to glycolysis (Elstrom et al., 2004; Fantin et al., 2006). These interrelated mechanisms lead to a level of metabolic demand that may exceed the ability of the cerebrovascular system to maintain adequate blood flow to prevent hypoxia and necrosis. The histological evidence of thrombosis and degenerating vessels with microhemorrhages are a common feature of GBM and likely reflect these biological processes.

Our group has a great experience in the study of GBM. In my PhD studies, together with a neurosurgery unit of the Catholic School of Medicine of Rome, we made up *in vivo* model-based studies that threw light on tumor progression processes and on

the role played by telomerase in these processes. More specifically, I tried to get insight into the complex molecular processes at the basis of GBM progression. Firstly, I focused my attention on the elucidation of telomerase involvement in GBM-induced angiogenesis. Then, in the second part of the work, I studied the consequences of HIF-1-inhibition on the development of GBM tumor. HIF-1 is a transcription factor that orchestrates cellular response to hypoxic conditions. Since histological analysis of GBM sections reveals the presence of extensive hypoxic areas, targeting HIF-1 could be an interesting strategy for GBM therapy.

Telomerase

Telomeres

Telomeres are among the most important structures in eukaryotic cells. Creating the physical ends of linear chromosomes, they play a crucial role in maintaining genome stability, control of cell division, cell growth and senescence.
In vertebrates, telomeres consist of repetitive DNA sequences and specific proteins, creating a specialized structure called the telosome that, through mutual interactions with many other factors in the cell, give rise to dynamic regulation of chromosome maintenance. Nearly 60 years ago, the first experiments identified telomeres as specific structures important for genome stability, at the ends of *Drosophila* and maize chromosomes. Telomeres are dynamic structures and their length varies among organisms or cells of different origin. For example, mice can have telomeres up to 150 kb long, while in humans the length can vary from 3 to 20 kb (Moyzis et al., 1988; Harley et al., 1990). Early analysis of telomeric heterochromatin showed that linear chromosomes end with short tandem repeats consisting of G-rich sequences, such as TTAGGG in vertebrates (de Lange et al., 1990). Electron microscope studies revealed a specific telomere structure in the form of a telomere loop (t-loop) or lariat (Griffith et al., 1999; Rubelj & Vondracek, 1999). The whole t-loop entity is held together by several telomere-specific proteins, as well as a number of other ubiquitous proteins involved in DNA processing and structure organization (de Lange 2005). The subtelomeric region adjacent to the t-loop is heterochromatic and contains repetitive, as well as corrupted telomeric sequences and can stretch up to 10–500 kb towards the centromere (Riethman et al., 2005).

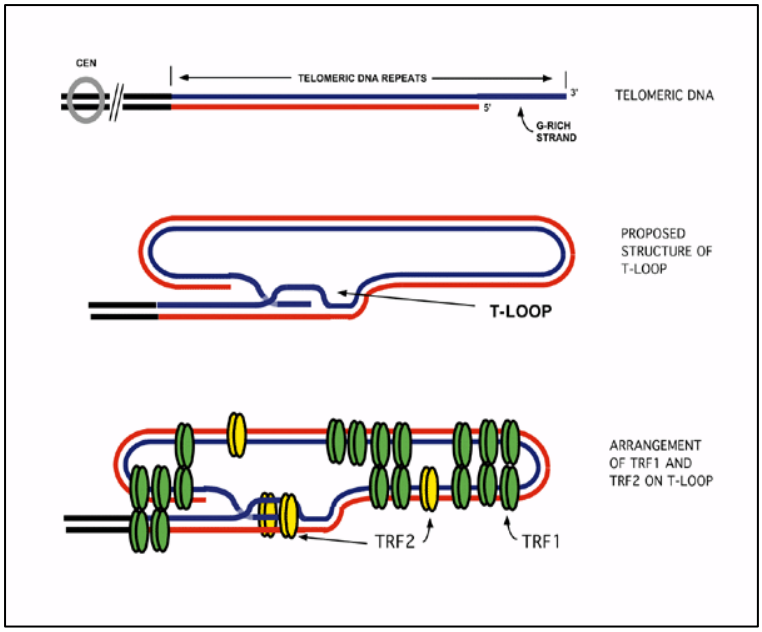

Figure 3. Represents the Telomeric ends forming a structural feature with their associated proteins that protects their ends.

Special histone and DNA modifications (such as acetylation and methylation) in subtelomeric and telomeric regions can regulate chromatin structure or processes that include replication and homologous recombination (Gonzalo et al., 2006). As part of the chromosome, telomeres contain histones forming nucleosomes, chromosome structural proteins (Nikitina and Woodcock, 2004) and some specific single-stranded DNA binding proteins with a great affinity for single-stranded telomeric sequences. Six proteins are considered to be strictly telomere specific. They meet the following criteria: they are specific for telomere DNA, present throughout the cell cycle and have functions restricted to the telomere. They have important roles in protection, elongation and regulation of the telomere. These proteins form a complex named *Shelterin*: TRF1, TRF2, hRap, TIN2, POT1, and TPP (Zhong et al., 1992; Bilaud et al., 1997). Each protein has a specific role in the

complex; such as inducing t-loop formation, protecting the telomere from nucleases, checkpoint functions or regulating telomere elongation in telomerase-positive cells.

In normal cells, telomeres shorten with each round of replication, due to the inability of DNA polymerase to synthesize the very end of the DNA lagging strand, as well as due to the presence of 5' exonuclease activity (Makarov et al., 1997). It is estimated that each passage through the cell cycle leads to shortening of telomeres by ~50–150 bp (Olovnikov, 1973; Makarov et al., 1997). Telomere erosion is considered to be a mitotic clock, which regulates the number of divisions before cells enter senescence.

The end replication problem

Semi-conservative DNA replication presents a problem when it comes to fully replicating a linear DNA molecule. Infact, DNA polymerase can only synthesize DNA in a 5'-3' direction and it needs a primer of RNA. This leads to complete replication of leading strand and an incomplete and discontinous synthesis of lagging strand. As originally pointed out by Alexi Olovikov in 1971, in this way, after several rounds of replication, the DNA molecule continues to get smaller and smaller. Telomerase complex solves this question by adding specific nucleotidic repetitions at the end of chromosomes, ensuring the maintenance of telomere length.

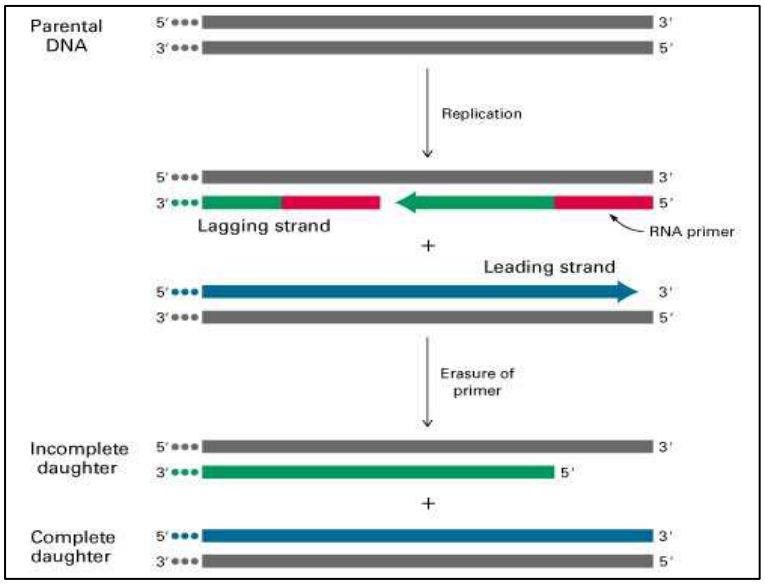

Figure 4. DNA polymerase requires an RNA primer to initiate synthesis in the 5'-3' direction. At the end of a linear chromosome, DNA polymerase can synthesize the leading strand until the end of the chromosome. In the lagging strand, however, DNA polymerase's synthesis is based on a series of fragments, called Okazaki, each requiring an RNA primer. Without DNA to serve as template for a new primer, the replication machinery is

unable to synthesize the sequence complementary to the final primal event. The result is the "end-replication problem" in which sequence is lost at each round of DNA replication

Telomerase

Telomerase was first identified biochemically more than 20 years ago (Greider and Blackburn, 1985) and shown to use an extraordinary mode of synthesis, relying on an intrinsic RNA, TR, that serves as a template for the polymerization of the telomeric DNA sequences, and a catalytic subunit, TERT, that functions as a reverse transcriptase (Greider and Blackburn, 1989; Yu et al., 1990).

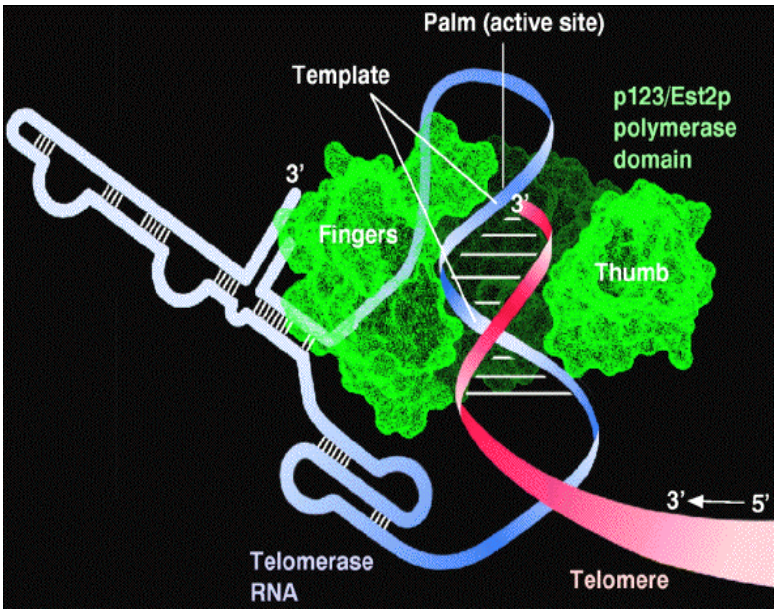

Figure 5. Structure of telomerase

TR

Unlike other polymerases responsible for replication of genomic DNA, telomerase activity depends on an essential RNA subunit. Telomerase was first shown to be an RNA-dependent DNA polymerase by characterization of the enzyme isolated from the unicellular ciliate *Tetrahymena*. The identification of a 159-nucleotide RNA component containing the sequence 5′-CAACCCCAA-3′, complementary to the $d(TTGGGG)_n$ telomeric repeat synthesized by *Tetrahymena* telomerase, suggested that this region of the RNA provides a template for telomere synthesis (Greider and Blackburn, 1989). The templating region of the telomerase RNA can be dissected into two functionally separable subdomains, employed in primer alignment and primer extension (Gilley and Blackburn, 1996). One end of the RNA template (3′-AAC-5′) serves to align the telomeric DNA primer for the extension step, via basepairing between the 3′ terminus of the primer and a portion of the template. Subsequent elongation occurs by copying the remaining six residues of the template onto this telomeric end. These first round products can be further elongated if the new telomeric terminus is translocated back to the primer alignment site, so that the primer is repositioned for another round of synthesis. Processivity is dictated by more than base pairing interactions at the primer alignment site; telomerase can also interact with telomeric substrates at a second, RNA-independent, primer binding site, called the anchor site, that contributes to processive elongation (Morin, 1989,1991). In addition to alignment and templating functions, several observations indicate that the template region of the RNA directly participates in enzyme action by contributing to both the structure and function of the enzyme active site

Catalytic subunit of telomerase (TERT)

The dependence of telomerase polymerase activity upon RNA formally defined the enzyme as a specialized type of reverse transcriptase (RT). During the last years, the discovery of the

catalytic component of telomerase revealed that it is in fact a reverse transcriptase, related to known RTs by both amino acid sequence and presumably by evolution. This has provided a key step toward a detailed understanding of the mechanism of chromosomal DNA synthesis by telomerase. Identification of this telomerase protein resulted from convergence of complementary biochemical and genetic strategies in the ciliate *Euplotes aediculatus* and the yeast *S. cerevisiae.* In *Euplotes,* biochemical fractionation of the enzyme identified two telomerase subunits, p123 and p43, that extensively co-purify with telomerase activity and are in apparent steichiometrically equivalent ratios with the RNA subunit (Lingner and Cech, 1996). An independent genetic approach recovered four yeast *EST* (ever shortertelomeres) genes that, when mutated, confer a telomere replication phenotype *in vivo* (Lundblad and Szostak, 1989). Comparison of the sequence of the yeast 103-kD Est2 protein with the *Euplotes* p123 subunit revealed that these two proteins are homologues, sharing ~20% sequence identity and more extensive sequence similarity over the length of both proteins. Most notable was the presence in both of a set of motifs common to RTs, marked by the presence of a number of highly conserved residues. A subset of these amino acid sequence motifs had previously been shown to form a conserved protein fold comprising the active site of reverse transcriptases (Kohlstaedt et al., 1992), with three invariant aspartates that are thought to be critical for catalysis (Larder et al., 1987). Single amino acid changes introduced into the comparable aspartates of the Est2 protein abolished yeast telomerase activity *in vitro* and conferred an *in vivo* telomere replication defect, demonstrating that these residues are essential for telomerase catalysis (Counter et al., 1997). Rapid on the heels of the characterization of the telomerase catalytic subunit in *Euplotes* and yeast has been the identification of the same component in *Schizosaccharomyces pombe* (Nakamura et al., 1997) and in humans (Harrington et al., 1997). These proteins, like those from *S. cerevisiae* and *Euplotes*, also show sequence and mechanistic similarity with known RTs, and hence this protein subgroup has been named TERT (Telomerase Reverse Transcriptases). The TERT protein family is most

similar in sequence to RTs such as non-LTR retrotransposons and group II introns that, like telomerase, extend their RNA-templated polymerization from DNA 3′ hydroxyl primers. However, despite the overall similarities with RNA-dependent polymerases, including the three aspartate residues required for enzyme catalysis, telomerases from disparate organisms are more related to one another than to other polymerases and thus appear to form a distinct subgroup (Nakamura et al., 1997). Several features distinguish telomerase RTs, such as a unique region of sequence conservation termed the "T motif," as well as a large amino-terminal basic domain (Nakamura et al., 1997). Prior to cloning of any of the TERT proteins, cross-linking studies with *Euplotes* telomerase indicated that the large subunit of the enzyme (presumably corresponding to the p123 catalytic component) contains a second site for telomeric DNA binding, called the anchor site (Hammond et al., 1997). The anchor site had been functionally defined by studies showing that primer recognition and processivity of the telomerase enzyme are influenced by the presence of G-rich telomeric sequences at the 5′ end of the primer, even when the 3′ terminus is non telomeric (Morin et al., 1989). This site is distinct from the binding that occurs between the 3′ end of the DNA primer and the template region of the RNA. Positioning the 5′ end of the primer in the anchor site is thought to contribute to processivity by preventing dissociation of the primer from the enzyme during translocation on the RNA template of the newly extended 3′ terminus. In studies with the *Euplotes* enzyme, in which the 3′ end of the primer was bound in the active site, cross-links between DNA and protein were localized 20–22 residues from the 3′ end, consistent with the prediction for an anchor site interaction with its primer (Hammond et al., 1997). Intriguingly, the use of partially duplex substrates with 3′ single-strand overhangs, which should resemble natural telomeres more closely, led to cross-links between protein and the duplex portion of the substrate. As expected, cross-links between the catalytic protein subunit and the telomerase RNA were also observed.

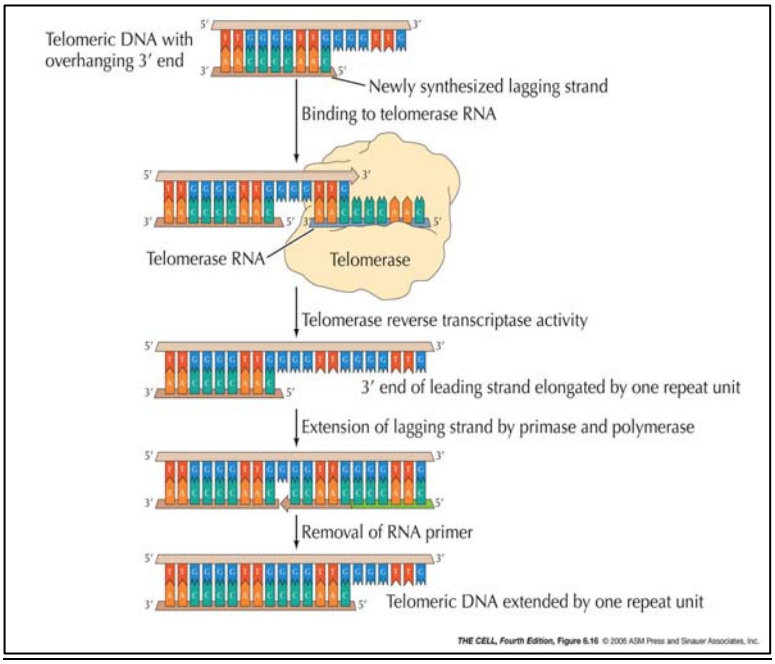

Figure 6. Action of telomerase. (Cooper and Hausman , 2007)

Regulation of telomerase activity

Most normal human cells have undetectable levels of telomerase activity and also fail to express hTERT. Strikingly, enzyme activity in telomerase-negative human cell lines can be restored by the ectopic expression of hTERT (Weinrich et al., 1997). Thus, the catalytic protein is the only limiting factor for telomerase activation in at least a subset of normal human cells, suggesting that regulation of hTERT expression may be a key target during cellular immortalization. By restoring telomerase activity to normal cells, this technique also has laid the groundwork for assessing whether conversion to telomerase

proficiency can reverse the mortal growth characteristics of normal cells. A complement to these *in vivo* experiments is the demonstration that coexpression of the hTERT protein and the human telomerase RNA in reticulocyte lysates is capable of reconstituting enzyme activity (Weinrich et al., 1997). An additional consequence is that this *in vitro* system may accelerate the search for inhibitors of telomerase activity; such inhibitors will be critical in testing the hypothesis that telomerase reactivation plays a role in oncogenesis.

Non canonical functions of telomerase

Various studies on telomerase suggest that this complex holds different roles other than canonical telomere maintenance. It was demonstrated that the expression of SV40 early genes, HRAS, and hTERT is sufficient to transform normal human cells (Hahn et al., 2002). Instead, the expression of SV40 and HRAS, together with ALT mechanism, does not induce transformation, suggesting that telomerase could hold other roles different from telomere elongation (Stewart et al., 2003). Moreover, telomerase ectopic expression in epithelial cells HMEC (Human Mammary Epithelial Cell) results in activation of growth promoting genes expression. L'EGFR (Epidermal Growth Factor Receptor) belongs to this group, and it was demonstrated that its inhibition abolished growth increment caused by telomerase (Smith et al., 2003). In previous studies, Li and colleagues analyzed the effects of telomerase inhibition in several human tumor cell lines. They observed that the expression of siRNA directed against TR, results in an inhibition of cell division, but it does not induce DNA damage response genes expression, telomere uncapping or strong shortening of these structures. Furthermore, by microarray, they observed that this inhibition results in an alteration of gene expression profile: as well as down regulation of cell cycle

genes, as Cdc27 and Cyclin G2, and genes involved in angiogenesis and metastatis, as integrin αV (Li et al., 2004; Li et al., 2005). Moreover, new studies about apoptosis revealed involvement of telomerase in these processes. Indeed, human fibroblasts in which telomerase is stably inhibited and treated by irradiation or chemiotherapic reagents, show a DNA damage response more weak than wild type counterpart. In these TERT-inhibited fibroblasts, they observed that chromosome structures are more sensitive to micrococcal DNAse than normal counterpart. These data, and the observations that there is increase of telomerase expression in S phase (Masutomi et al., 2003), demonstrate the involvement of telomerase in chromatidic structures regulation during replication phase (Masutomi et al., 2005).

Telomerase and cancer

Telomerase is expressed in the majority of human cancers, making it an attractive therapeutic target. In cellular *in vitro* models, for example in the case of CD8 positive T cells, hTERT over-expression significantly enhances proliferation and cell survival (Dagarag et al., 2004). Similar observations have been made with many different cell types. *In vivo* findings in animal tumor models showed that *mTERC* was upregulated early in tumorigenesis and that telomerase became activated in late stages of tumor progression (Blasco et al., 1996). These studies led to the examination of what the effects of constitutive expression or overexpression of TERT would be. mTert overexpression was shown to be associated with spontaneous mammary epithelial neoplasia and invasive carcinoma in aged mice (Artandi et al., 2002), while constitutive expression of mTert in thymocytes promotes T-cell lymphoma (Canela et al., 2004). More recently, work on targeted overexpression in specific tissues showed faster wound healing and increased

tumorigenesis in the skin of K5-m*Tert* mice (where m*Terc* is required for the tumor promoting effect) (Cayuela et al., 2005). In addition, conditional induction (using a tetracycline-inducible system) in a mouse model showed that mTert causes the proliferation and mobilization of hair follicle stem cells (Sarin et al., 2005). This was visualized *in situ* as well as through the observation of exacerbated hair growth and faster hair regrowth in a manner independent from telomere synthesis. How TERT protein can also modulate the proliferation of stem cells in the skin even in the absence of telomerase RNA is currently not understood. The link between telomere biology and oncogenesis was first proposed when telomerase expression was found to be a hallmark of human cancer: telomerase expression or reexpression and activity can be detected in >90% of tumor samples. Telomerase deficiencies and cancer appear to lie at opposite ends of a spectrum similar to p53: loss of p53 is observed in most tumors and is tumor promoting in mouse models, whereas mice with enhanced p53 responses exhibit increased cancer resistance, a shortened life span, and a number of early aging-associated phenotypes (Donehower, 2002). In both models aging appears to be driven in part by a gradual depletion of the functional capacity of stem cells. The link between p53 and telomeres is further illustrated in Li-Fraumeni syndrome (LFS), a cancer predisposition syndrome associated with germ line *TP53* mutations. It was shown that the progressive earlier age of cancer onset in LFS is related to a measurable decrease in telomere length, with each generation providing the first rational biological marker for clinical monitoring of LFS patients (Tabori et al., 2007). Ectopic *hTERT* expression can allow post-senescent cells to proliferate beyond crisis, in a process that could to be independent of catalytic activity (Counter et al., 1998). Tumorigenesis is often associated with the upregulation of c-Myc that can be induced by retroviral insertion or translocation. c-Myc binding sequences are described within the *hTERT* promoter, and the MYC protein stimulates *hTERT* transcription (Wu et al., 1999), which may in turn contribute to tumorigenesis or tumor progression. The flip side of continued expression or reexpression of *hTERT* in genetically stable primary cells and in

animal models is enhanced longevity and a delay of senescence during *in vitro* culture (Gonzalez-Suarez et al., 2005). However, sustained (over)expression of telomerase in CD4- or CD8-positive T cells over longer periods in culture were shown to promote genomic instability (Roth et al., 2005). This may be directly due to hTERT overexpression or may be a consequence of extended proliferation and replication errors that may be exacerbated by culture conditions. In addition, gain of expression of *hTERC* due to the presence of multiple gene copies has also been recently associated with cervical dysplasia and invasive cancer progression.

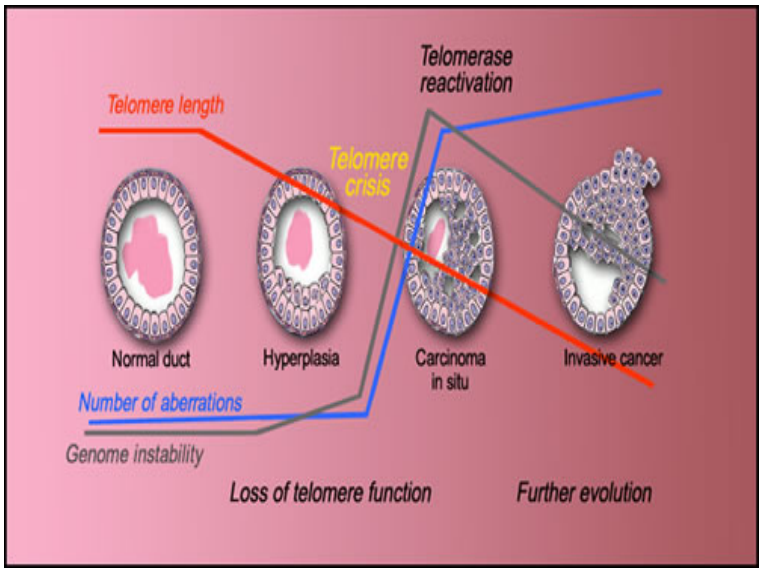

Figure 7. In the march to malignancy, there is a progressive shortening of telomere lengths that is accompanied by an increase in genomic instability. In some cases, this genomic instability can give rise to genetic aberrations that lead to invasive cancer.

Telomerase involvement in tumor angiogenesis

One of the most important demonstrations of telomerase involvement in tumor angiogenesis derives from the observation, made by our group, that hTERT is expressed by the endothelial cells of tumor vessels. This expression is a peculiar feature of tumor vessels, since we didn't observe any hTERT reactivation in endothelial cells proliferating in contexts of non neoplastic angiogenesis. Moreover, histological analysis of human astrocytomas revealed that hTERT expression by the tumor endothelial cells is related to the histological grade of the tumor itself. Indeed, hTERT is expressed by 100% of endothelial cells in GBM, by 56% in AA, by 29% in low grade astrocytomas. The percentage of low grade astrocytomas that progress to a more aggressive phenotype (29%) is comparable to tumors whose endothelial cells reactivate hTERT expression (Pallini et al., 2001). hTERT reactivation in tumor endothelial cells could be necessary for telomere maintenance of fast growing cells. Indeed, in mTERT knockout mice, the presence of short telomeres inhibits angiogenesis (Franco et al., 2002). But the observation that there is not telomerase reactivation in non neoplastic angiogenesis support the idea that telomerase holds non canonical roles in tumor angiogenesis (Pallini et al., 2001).

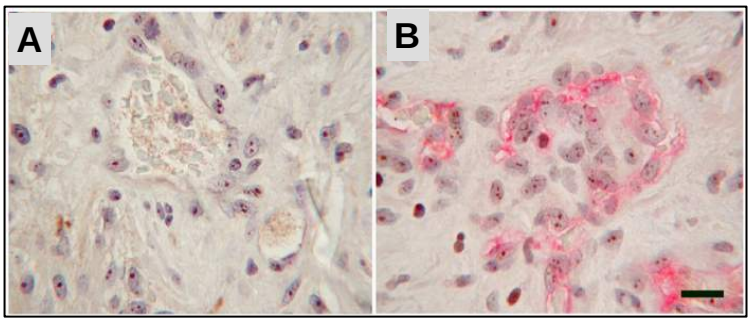

Figure 8: Immunostaining on human glioblastoma section. A: Nuclear staining with hTERT antibody both on glial neoplastic cells and endothelial cells. B: double immunostaining with hTERT and CD31 antibodies in endothelial cells (Scale bar 40 μm).

Hypoxia-Inducible Factor-1 (HIF-1)

Hypoxia and HIF-1

Oxygen (O_2) is essential for the survival of all aerobic organisms. O_2 is required for aerobic metabolism that maintains intracellular energy balance. Aerobic energy metabolism is dependent on oxidative phosphorylation, in which the oxido-reduction energy of the mitochondrial electron transport is converted into the high-energy phosphate bond of ATP. In this process, O_2 serves as the final electron acceptor. Depending largely on the distance from the nearest functional blood vessel, cells in mammalian tissues typically experience O_2 concentrations in the 40–60 mm Hg range. Hypoxia, defined as a state of reduced O_2 level below normal values, occurs under various physiological (embryonic development, adaptation to high altitudes, wound healing) as well as pathological (ischemic diseases, cancer) conditions. In order to cope with hypoxia, organisms undergo a variety of systemic and local changes to restore O_2 homeostasis and limit the effect of low O_2. Systemic adjustments include enhanced O_2 delivery by the bloodstream, whereas angiogenesis features prominently among the local adjustments. At the cellular level, the most noticeable response to hypoxia is reduction in oxidative phosphorylation, accompanied by increased glycolysis to compensate for lower ATP production.

Although hypoxia generally inhibits mRNA synthesis, transcription of subsets of genes increases dramatically. At the molecular level, the master switch orchestrating the cellular response to low O_2 tension is generally considered to be the transcription factor Hypoxia-Inducible Factor (HIF). HIF is a transcription factor found in mammalian cells cultured under reduced oxygen tension and plays a key role in the cellular response to hypoxia. HIF is a heterodimer consisting of two subunits, the oxygen-sensitive HIF-α and the constitutively

expressed HIF-ß (also known as aryl hydrocarbon receptor nuclear translocator (ARNT), the heterodimeric partner of aryl hydrocarbon receptor (Ahr) (Wang et al., 1995). Both the subunits are members of the basic helix–loop–helix-*Drosophila* period clock protein (PER)-ARNT-*Drosophila* single-minded protein (SIM) (HLH-PAS) family of transcription factors (Jiang et al., 1996).

Three HIF-α homologues have been identified: HIF-1α, HIF-2α and HIF-3α (Ema et al., 1997; Tian et al., 1997; Gu et al., 1998). HIF-1α and HIF-2α share a high degree of sequence identity, which is highlighted by their common ability to heterodimerize to HIF-ß (Ema et al., 1997; Tian et al., 1997). Heterodimers that contain HIF-1α or HIF-2α appear to have overlapping but distinct tissue-specific expression patterns and target genes. Less is known about HIF-3α compared with the other HIF-α homologues. It has been shown that the inhibitory PAS domain protein (IPAS) is an alternatively spliced variant of HIF-3α and functions as a dominant-negative regulator of HIF-α, adding to the complexity in the regulation of hypoxia-inducible genes by the HIF family of transcription factors (Makino et al., 2002).

HIF-1α has two transactivation domains located in its COOH-terminal half: the NH_2-terminal transactivation domain or (N-TAD) (amino acids 531-575) and the COOH-terminal transactivation domain or C-TAD (amino acids 786-826; Li et al., 1996; Jiang et al., 1997; Pugh et al., 1997).

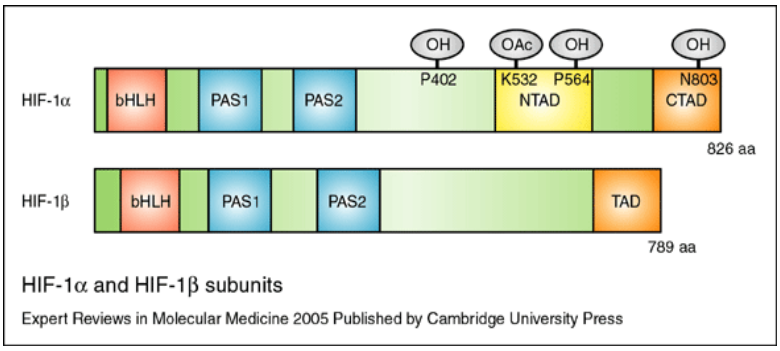

Figure 9. Hypoxia-inducible factor (HIF)-1a and HIF-1b contain one basic–helix–loop–helix (bHLH) domain and two PER–ARNT–SIM (PAS1 and PAS2) domains in their N-terminal regions. The positions of post-translational hydroxylation (OH) and acetylation (OAc) of HIF-1a are indicated. Hydroxylation of two proline residues (at P402 and P564) and acetylation of lysine (at K532) within the oxygen-dependent degradation (ODD) domain (residues 401–603) and close to the N-terminal transactivation domain (NTAD) confers recognition by pVHL (the product of the von Hippel–Lindau tumour suppressor gene), leading to degradation of the a-subunit. Hydroxylation at N803 in the C-terminal transactivation domain (CTAD) of HIF-1a inhibits recruitment of coactivators required for HIF-1a transcriptional activity. HIF-1b contains one transactivation domain (TAD) in its C-terminus.

Downregulation of HIF-1α protein levels in normoxia

In normoxia, the von Hippel-Lindau tumour suppressor (pVHL), which is the recognition component of an E3 ubiquitin ligase complex, targets HIF-1α (Iwai et al., 1999; Lisztwan et al., 1999), leading to its ubiquitylation and consequent proteasomal degradation (Lisztwan et al., 1999; Cockman et al., 2000; Kamura et al., 2000; Ohh et al., 2000; Tanimoto et al., 2000). The oxygen-dependent degradation domain (ODDD), which overlaps the N-TAD, controls the degradation of HIF-1α by the ubiquitin–proteasome pathway. Deletion of this entire domain renders HIF-1α stable even in normoxic cells (Huang et al., 1998). It has been shown that the interaction of pVHL with HIF-1α is regulated by the hydroxylation of two proline

residues, proline-402 and proline-564, located within the ODDD, which are conserved between HIF-1α and HIF-2α (Ivan et al., 2001; Jaakkola et al., 2001; Masson et al., 2001). Further, detailed analysis has revealed two subdomains within the ODDD: an NH_2-terminal subdomain or NODDD (amino acids 380-417; Masson et al., 2001) and a COOH-terminal subdomain or CODDD (amino acids 549–582) that overlaps the N-TAD (Pugh et al., 1997).

In 2001 Epstein and colleagues identified egg-laying defect (EGL)-9 as a prolyl hydroxylase capable of hydroxylating HIF-1α in *Caenorhabditis elegans*. Three prolyl hydroxylase domain (PHD) enzymes, known as PHD1, PHD2 and PHD3, were subsequently identified in mammalian cells and shown to hydroxylate HIF-1α, although at varying levels of activity (Bruick & McKnight, 2001; Epstein et al., 2001). This post-translational modification of HIF-1α by the PHDs is oxygen, iron, 2-oxoglutarate and ascorbate dependent, which may be part of the mammalian oxygen-sensing mechanism (Kivirikko & Myllyharju, 1998). Interestingly, each of the PHDs hydroxylates human HIF-1α at proline-564, whereas only PHD1 and PHD2 hydroxylate the second site of prolyl hydroxylation, proline-402. Both proline residues subjected to hydroxylation lie within the ODDD, conserved between the worm and the mammalian HIF-1α isoforms (Epstein et al., 2001). The relative role of the three mammalian PHDs in terms of their oxygen-sensing capabilities and target proteins for modification remains to be determined. PHD2 has been shown in certain cell lines to be the predominant enzyme that hydroxylates HIF-1α in normoxia, on the basis that inhibition of PHD2 expression with RNA interference (RNAi) stabilized HIF-1α in normoxia, where inhibition of PHD1 and PHD3 had no effect (Berra et al., 2003). PHD genes have been shown to be induced in hypoxia, and the hypoxic induction is mediated by HIF-1α (Epstein et al., 2001; Berra et al., 2003; Metzen et al., 2003). The increase in PHD expression under hypoxia may reflect the function of PHDs in degrading HIF-1α upon reoxygenation or alternatively may be part of the mechanism to balance HIF-1α in hypoxia. Since PHDs are components of the HIF pathway, induction of PHDs

by hypoxia suggests a regulatory feedback loop in this signalling pathway.

The interaction of HIF-1α and pVHL was reported to be enhanced by acetylation of lysine-532 through a mouse homologue of an N-acetyltransferase, ADP-ribosylation factor domain protein 1 (ARD1) (Jeong et al., 2002). However, further studies have failed to validate this finding, reporting that human ARD1 (hARD1) does not affect HIF-1α stability (Murray-Rust et al., 2006).

An additional mechanism for negatively regulating HIF-1α protein levels involves interaction of the p53 tumor suppressor gene with HIF-1α, either directly or indirectly via Mdm2, itself a downstream target of p53 (Bardos & Ashcroft, 2005).

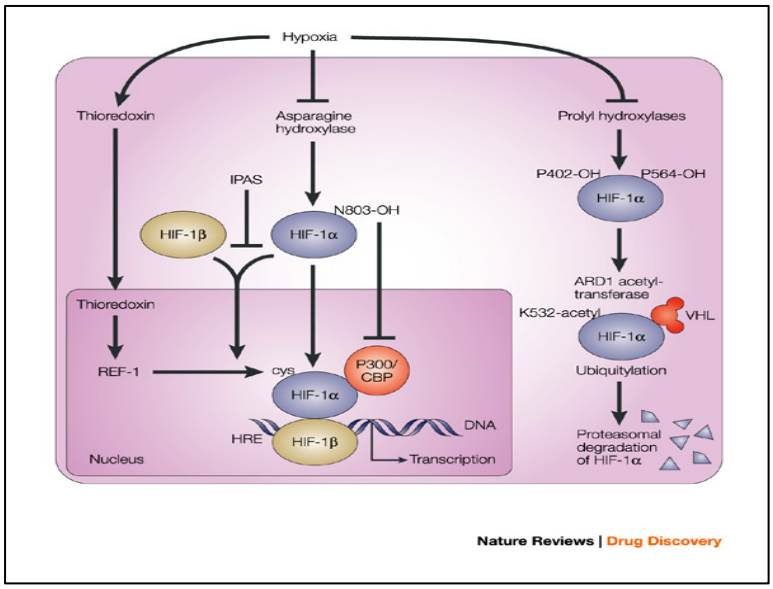

Figure 10. Under aerobic conditions, HIF-1α is hydroxylated on proline 402 and proline 564. The proline hydroxylations are necessary for binding to von Hippel-Lindau (VHL) and ubiquitin-mediated degradation by the proteasome. The asparagine hydroxylation prevents binding to p300/CBP. A splice derivative of HIF-3 α called inhibitory PAS (IPAS), as it only

possesses the PAS domain, competes for HIF-1β binding. Maintenance of cysteine in a reduced state in the transactivation domain (TAD) is essential for p300/CBP binding. Compounds that inhibit thioredoxin inhibit HIF-1α-mediated transactivation. HIF-1α and HIF-1β both translocate to the nucleus to transactivate genes such as vascular endothelial growth factor (VEGF) that possess hypoxia-response elements (HREs). PAS, PER/ARNT/SIM; REF-1, redox factor 1. (Giaccia A et al., 2003).

Hypoxic induction of HIF-1

Inhibition of oxygen dependent hydroxylation

In hypoxia, the proline residues within the ODDD are not hydroxylated and thus HIF-1α is stabilized and the protein levels increase. Stabilized HIF-1α is translocated to the nucleus where it dimerizes with HIF-1ß (ARNT) and associates with co-activators, such as CREB-binding protein (CBP)/p300. To be transcriptionally active, the HIF complex has to assemble on the HRE in the regulatory regions of target genes. HIF induces the transcription of several hypoxia-response genes, such as the proangiogenic vascular endothelial growth factor (VEGF), by binding to hypoxia-response elements in their promoters. The C-TAD of HIF-1α is involved in modulating the transcriptional activation of HIF-1α under hypoxic conditions, in contrast to the N-TAD, which is involved in the stabilization of HIF-1α. Under hypoxia, the C-TAD is able to interact with transcriptional co-activators, such as CBP/p300. This interaction is unable to occur under normoxia due to the oxygen-dependent hydroxylation of asparagine-803, located within the C-TAD. Hydroxylation of asparagine-803 is mediated by an asparaginyl hydroxylase, known as factor inhibiting HIF-1 (FIH-1), which prevents HIF-1α from interacting with the transcriptional co-activators CBP/p300. An additional mechanism of controlling HIF-1 transactivation function is through redox (reduction–oxidation)-dependent processes. Transfection of thior-edoxin-1 (Trx-1), belonging to the thioredoxin family of small redox active proteins, increases HIF-1α protein levels under both normoxic and hypoxic conditions. This increase is associated

with increased HIF-1 transactivation and the expression of downstream targets including VEGF and nitric oxide synthase-2 (Welsh et al., 2002). Redox effector factor-1 (Ref-1) is a protein which functions not only as a DNA repair endonuclease but also as a redox regulatory factor maintaining transcription factors in an active reduced state. Thiolredox regulation of C-TAD activity by Trx-1 via the Ref-1 system has been reported to promote interaction of the C-TAD with CBP/p300 resulting in increased HIF-1 transactivation (Ema et al., 1999).

HIF-1 target genes

Given that cells and organs need to adapt to changes in oxygen supply, it would not be surprising to find that a significant variety of the HIF-1 target genes are regulated in a tissue-specific manner. To date, there are more than 100 HIF-1 downstream genes identified with varying functions. HIF-1 activates the expression of these genes by binding to a 50-base pair *cis*-acting HRE located in their enhancer and promoter regions (Semenza et al., 1991). Moreover, by using DNA microarrays, it has been reported that more than 2% of all human genes are regulated by HIF-1 in arterial endothelial cells, directly or indirectly (Manalo et al., 2005).

Erythropoiesis/Iron Metabolism

In response to hypoxia, the capacity of red blood cells to transport oxygen is up-regulated by the expression of genes involved in erythropoiesis and iron-metabolism. Hypoxia increases the expression of EPO, which is required for the formation of red blood cells. An increase in the number of erythrocytes enhances the delivery of oxygen to tissues. Products of iron-metabolizing genes control the major erythropoietic rate-limiting step of heme production. Hypoxia up-regulates transferrin (Tf), which transports Fe^{3+} into cells; the transferrin receptor (Tfr), which binds Tf and enables cellular transferrin uptake; and ceruloplasmin (also known as a

ferroxidase), which is required to oxidize ferrous (Fe^{2+}) to ferric (Fe^{3+}) iron. Increasing of these genes supports iron supply to erythroid tissues (Rolfs et al., 1997).

Angiogenesis

Angiogenesis is a complex process that involves multiple gene products expressed by different cell types. A large number of genes involved in different steps of angiogenesis have been shown to increase by hypoxia challenge. Among them, the vascular endothelial growth factor (VEGF) is the most potent endothelial-specific mitogen, and it directly participates in angiogenesis by recruiting endothelial cells into hypoxic and avascular area and stimulates their proliferation. Therefore, the induction of VEGF and various other proangiogenic factors leads to an increase in the vascular density and hence a decrease in the oxygen diffusion distance. In addition, HIF-1 regulates genes involved in governing the vascular tone such as nitric oxide synthase (NOS2), heme oxygenease 1, endothelin 1 (ET1), adrenomedulin (ADM), and the 1β-adrenergic receptor. Moreover, hypoxia induces genes involved in matrix metabolism and vessel maturation such as matrix metalloproteinases (MMPs), plasminogen activator receptors and inhibitors (PAIs), and collagen prolyl hydroxylase.

Glucose Metabolism

Under low oxygen supply, cells switch their glucose metabolism pathway away from the oxygen-dependent tricarboxylic acid (TCA) cycle to the oxygen-independent glycolysis (Dang and Semenza, 1999). With only 2 ATP molecules from each glucose molecule produced by glycolysis, instead of 38 ATP provided by TCA cycle, hypoxic cells elevate their ability to generate ATP by increasing the glucose uptake. This is achieved by up-regulating the expression of glycolytic enzymes and glucose transporters (Wenger, 2002). Hypoxia and HIF-1 increase virtually all the enzymes in the glycolytic pathway, as well as the glucose transporters 1 and 3

(GLU1, GLU3) (Chen et al., 2001). Furthermore, the glycolysis metabolic products, such as lactate and pyruvate, have been reported to cause HIF-1α accumulation under normoxia and regulate hypoxia-inducible gene expression, hence establishing a potential positive feedback loop (Lu et al., 2002).

Cell Proliferation/Survival

Hypoxia and HIF-1 induce growth factors, such as insulin-like growth factor-2 (IGF2) and transforming growth factor-β α (TGF- β) (Krishnamachary et al., 2003). Binding of such growth factors to their cognate receptors activates signal transduction pathways that lead to cell proliferation/survival and stimulates the expression of HIF-1α itself (Semenza, 2003). Cytokines and growth factors, as well as hypoxia in some cell types, can activate signaling pathways MAPK and PI3K, which promote cell proliferation/survival as well as contribute to HIF-1 activity. This leads to increased HIF-1 transcriptional activity of target genes, including those encoding IGF2 and TGF-α, thereby contributing to autocrine-signaling pathways that are crucial for cancer progression (Semenza, 2003).

HIF-1-induced Apoptosis

Paradoxically, cell adaptation to hypoxia leads not only to cell proliferation/survival but also to cell death in some circumstances. Hypoxia has been shown to induce apoptosis, where HIF-1 plays a complex role (Carmeliet et al., 1998). Genetic studies using embryonic stem cells harboring a deletion of HIF-1α showed decreased apoptosis compared with wild type when challenged with low oxygen (Carmeliet et al., 1998). Activation of caspase-3 and Apaf-1-mediated caspase-9, and the release of cytochrome *c*, have been reported in several cell types under hypoxic conditions. It has also been demonstrated that the expression of HIF-1α significantly correlated with apoptosis and the pro-apoptotic factors, such as caspase-3, Fas, and Fas ligand (Volm and Koomagi, 2000). Moreover, hypoxia depressed the antiapoptotic protein Bcl-2 (Carmeliet et al.,

1998), whereas the proapoptotic protein Bcl-2/adenovirus EIB 19-kDa interacting protein 3 (BNip3) and its homolog Nip3-like protein X (NIX) were up-regulated in a HIF-dependent manner (Bruick, 2000). Some genes involved in cell cycle control, such as p53 and p21, were also found to be HIF-dependent (Carmeliet et al., 1998). In addition, p53 has been implicated in regulating hypoxia-induced apoptosis through induction of apoptosis-related genes such as *Bax, NOXA, PUMA*, and *PERP*. In addition to the above classes of genes, HIF-1 also regulated many other target genes implicated in diverse processes such as adipogenesis, carotide body formation, B lymphocyte development, and immune reactions. Although there are some studies showing a role of HIF-2α in the VEGF induction (Akeno et al., 2001; Compernolle et al., 2002), no *bona fide* target genes have yet been identified for HIF-2α or HIF-3α. However, a recent study using a genetic "knock-in" strategy has shown that targeted replacement of HIF-1α with HIF-2α results in expanded expression of HIF-2α -specific target genes (i.e., Oct-4, a transcription factor essential for maintaining stem cell pluripotency) (Covello et al., 2006).

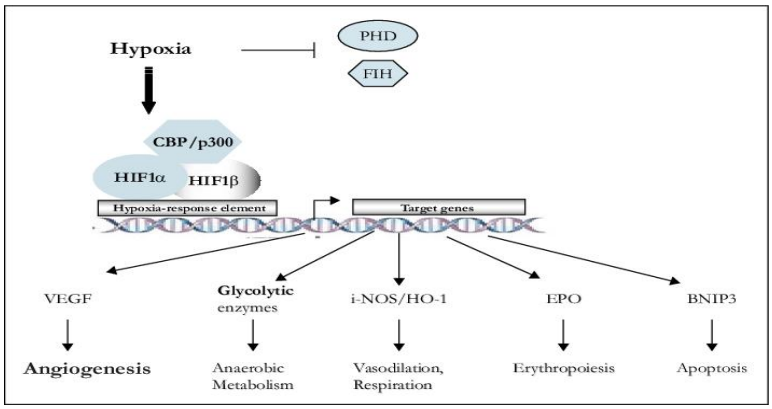

Figure 11. Under hypoxic conditions the alpha subunit of HIF is stable and translocates into the cell nucleus where it heterodimerises with the beta subunit inducing binding to the DNA of target genes carrying a hypoxia-response element (HRE). Interaction with the co-activator CBP/p300 initiates the induction or repression of a large number of genes involved in angiogenesis, anaerobic glycolysis, vasodilation and respiration, erythropoiesis, and apoptosis.

Role of HIF in cancer disease

In order for solid tumors to grow, an increase of oxygen delivery to cells, via angiogenesis and activation of glycolysis, have been observed and named, the Warburg effect (Seagroves et al., 2001). Given the importance of HIF-1 in the activation of genes essential to these processes, it is not surprising that both HIF-1α and HIF-2α have been strongly implicated in tumor progression and grade, hence conferring a selective advantage to tumor cells. Overexpression of HIF-1α and HIF-2α was found in various human cancers, probably as a consequence of intratumoral hypoxia or genetic alteration (Talks et al., 2000). The interior of the tumor mass becomes progressively hypoxic as its size increases until adequate blood vessels are obtained by tumors. Hypoxic conditions within tumors can result in increased HIF-1 stability and activity. Immunohistochemical analyses demonstrated that there are detectable levels of HIF-1α

protein in benign tumors, elevated levels in primary malignant tumors, and a marked amount in tumor metastases, in contrast to its absence in normal tissues. Expression of HIF target genes is generally consistent with the levels of HIF-1α. There is a remarkable frequency of common genetic alterations in cancer cells associated with increased HIF-1α expression. As mentioned in VHL disease, for example, loss of function of VHL resulted in constitutively expressed HIF-1α (Iliopoulos et al., 1996). In addition, loss of function of wild-type p53, which is inactivated in most of human cancers, increased HIF-1α levels and enhanced HIF-dependent transcription in tumors (Ravi et al., 2000). Loss of function of tumor suppressor gene PTEN in glioblastoma-derived cell line resulted in increased HIF-1α levels and HIF-1-mediated gene expression, probably via activating the PI3K/AKT signaling cascade (Zundel et al., 2000). The transforming potential of the v-Src oncogene is thought to be due in part to its induction of HIF and gain of function of v-SRC increased expression of HIF-1α and HIF-dependent genes (Jiang et al., 1997). Moreover, enhanced HER2 receptor tyrosine kinase signaling has been shown to increase the rate of synthesis of HIF-1α (Laughner et al., 2001). Increased activity of the HER2 receptor tyrosine kinase is a prevalent and important genetic alteration in breast cancer, correlating with tumor aggressiveness and decreased patient survival. Therefore, it seems that HIF-1α overexpression confers selective advantages to tumor cells. A correlation between HIF-1 overexpression and patient mortality, poor prognosis, or treatment resistance has been oserved in many studies (Semenza, 2003).

The Warburg effect

ATP required for normal cell proliferation and survival comes primarily from two sources. The first is glycolysis, which comprises a series of reactions that metabolizes glucose to pyruvate in the cytoplasm to produce a net of 2 ATP from each

glucose. The other is the tricarboxylic acid (TCA) or Krebs cycle, which uses pyruvate formed from glycolysis in a series of reactions that donate electrons via NADH and $FADH_2$ to the respiratory chain complexes in mitochondria. With oxygen serving as the final electron acceptor, electron transfer creates across the mitochondrial inner membrane a proton gradient the dissipation of which through ATP synthase forms 36 ATP per glucose molecule. With limited oxygen, such as with muscles that have undergone prolonged exercise, pyruvate is not used in the TCA cycle and is converted into lactic acid by lactate dehydrogenase (LDH) in a process termed anaerobic glycolysis. Many cancer cells consume glucose avidly and produce lactic acid rather than catabolizing glucose via the TCA cycle, which is the key for generating ATP in nonhypoxic normal cells. The avid uptake of glucose by tumors is the foundation for the detection and monitoring of human cancers by fluorodeoxyglucose positron emission tomography. Many years ago, the renowned biochemist Otto Warburg observed that thin slices of human and animal tumors *ex vivo* displayed high levels of glucose uptake and lactate production. The shift toward lactate production in cancers, even in the presence of adequate oxygen, is termed the Warburg effect or aerobic glycolysis (Warburg, 1956). To account for the conversion of glucose to lactate by cancer cells in the presence of oxygen, Warburg speculated that tumor mitochondria are decreased or functionally impaired. In fact, Warburg suggested that impaired mitochondrial function contributes to tumorigenesis. Recent studies suggest that mutations affecting mitochondrial DNA (mtDNA) or enzymes of the TCA cycle might contribute to the Warburg effect. Mutations of mtDNA, which are prevalent in human cancers, could render the mtDNA encoded components of the respiratory chain defective complexes. Intriguingly, the subunits of the TCA cycle enzyme SDH (SDHB, SDHC, and SDHD) behave as classic tumor suppressors in pheochromocytoma or paraganglioma. Furthermore, FH is a tumor suppressor in leiomyoma and renal cell carcinoma. Although these observations suggest that mitochondrial function may be compromised by mutations in mitochondrial enzymes, there is no direct evidence that these mutations are sufficient for

tumorigenesis. In this regard, there is no evidence that respiration is, in fact, less active in cancer cells than in normal cells. Hence, further studies are required to address whether impaired mitochondrial function sufficiently contributes to tumorigenesis. Several oncogenes have been implicated in the Warburg effect. The *AKT* oncogene, which encodes a protein serine-threonine kinase, is associated with enhanced glucose uptake and aerobic glycolysis seemingly independent of HIF-1. The *MYC* oncogene, which is widely activated in human cancers, has also been implicated in the direct activation of aerobic glycolysis. Elevated and sustained activation of MYC, however, is tightly associated with increased mitochondrial reactive oxygen species, which may cause mtDNA mutations that in turn contribute to dysfunctional mitochondria. In addition to oncogenic activation of aerobic glycolysis, the activation of HIF and its direct transactivation of glycolytic enzyme genes significantly contributes to the conversion of glucose to lactate. Two recent studies provide insight into the Warburg effect via a novel HIF-1-mediated mechanism that actively inhibits mitochondrial function (Papandreou et al., 2006). PDK1, which is one of four family members, was identified as a direct HIF-1 target gene in hypoxic cells. PDK1 phosphorylates and inactivates the mitochondrial pyruvate dehydrogenase (PDH) complex. Suppression of PDH by PDK1 inhibits the conversion of pyruvate to acetyl-CoA, thereby attenuating mitochondrial function and respiration. Because nonhypoxic stabilization of HIF through oncogenic events has been observed in many types of tumors, we hypothesize that PDK1 levels may be up-regulated in nonhypoxic tumor cells by HIF, which would divert pyruvate from PDH and result in the increased lactate production. A recent immunohistochemical study further provided evidence that PDK1 expression is elevated in non–small-cell lung cancers (Koukourakis et al., 2005). Intriguingly, PDH expression seems to be reduced in high PDK1-expressing cancer cells. These studies suggest that PDK1 activation may be a key regulatory switch contributing to the Warburg effect. In aggregate, the activation of oncogenes, such as *AKT* and *MYC* along with the stabilization of HIF can enhance aerobic glycolysis or the Warburg effect through

increased glycolytic flux and attenuation of mitochondrial function.

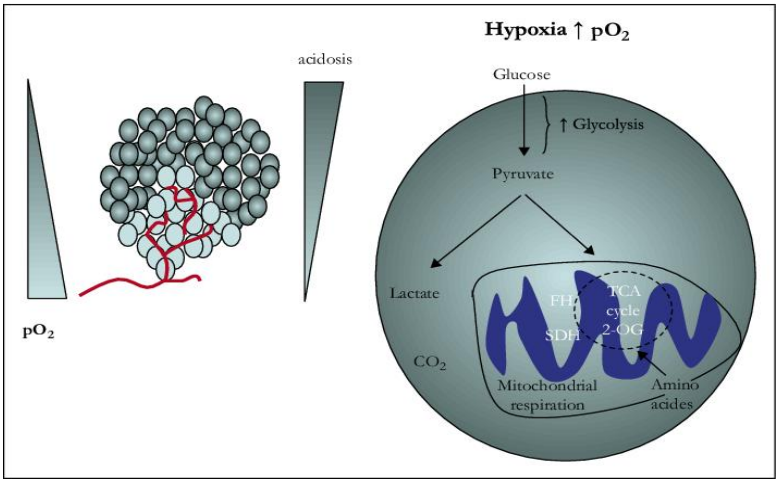

Figure 12. In normal cells the pyruvate generated by glycolysis is metabolized through the tricarboxylic acid (TCA) cycle and oxidative phosphorylation, which is efficient in energy production. In hypoxic tumour cells pyruvate is converted to lactate because oxidative phosphorylation that requires oxygen is limiting. Since this option is less efficient in producing energy the tumour cells increase their uptake and consumption of glucose through an increase in the production of glucose transporters and enzymes of the glycolytic pathway. The increase in lactate production in turn contributes to the acidosis characteristic of tumours. In addition, one of the metabolites of the TCA cycle the 2-oxoglutarate (2-OG) (α-ketoglutarate) is required for the activity of the PHD and FIH hydroxylases. Catabolism of amino acids is also a source of 2-OG. The production of succinate or fumarate by enzymes of the TCA cycle, respectively succinate dehydrogenase (SDH) and fumarate dehydrogenase (FH) leads to feedback inhibition of these hydroxylases.

AIM OF THE PROJECT

The aim of my PhD studies was to explore the consequences of targeting angiogenesis on the development of human GBM. To address this purpose, I selected two parallel strategies: inhibition of telomerase expression in tumor endothelial cells and inhibition of HIF-1 in glial tumor cells.

Part 1: Telomerase inhibition

As observed in previous studies by our laboratory, telomerase is selectively reactivated by endothelial cells of astrocytoma vessels (Pallini et al., 2001). Moreover, we demonstrated that GBM cell lines transactivate telomerase reactivation in HUVEC cells when co-cultured *in vitro* (Falchetti et al., 2003). The meaning of this reactivation has not been fully understood. Since telomerase reactivation was exclusively observed in tumor-irrorating vessels, our hypothesis was that telomerase may contribute to endothelial cell survival in the tumor stressing microenvironment. In order to verify this hypothesis, we observed, *in vitro* and *in vivo*, under stressing conditions, survival rate of HUVEC wt, HUVEC engineered for telomerase overexpression, and HUVEC that cannot reactivate telomerase even if appropriately stimulated. This last population was obtained by stable expression of siRNA directed against hTERT in HUVEC cells. We therefore set up an *in vivo* model in nude mice in which the three different HUVEC cell lines described above were grafted subcutaneously as single graft, or co-injected together with GBM cell lines.
This model allowed to demonstrate that:

HUVEC-TERT show an extended proliferation rate *in vitro*, but they do not grow and poorly survive when injected in nude mice;

HUVEC cells when co-grafted with GBM cells survive and form net-like structures. Telomerase over-expression in HUVEC-TERT amplifies this effect.

Instead, inhibition of telomerase reactivation by RNAi abolished this behavior even in co-grafts.

This result may have clinical impact for developing adjuvant therapies in highly angiogenetic malignancies.

The results described above were published on International Journal of Cancer (Falchetti et al., 2008).

Part 2: HIF-1 inhibition

Deregulation of HIF-1, a recurrent lesion in many solid tumors, is believed to contribute to cancer initiation and progression. Hystological analysis on GBM sections reveals that these tumors are characterized by extensive hypoxic areas. Moreover, GBM derived cell lines express HIF-1 signature even in normoxic conditions. In this study we investigated the consequences of down-regulation of HIF-1 function in a human GBM cell line, in terms of both cell proliferation *in vitro* and tumorigenicity *in vivo*. For HIF-1 inhibition we used RNAi technique for stable expression of siRNA targeting the O_2-regulated HIF-1 subunit in GBM cell lines. HIF-1 down-regulation *in vitro* did not impair growth rate of GBM cells. Conversely long term co-cultures of wild type and HIF-1 inhibited cells resulted in the overgrowth of the wild type cells. The most interesting result came from the *in vivo* model. Similarly to the approach already performed to test the consequences of telomerase inhibition, we engrafted subcutaneously in immunocompromised mice wild type GBM cells or HIF-1-inhibited cells or a 1:1 mixture of the two cell populations. Single grafting of wild type or of HIF-1 inhibited cells lead to comparable tumor formation and growth. Surprisingly, co-grafting of the two mixed populations resulted in more aggressive tumors, both in terms of tumor appearance and tumor growth.
This suggests that heterogeneity of the cellular populations in their ability to mount a response to hypoxia may promote tumor aggressiveness.

MATERIALS and METHODS- Part 1

Cell cultures

TB10 cell line was established in our laboratory from a human GBM tumor. TB10 was grown in DMEM (high glucose, Invitrogen Italia, Milano, Italy) supplemented with 10% heat-inactivated fetal bovine serum. Immunohistochemistry for GFAP was routinely performed to check maintenance of the glial phenotype. The cells were regularly tested for mycoplasma contamination. HUVECs (Bio-Wittaker, Walkersville, MD) were maintained in complete endothelial cell growth medium (EGM -2; Bio-Wittaker) containing endothelial cell basal medium (EBM-2; Bio-Wittaker) supplemented with endothelial cell Bullet kit (Bio-Wittaker; 2% FBS, hEGF-2, hVEGF, R3-IGF-1, ascorbic acid, hydrocortisone, heparin, gentamicin and amphotericin-B). Cells were grown at 37°C in a humidified atmosphere of 5% CO2-95% air. HUVECs used for the experiments were between passage 2 and 5. Hypoxic culturing conditions were achieved by Modular Incubation Chamber MIC-101 (Billups-Rothenberg, Inc., Del Mar-CA).

Plasmids (For plasmid maps see Appendix A)

p-BABE-puro-hTERT and p-BABE-puro-DN-hTERT
p-BABE-puro-hTERT and p-BABE-puro-DN-hTERT were kindly provided by Robert A. Weinberg (Whitehead Institute for Biomedical Research-Cambridge) (Counter et al., 1998).

pRETROSUPER
The pRETROSUPER vector is derived from the Murine Embryonic Stem Cell virus (pMSCV). It contains the pSUPER shRNA expression cassette. The hairpin oligonucleotides are cloned downstream of the polymerase III Histone H1-RNA promoter (H1). pRETROSUPER expresses a transcript containing the viral packaging signal, the H1- shRNA cassette

and the puromycin resistance gene. The pRETROSUPER has a specifically designed 3' LTR that has a deletion in the LTR promoter elements. This deletion results in inactivation of the LTR mediated transcription upon retroviral integration. The phosphoglycerate kinase promoter (PGK) drives the expression of the puromycin resistance gene (puro) for selection in eukariotic cells. The pRETROSUPER plasmid can be propagated in E. coli under ampicillin (AMP) selection.

pCCLsin.PPT.hPGK.GFPpre
pCCLsin.PPT.hPGK.GFPpre is a lentiviral vector described in Dull T et al., 1998. This vector contains the GFP gene driven by the human phosphoglicerate kinase promoter (hPGK).

RNA interference

To target hTERT by RNAi, we used the siTERT1 sequence cloned in pRETRO-SUPER, that we have previously characterized in its ability to down regulate hTERT expression and telomerase activity. From the original construct p-RETRO-SUPERsiTERT1, a fragment encompassing H1 promoter and siTERT1 sequence was subcloned in the XhoI site of the lentiviral vector pCCLsin.PPT.hPGK.GFPpre.

Production of viral stocks and cell infections

Amphotropic retroviruses were generated in HEK 293T packaging cells upon transfection of the retroviral vectors by Lipofectamine reagent (Invitrogen Italia), according to the manufacturer's instructions. Forty-eight hours post-transfection, the viral supernatant was used to infect HUVECs after addition of 2µg/ml polybrene. Cells were infected twice for 6 hr and, after 48 hr, selected with puromycin. Resistant HUVECs over-expressing hTERT or alternatively DN-hTERT were designed

HUVEC-TERT and HUVEC-DN respectively. Amphotropic lentivirus was generated as described. Briefly, pCCLsin.PPT.hPGK.GFPpre construct was cotransfected in HEK 293 packaging cells with pMDL, pRSV-REV and pVSV-G by Lipofectamine reagent. Forty-eight hours post-transfection, the viral supernatant was used to infect HUVECs after addition of 8 μg/ml polybrene. Cells were infected twice for 6 hr. Infection efficiency was monitored through GFP expression. Typically, one cycle of infection is sufficient to obtain virtually 100% of transduced HUVECs. HUVEC stably transduced with siTERT1 sequence or alternatively with empty vector were designed as HUVEC-siTERT and HUVEC-GFP respectively. As negative control of interference, we used the rat sequence for the VGF gene, a neuronal specific mRNA that is not expressed in endothelial cells, generating HUVEC-siVGF.

Immunocytochemistry

For immunostaining of cultured HUVECs and TB10, cells were plated onto poly-L-ornithine coated glass coverslips in serum-free medium. Cells were then fixed with 4% paraformaldehyde and stained with antibody directed against CD31 (Dako, Glostrup, Denmark), TERT protein (Novocastra Laboratories, Newcastle upon Tyne, UK), glial fibrillary acid protein (GFAP; Dako, Glostrup, Denmark), and GFP (BD Biosciences Clontech, Palo Alto, CA). Appropriate secondary antibodies (goat anti mouse IgG affinity purified TRITC-conjugate; Chemicon; goat anti rabbit IgG FITC-conjugate; Chemicon) were used.

Semi quantitative RT PCR

RNA was extracted according to Chomczynski and Sacchi (Chomczynski et al., 1987). An amount of 5 µg of total RNA were retro-transcribed by oligo (dT) primer (Promega, Madison, WI) and 1/5 of the resulting cDNA amplified via PCR.
The primer sets used were:
F-TERT/3280 (ACCAAGCATTCCTGCTCAAGCTG)
R-TERT/3685 (CGGCAGGTGTGCTGGACACTC)
F-G3PDH/4205 (ACCACAGTCCATGCCATCAC)
R-G3PDH/4762 (TCCACCACCCTGTTGCTGTA)
PCR was performed using 1.5 mM MgCl2, 200 µM dNTPs, 10 pmol of each primer and 2 U of Taq polymerase (Promega, Madison, WI).
CDNA was amplified by 35 cycles with the following settings: 94°C for 30 s; 65°C for 45 s; 72°C for 30 s, for hTERT. 94°C for 30 s; 60°C for 45 s; 72°C for 30 s, for G3PDH.

Real Time RT-PCR

hTERT expression was measured by Real-Time quantitative RT-PCR, based on TaqMan methodology, using ABI PRISM 7900 Fast Real Time PCR System (Applied Biosystems). To normalize the amount of total RNA present in each reaction, a housekeeping gene, TBP, was amplified, which is assumed to be constant in all samples. Primers and probes were purchased from Applied Biosystems, Assay-on-Demand Gene Expression Products, TERT assay ID Hs001162669_m1 and TBP ID Hs99999910_m1.

Telomeric Repeat Amplification Protocol (TRAP) Assay

The PCR-based TRAP assessed telomerase activity as described in (Falchetti et al., 1998). One/fifth of the PCR reaction was electrophoresed on 10% polyacrilamide non-denaturing gel and visualized by autoradiography.

Growth Curve

Growth rate of HUVEC-GFP, HUVEC-TERT, HUVEC-siTERT and HUVEC-DN was studied by CellTiter 96 Aqueous One Solution Cell Proliferation Assay (Promega Italia, Milano, Italy). Briefly, 5000 cells per well were plated in a 96 multiwell plate. The data were averaged from four wells and expressed as mean±SD of cell numbers per well. After 48 hr treatment the assay was performed according to the manufacturer's instructions.

FACS analysis

HUVEC-TERT and HUVEC-GFP were treated with 0.75 mM H2O2 for 3 hr. After 15 hr of recovery in fresh EGM2 medium, cells were harvested, washed in PBS and fixed with cold 70% ethanol for at least 1 hour. After removing the alcoholic fixative, cells were stained for the analysis of the DNA content in a solution containing 50 μg/ml propidium iodide (Sigma) and 75 KU/ml RNase (Sigma) in PBS, for 30 min at room temperature in the dark. Samples were measured by using a FACScan cytofluorimeter (Becton Dickinson, CA) and the analysis was performed by means of the CellQuest software package (BD). Cell death was evaluated as percentage of the cells in the sub-G1 region in each DNA histogram, which is

indicative of apoptosis. For the Annexin V assay, we used HUVEC and HUVEC-TERT with no GFP labeling. Cells were harvested, washed once in cold PBS and processed accordin to manufacturer's instructions (Annexin V-FITC Apoptosis Detection Kit, MBL International). Ten thousand events/samples were acquired using a FACScan cytofluorimeter (Becton Dickinson, CA) and the analysis was performed by means of the CellQuest software package (BD).

HUVEC and Glioblastoma Cells Xenografting in Immunodeficient Mice

Four-week-old male nude mice (Harlan, Udine, Italy) were used as hosts for the *in vivo* models of angiogenesis. The experiments on animals were approved by the Ethical Committee of the Catholic University School of Medicine, Rome. HUVEC-GFP, HUVEC-TERT, HUVEC-siTERT, HUVEC-siVGF and HUVEC-DN were harvested, washed twice, and resuspended in cold PBS at the concentration of 1 x 10^4/µl. Then, 100 µl of cells were mixed with 100 µl of Matrigel (BD Bioscience, Bedford, MA) on ice, and the mixture was implanted by subcutaneous injection using a 25-gauge needle. Only one injection was performed on a single mouse. In TB10-HUVEC cografts, 5 x 10^5 TB10 cells and 5 x 10^5 HUVEC cells were resuspended in 100 µl of cold PBS, and the suspension was mixed with an equal volume of cold Matrigel. The animals were kept under pathogen-free conditions in positive-pressure cabinets (Tecniplast Gazzada, Varese, Italy).

Histology, Immunohistochemistry, and Fluorescence Microscopy

The Matrigel implants were removed by one to 4 weeks after grafting. The mice were deeply anesthetized and transcardially

perfused with 0.1 M PBS (pH 7.4), followed by 4% paraformaldehyde in 0.1 M PBS. The implants were surgically removed, stored in 30% sucrose buffer overnight at 4°C, and either embedded in paraffin or cryotomed. In paraffinized sections (5µm thick), a previous step of heat-induced antigen retrieval technique by microwave oven processing (2 cycles of 5 minutes, 750W) in citrate buffer was used. The sections were then incubated with anti-GFP (BD Biosciences Clontech, Palo Alto, CA). After incubation with the primary antibody, immunodetection was performed using the avidin biotin complex peroxidase method (ABC-px method) (LSAB-Dako, Golstrup, Denmark) using freshly made diaminobenzidine as a chromogen. Alternate sections were stained with H&E for morphological analysis. The material was studied under light field illumination and images were captured with a Leitz microscope equipped with a Nikon Coolpix 995 camera and connected to a PC. For fluorescence microscopy, cryotomed sections (20 µm thick) were collected in distilled water, mounted on slides, and cover-slipped with Eukitt. Images were obtained with a Laser Scanning Confocal Microscope (IX81, Olympus Inc, Melville, NY). For quantitative analyses, 10 separate fields were randomly selected per tissue section and the number of surviving GFP-positive HUVECs (20x fields) as well as the net-like tubule structures (10x fields) was counted and averaged. Representative images from each slide were acquired using the confocal microscope with fixed optical parameters, light intensity, filter settings, and magnification. Acquired images were stored as TIFF files and evaluated using Adobe Photoshop 6.

Statistical Analyses

Results are expressed as the mean $\pm$ standard deviation (SD). The significance of differences was assessed by the unpaired two-tail Student-*t* test. Significance was set at $p < 0.05$.

RESULTS- Part 1

Preparation of engineered HUVEC cell populations

All the HUVEC populations used in the following experiments were engineered for the expression of GFP by lentiviral infection. Preliminary studies have shown that GFP expression in HUVECs does not alter their phenotype or culture behavior or telomerase expression.

a) Generation of hTERT over-expressing HUVECs

To test the effect of sustained telomerase expression in endothelial cells (EC), we generated, via retroviral infection with pBabe-puro-hTERT (see mat & met section), a population of HUVECs over-expressing hTERT (HUVEC-TERT). As a positive control we infected HUVECs with pBabe-puro-DNTERT (HUVEC-DNTERT), which allows the stable expression of a dominant negative allele of hTERT subunit. We confirmed by RT-PCR the expression in both the HUVEC strains obtained of hTERT mRNA (Figure 13A). Then, by TRAP assay, which detects telomerase activity in cellular lysate, we demonstrated the reactivation of telomerase activity exclusively in HUVEC-TERT cell population (Figure 13B and data not shown). As previously reported, human ECs delay replicative senescence after ectopic expression of hTERT, due to reactivation of telomerase activity which parallels hTERT over-expression. More specifically, HUVEC cells over-expressing an ectopic hTERT maintain their angiogenic potential *in vitro* and do not show neoplastic features: their growth is contact-inhibited, serum-dependent, and anchorage-dependent. Notably, HUVEC-TERT lines maintain normal p53-dependent checkpoint control, inducing expression of p21 (Cip1/Waf1) in response to DNA damage.

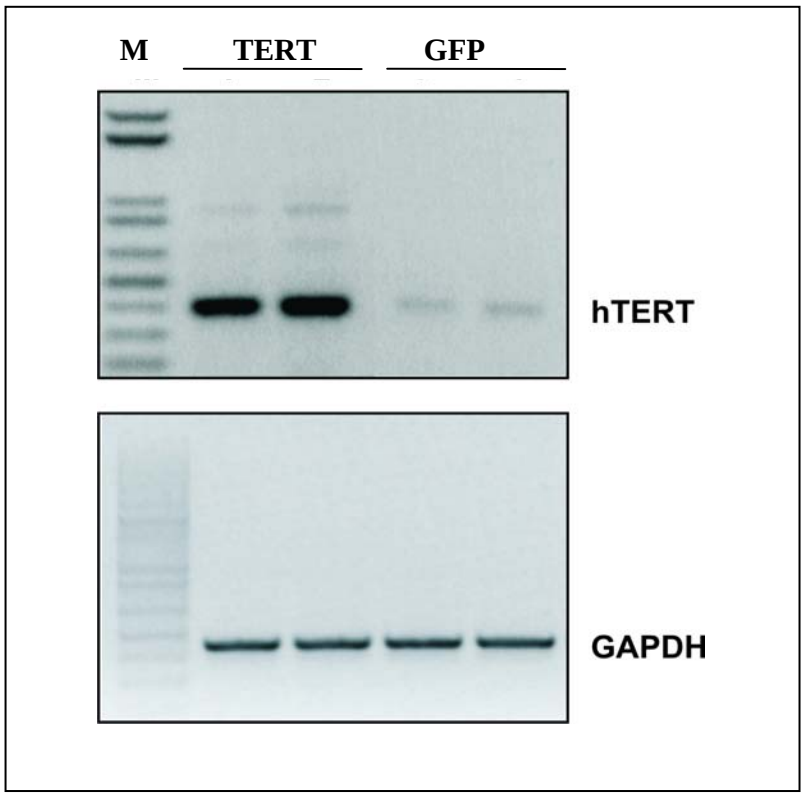

Figure 13A: hTERT and GAPDH RT-PCR. GAPDH expression was used for normalization.

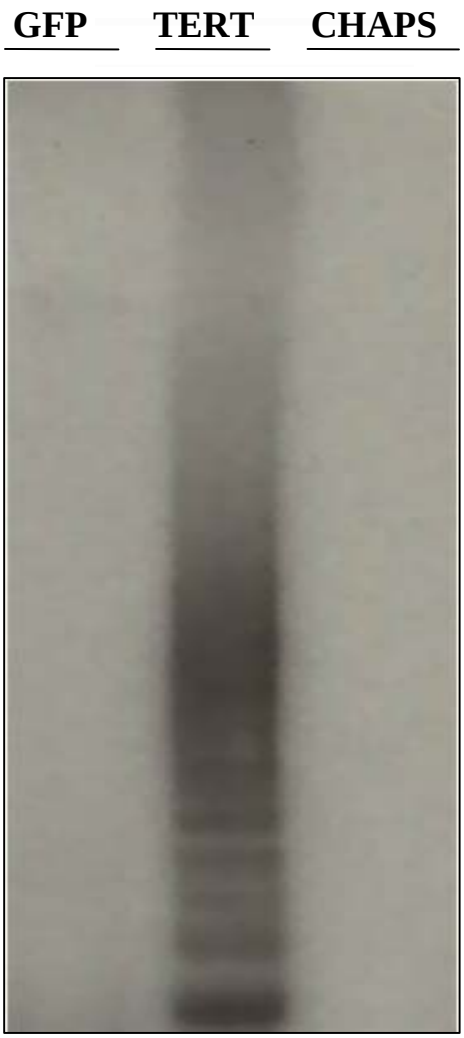

Figure 13B: TRAP assay.

b) Inhibition of hTERT expression in HUVECs

Since we have previously observed that HUVECs reactivate telomerase when co-cultured with human GBM cell lines, we generated HUVECs unable to enhance telomerase activity upon exposure to GBM. To this purpose, HUVECs were infected with a lentiviral construct, pCCL, which allows stable transduction of short hairpin RNAs (shRNAs) that are processed to siRNAs in mammalian cells. The si1 oligonucleotide encoding for shRNA complementary to hTERT was chosen based on its efficiency in inhibiting hTERT expression as well as telomerase activity in GBM cells. The resulting cell population was named HUVEC-siTERT. As control of RNAi, we generated a cell line, HUVEC-siVGF, obtained by lentiviral infection of a shRNA targeting the rat sequence of VGF gene, a neuronal specific mRNA that is not expressed in ECs (see mat & met section). To test the efficacy of si1 sequence to down-regulate hTERT in the HUVEC cell system, we performed Real Time RT-PCR on HUVEC-TERT transduced with the si1 construct (HUVEC-TERT-si1), observing a five-fold down-regulation of hTERT with respect to HUVEC-TERT, therefore demonstrating that the si1 sequence is efficient in inhibiting hTERT in HUVECs even when hTERT is abundantly expressed (Figure 14). As expected, shRNA targeting VGF has no effect on hTERT mRNA expression (Data not shown).

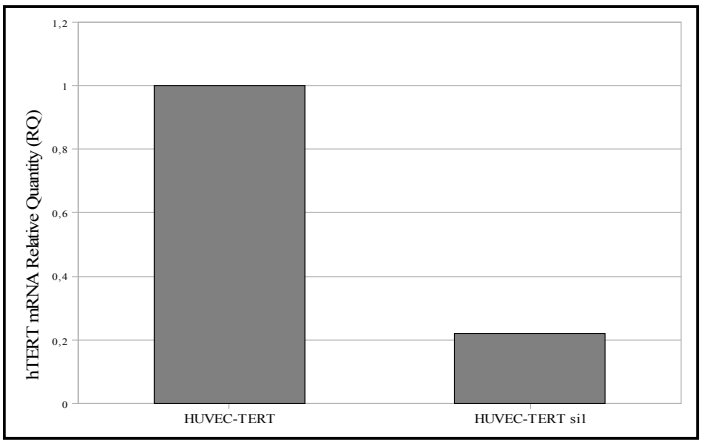

Figure 14: Real Time PCR. hTERT results efficiently inhibited in HUVEC TERTsi1 by siRNA.

Immunohistochemical characterization of engineered HUVECs

Morphologically, HUVEC-TERT, HUVEC-siTERT and HUVEC-DN were identical to HUVEC-GFP, with characteristic cell extensions such as lamellipodia and pseudopodia, and expressed the endothelial specific antigen CD31 (Figure 15). Immunostaining with anti-TERT antibody revealed that the low-passage subconfluent HUVEC-GFP had either a weak positive reaction, which stained diffusely the cell nucleus, or discrete granular staining outlining the nucleoli. In the HUVEC-siTERT, the degree of TERT immunostaining was similar to that of HUVEC-GFP, however about 20% of the cells did not stain at all (Figure 15). Conversely, HUVEC-TERT and HUVEC-DN showed an intense immunoreaction that diffusely stained cell nucleus obscuring any nucleolar detail (Figure 15). The strong immunoreaction for TERT in DN-HUVEC is due to

the accumulation of catalytically inactive hTERT which was recognized by the anti-TERT antibody.

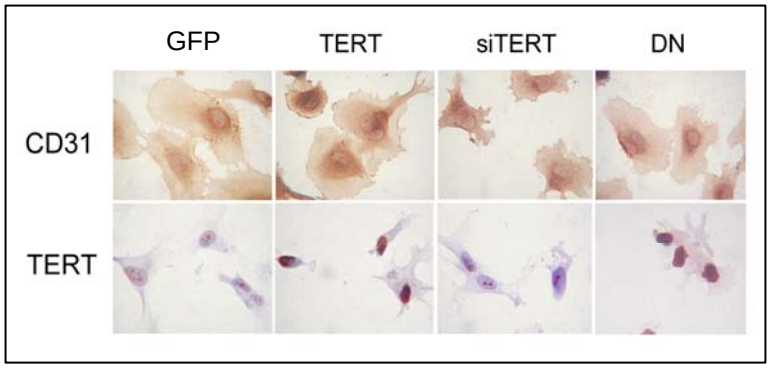

Figure 15: Immunocytochemical characterization of different HUVEC populations. Telomerized HUVEC (HUVEC-TERT) are identical to control HUVECs (HUVEC-GFP, HUVEC-siTERT and HUVEC-DN), and express the endothelial specific antigen CD31 (upper panel). Staining intensity with the anti-TERT antibody parallels the different degrees of hTERT expression by the different HUVEC strains (lower panel).

Could hTERT expression give any proliferative advantage to the cell?

The main consequence of hTERT ectopic expression was that HUVEC-TERT showed an extended lifespan *in vitro*. We passaged HUVEC-TERT up to 50 PDs, and we did not observe any change in their doubling time. As expected, both HUVEC with a canonical hTERT expression (HUVEC-GFP) and HUVEC with reduced telomerase activity, either HUVEC-siTERT and HUVEC-DN, became senescent, flattened, and underwent into growth arrest within a few passages. Anyway, HUVEC-TERT did not exhibit features of transformed cells since they could not be cloned and they were not tumorigenic in immunodeficient mice (see below). To address if telomerized

HUVECs had any proliferative advantage with respect to primary or to telomerase-inhibited HUVECs, we evaluated the proliferation rate of HUVEC-TERT and of early passage HUVEC-GFP, HUVEC-siTERT and HUVEC-DN, either under standard culture conditions or under cell stressing conditions. To mimic the tumor microenvironment conditions, we conducted the experiment in low serum (0.5% FBS), in glucose deprivation - adding to cell medium 1 or 5mM deoxyglucose (DG) - or under hypoxic conditions, in hypoxic chamber (see methods section). After 48 hours treatment, cells were analyzed by CellTiter 96 Aqueous One Solution Cell Proliferation Assay (Promega). HUVEC-TERT exhibited a slight but statistically significant increase in proliferation rate with respect to control ($p < 0.01$, Student *t*-test), except under hypoxic conditions, where all the groups displayed the same growth rate (Figure 16).

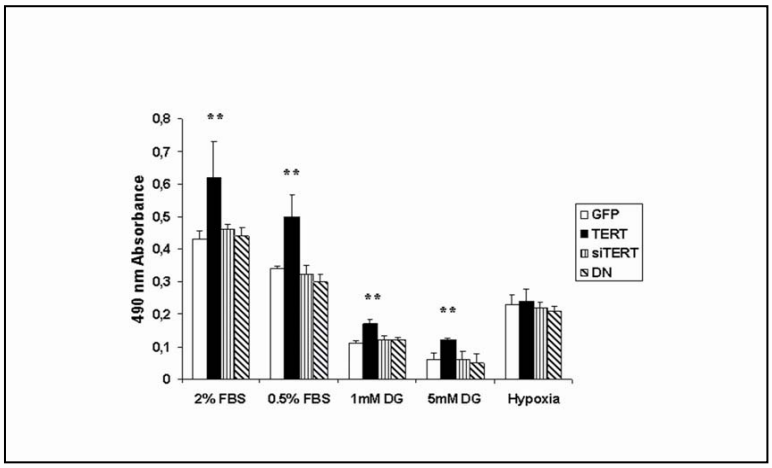

Figure 16: Proliferation rate of HUVEC-GFP, HUVEC-TERT, HUVEC-siTERT and HUVEC-DN under standard (2% FBS) or stressing culture conditions (0.5 % FBS, 1 or 5 mM DG and hypoxia), as assessed by a

colorimetric assay which determines the number of viable cells as a direct proportion to the amount of 490 nm absorbance. The experiment was performed three times. Data were averaged from four wells/experiment and expressed as mean±SD of cell numbers per well. HUVEC-TERT exhibit a significant difference in cell number under all experimental conditions, with the exception of hypoxia (**, $p<0.01$, Student *t*-test).

hTERT protects ECs from oxidative stress induced apoptosis

It has been reported that hTERT over-expression confers to ECs an augmented resistance to apoptotic stimuli. We therefore treated control and HUVEC-TERT with hydrogen peroxide (H_2O_2). H_2O_2 is a well characterized mediator of oxidative stress which is known to generate a variety of different types of oxidative DNA lesions, including base modifications, frameshift mutations, and DNA strand breaks. FACS analysis revealed a protection effect from apoptosis in HUVEC-TERT with respect to the other experimental groups, which displayed a homogeneous percentage of cells in sub-G1 in response to H_2O_2 treatment (Figure 17A). Moreover, staining with Annexin-V confirmed that the cell population in sub-G1 was an apoptotic population (Figure 17B).

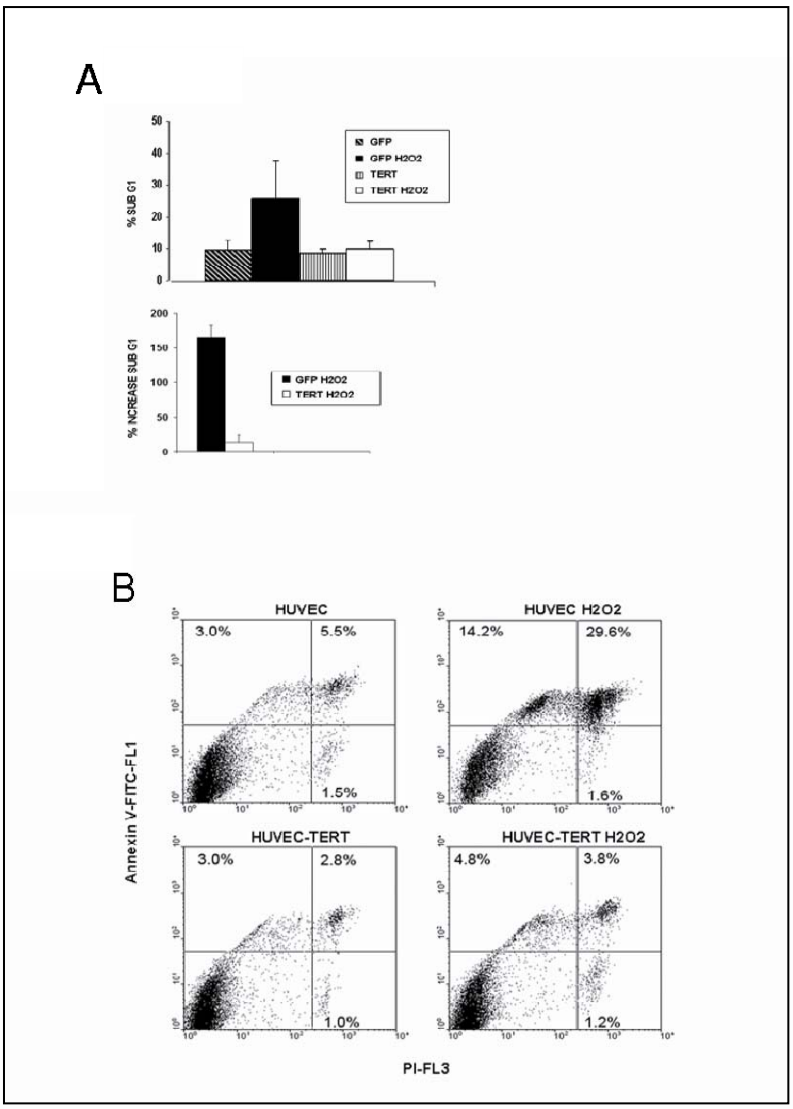

Figure 17: A: FACS determination of the percentage of sub G1 cells in HUVEC-GFP *vs* HUVEC-TERT populations after 3 hours treatment with 0.75 mM H_2O_2. Data were averaged from three different experiments and expressed as mean±SD. The percentage of cells in sub G1 is comparable in the two experimental groups under standard conditions. Under oxidative stress induced by H_2O_2, hTERT over-expression exerts a protection effect from apoptosis. B: Staining with Annexin-V confirmed that the cell population in sub-G1 was an apoptotic population.

hTERT inhibition abolishes the angiogenic behavior of HUVECs in GBM xenografts

Subcutaneous grafting of human ECs as Matrigel assay in immunosuppressed mice has previously been used to investigate survival of these cells under unfavorable *in vivo* conditions. For example, it has been demonstrated that primary human dermal microvascular ECs show poor survival and tubule formation when subcutaneously implanted in immunosuppressed mice, whilst their telomerized counterparts survive and form microvascular structures. Therefore, we used this model to test the hypothesis whether the presence of GBM tumor cells might affect the survival and the angiogenic behavior of grafted HUVECs through mechanisms that involve telomerase activation in these cells. In our bioassay of tumor angiogenesis, HUVECs with different degrees of telomerase expression and human GBM derived TB10 cells (see mat & met), were cografted as Matrigel implants into the subcutaneous tissue of athymic nude mice. On histological examination, clusters of TB10 cells and neoformed vessels were found in Matrigel implants examined by one week after grafting (*n*, 5; Fig). Immunostaining with anti-GFP and direct fluorescence microscopy revealed that HUVEC-GFP not only survived in the implant but even contributed to new vessel formation. At two and 4 weeks after grafting, the tumor xenografts (*n*, 12) were supplied by murine-human chimeric microvessels which were viable to circulating erythrocytes (Figure 18B). In experiments where HUVEC-TERT were used (*n*, 13), the overall picture was qualitatively similar to that of HUVEC-GFP (*n*, 12), although the number both of surviving cells and of tubule structures was significantly higher ($P < 0.0001$, *t*-test) (Figure 19B). Conversely, Matrigel implants containing HUVEC-siTERT (*n*, 16) or HUVEC-DN (*n*, 8) appeared completely devoid of GFP-labeled net-like structures, with only a few cells surviving (Figures 19A and 19B).

The total number of GFP-positive HUVECs was significantly lower in specimens containing either HUVEC-siTERT or HUVEC-DN relative to control HUVECs (HUVEC-GFP or

HUVEC-siVGF) ($p < 0.0001$, *t*-test) (Figure 19B). These data demonstrate that telomerase inhibition is sufficient to suppress the angiogenic behavior of the HUVECs in the tumor environment.

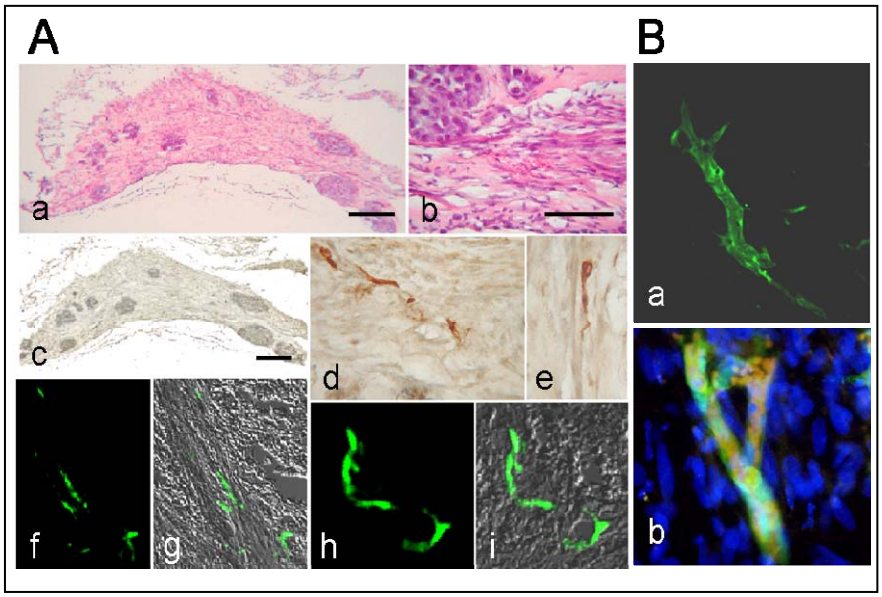

Figure 18: *In vivo* Matrigel assay of tumor angiogenesis in nude athymic mice xenografted with human GBM cells and HUVEC-GFP.

Appearance of Matrigel implant at one week after xenografting. Clusters of GBM tumor cells within the implant (***a***) are approached by capillary networks (***b***). H&E staining. HUVEC-GFP lying along the path of capillary networks (brown in ***c-e***, immunostaining with anti-GFP antibody; green in ***f-i***, fluorescence microscopy in ***f*** and ***h***; confocal microscopy in ***g*** and ***i***). Scale bars: **a**, 200 µm; **b**, 80 µm; **c**, 200 µm; **d-i**, 30 µm.

Four weeks after grafting, HUVEC-GFP contribute to the formation of vessel walls (***a***). Red blood cells are visible within the lumen of HUVEC containing microvessels (***b***); nuclear staining with DAPI), showing that the neoformed vascular structures communicate with the host murine circulatory system (fluorescence microscopy). Scale bar: **a-b**, 50 µm.

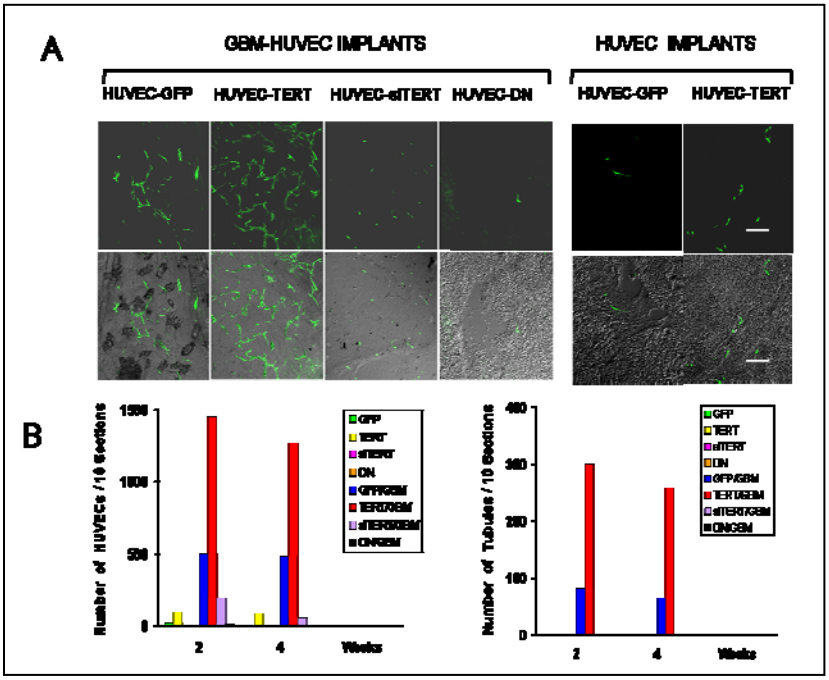

Figure 19: *In vivo* survival and tubule formation by GFP-positive HUVECs subcutaneously xenografted in nude athymic mice as Matrigel implants.

In Matrigel implants containing HUVECs and human GBM cells, both HUVEC-GFP and HUVEC-TERT formed abundant capillary networks. Tubule formation was completely inhibited by the HUVECs where telomerase expression was down-regulated (HUVEC-siTERT and HUVEC-DN). In Matrigel implants containing HUVECs alone, a few HUVEC-GFP and HUVEC-TERT survived at two weeks after xenografting. Scale bars: 80 µm.

Graphic representation of HUVEC (*left*) and tubule (*right*) density in Matrigel implants at two and four weeks after implantation. In Matrigel implants containing HUVECs and human GBM cells, telomerase down-regulation in HUVECs both by siTERT and by DN-TERT significantly reduced the number of GFP-positive HUVECs per ten random high-power fields (*, $P < 0.001$ and **, $P < 0.0001$, respectively). Fluorescent tubule structures were not found in implants grafted both with HUVEC-siTERT and with HUVEC-DN. Averages and standard deviations are presented, and each time point came from at least five independent experiments.

hTERT expression is not sufficient for angiogenic behavior of HUVECs in subcutaneous grafts

In order to evaluate at which extent telomerase expression alone influences the behavior of HUVECs in subcutaneous grafts, we made single graft injections with HUVEC-GFP, HUVEC-siTERT, HUVEC-DN and with HUVEC-TERT. In these single implants (*n*, 12), only a few HUVEC-GFP and HUVEC-TERT survived (Fig. 19A), whilst both HUVEC-siTERT and HUVEC-DN did not (Fig. 19A). Surviving HUVEC-TERT were interspersed within the Matrigel matrix as single cells without forming net-like structures.

These findings demonstrate that primary HUVECs do not survive in Matrigel implant xenografts, and that hTERT up regulation, although increases to some extent HUVECs survival, is not sufficient for these cells to elicit their contribution to angiogenesis.

DISCUSSION- Part 1

We have previously shown that in human GBM the proliferating endothelial cells of the tumor vasculature over-express hTERT, and that hTERT expression by the ECs of the tumor vessels heralds the malignant progression of astrocytic brain tumors (Pallini et al., 2001). A mechanism was postulated where GBM-derived factor/s would induce hTERT expression in the ECs of newly formed vessels. In fact, as demonstrated by in vitro experiments, in co-cultures of GBM derived cells and ECs, GBM induces reactivation of TERT expression in ECs counterpart (Falchetti et al., 2003). Increased transcription of hTERT may be a by-product, with no functional role, of the activation in ECs of a transcriptional program in response to angiogenic stimuli released by tumor cells. We have previously shown that ECs of astrocytoma tumors express high levels of c-Myc (Pallini et al., 2001). Since this oncogene is an established positive regulator of hTERT transcription it is possible that hTERT expression is consequently up-regulated without a specific role (Falchetti et al., 1999). Conversely hTERT expression, and the consequent up regulation of telomerase activity, may be important for tumor angiogenesis. Accordingly, it has been demonstrated that tumor vascularization is impaired in telomerase-negative mice with short telomeres (Franco et al., 2002). In the attempt to address this point we generated both HUVEC where telomerase was up regulated, and HUVEC where telomerase up regulation was prevented either by RNAi targeting hTERT or by the over-expression of a dominant negative allele of hTERT. Then, we analyzed survival and tubule formation of these HUVEC strains in subcutaneous xenografts containing human GBM cells. This model should simulate the interactions between GBM tumor cells and human ECs. We found that hTERT expression in HUVECs is essential for their ability to survive and form tubule structures in the tumor environment. The angiogenic potential of HUVECs was strongly influenced by hTERT expression in this model. When hTERT is over-expressed, HUVECs survive in the implant and even form chimeric murine-human microvessels. Conversely, when hTERT reactivation is

prevented, no tubule formation is present in the xenograft and only a few HUVECs survive. Since the same finding holds true upon over-expression of DN-TERT, we conclude that telomerase activity and not simply hTERT expression is required for HUVECs survival in the cograft with GBM. It is important to note that the angiogenic behavior of engrafted HUVECs depends on the presence of GBM cells, in fact telomerized HUVECs show poor survival when subcutaneously grafted in nude mice as single culture. Thus, telomerase over-expression is a necessary condition but not a sufficient one to allow HUVEC survival and formation of vascular structures in subcutaneous Matrigel implants.

The issue whether hTERT over-expression is a condition sufficient *per se* to allow proliferation and ECs organization in net-like structures is controversial. Our study demonstrates that hTERT over-expression might allow only a very limited survival, which is not sufficient to elicit any angiogenic behavior of HUVECs in the Matrigel implant. Conversely, Yang and colleagues showed that retroviral-mediated transduction of hTERT in HDMECs resulted in cell lines that form microvascular structures when subcutaneously implanted in SCID mice, with functional murine-human vessel anastomoses (Yang et al., 2001). In agreement with our data, however, Freedman and Folkman showed that telomerized HUVECs, though capable of extended proliferation *in vitro*, do not grow or survive when implanted subcutaneously in immunocompromised mice (Freedman and Folkman, 2004). The orthotopic model used for HDMEC xenografting vs the heterotopic one used for HUVECs might be influential in explaining such discrepant results. Beside this, the key aspect of the present study is that the pro-angiogenic effect of GBM-related factor/s is nearly abolished when we prevent the ability of HUVECs to reactivate hTERT.

Telomerase has also been demonstrated to be an important inducer of angiogenic phenomena in non neoplastic contexts. For example, Murasawa and co-workers demonstrated that telomerase activity contributes to endothelial progenitor cells angiogenic properties: mitogenic activity, migratory activity, and cell survival resulted significantly enhanced by hTERT

over-expression (Murasawa et al., 2002). In our model system we found no evidence of HUVECs proliferation within the graft, in fact the number of HUVECs in the xenograft at any survival time was smaller than the number of grafted cells. Thus it is unlikely that the higher number of surviving telomerized HUVEC is due to an increase in replication potential provided by telomerase activity. We favour the hypothesis that telomerase expression increases resistance of HUVECs to apoptotic stimuli. Several reports describe increased cell death in normal and transformed cells upon telomerase inhibition independently of telomere shortening (Li et al., 2004) as well as protection from cellular stresses of non transformed cells upon telomerase over-expression (Oh et al., 2001). Recently it was shown that inhibition of telomerase expression in normal human fibroblasts abrogates the cellular response to DNA double strand breaks, impairs the DNA damage response and decreases DNA repair (Masutomi et al., 2005). In addition, low level of telomere dysfunctions in presenescent normal human mammary epithelial cells was shown to lead to a sub threshold activation of p53, a phenomenon abrogated by ectopic expression of telomerase (Beliveau et al., 2007). p53 appeared to be capable of integrating signals originating from telomere dysfunctions and from growth factor deprivation, thus inducing cell cycle arrest. Thus signals from telomere dysfunctions can be similarly integrated with different forms of cellular stresses leading to apoptosis. Our finding showing that telomerized HUVEC are more resistant to oxidative stress induced by a pulse of H_2O_2 is compatible with this hypothesis.

In conclusion, this study demonstrates that the selective inhibition of telomerase in the ECs of GBM xenografts abolishes the angiogenic behavior of these cells in the tumor environment. Other than a direct effect on GBM tumor cells, antitelomerase compounds might hinder tumor growth through an antiangiogenetic mechanism directed towards the ECs of the tumor vasculature. Compared with the poorly vascularized core region of the tumor, the endothelial cells represent a much more attractive target for drugs delivered into the blood stream.

MATERIALS and METHODS- Part 2

Cell cultures and generation of stably transduced cell lines

HEK 293T cells and TB10, a cell line established in our laboratory from a secondary human GBM tumor, were grown in DMEM (high glucose, Invitrogen Italia, Milano, Italy) supplemented with 10% heat-inactivated fetal bovine serum. The cells were regularly tested for mycoplasma contamination. For experiment requiring hypoxic conditions the cells were placed in a modular incubator chamber flushed with a gas mixture containing 2% O_2, 5% CO_2, 93% N_2 at 37 °C. Anoxia was similarly achieved by culturing cells in a 5% CO_2 and 95% N_2 atmosphere. As a hypoxic mimetic the PHD inhibitor deferoxamine was used at the concentration of 100 μM.

Plasmids (For maps see Appendix A)

pRETROSUPER

The pRETROSUPER vector is derived from the Murine Embryonic Stem Cell virus (pMSCV). It contains the pSUPER shRNA expression cassette. The hairpin oligonucleotides are cloned downstream of the polymerase III Histone H1-RNA promoter (H1). pRETROSUPER expresses a transcript containing the viral packaging signal, the H1- shRNA cassette and the puromycin resistance gene. The pRETROSUPER has a specifically designed 3' LTR that has a deletion in the LTR promoter elements. This deletion results in inactivation of the LTR mediated transcription upon retroviral integration. The phosphoglycerate kinase promoter (PGK) drives the expression of the puromycin resistance gene (puro) for selection in eukariotic cells. The pRETROSUPER plasmid can be propagated in E. coli under ampicillin (AMP) selection.

pEGFP-C1

pEGFP-C1 encodes a red-shifted variant of wild-typeGFP which has been optimized for brighter fluorescence and higher expression in mammalian cells. pEGFP- C1 encodes the GFPmut1 variant which contains the double-amino-acid substitution of Phe-64 to Leu and Ser-65 to Thr. SV40 polyadenylation signals downstream of the EGFP gene direct proper processing of the 3' end of the EGFP mRNA. A neomycin resistance cassette, consisting of the SV40 early promoter, the neomycin/kanamycin resistance gene of Tn5, and polyadenylation signals from the Herpes simplex virus thymidine kinase gene, allows stably transfected eukaryotic cells to be selected using G418. A bacterial promoter upstream of this cassette expresses kanamycin resistance in E. Coli.

pRetroQ-DsRed Monomer-C1

pRetroQ-DsRed Monomer-C1 is a high-titer, self inactivating retroviral vector that facilitates efficient delivery and expression of DsRed-monomer (DsRed.M1) as well as C terminal fusion of DsRed monomer to target cells. This vector also contains a puromycin resistance cassette driven by PGK promoter for selection of positively infected cells. pRetroQ-DsRed Monomer-C1 contains a bacterial origin of replication, an E.coli Ampr gene for propagation and selection in bacteria, and an SV40 origin for replication in mammalian cells expressing the SV40 T antigen.

RNA interference and viral infections

Silencing of HIF-1α was obtained by retroviral mediated expression of shRNA targeting nucleotide 528-547 of HIF-1 α sequence (GenBank™ accession number NM_001530) using pRETRO-Super vector. Control shRNA had the following sequence
5’ GGGATATCCCTCTAGATTA 3’. Neither the HIF-1α targeting shRNA nor the control sequence (sh random, siR5) have any homology with other human gene, as tested by BLAST (http://ncbi.nln.nih.gov/BLAST).

shRNA expressing retroviruses were produced in 293T cells by cotransfecting pRETRO-Super together with plasmids encoding for gag, pol and VSV-G proteins. Viral supernatant was collected 48 h post-transfection, filtered through a 0.45 μm pore size filter and added to the cells in the presence of 4 μg/ml polybrene. 48 h post infection cells were selected by 1 μg/ml of puromycin. TB10 expressing green or red fluorescent proteins were similarly obtained by infection with recombinant retroviruses prepared from pEGFP-C1 and pRetroQ-DsRed Monomer C respectively (Clontech Laboratories, Inc). Cells were subjected to three consecutive rounds of infection and more than 80% of the cells expressed the florescent protein.

Real Time RT-PCR

Total RNA (2 μg) was retrotranscribed according to standard procedures and 1/10 of the cDNA was used to quantify the transcripts by real time RT-PCR, using probes from the Universal ProbeLibrary (Roche Applied Science) and gene specific-primers designed by the Probe Finder software (Roche Applied Science). RQ were calculated relative to TBP mRNA assumed to be constant. The real time PCR was performed with the 7900HT Fast Real-Time PCR System by Applied Biosystem.

Western Blotting

Approximately 10^6 cells were lysed in 10Mm HEPES pH 8.0, 50 mM NaCl, 500 mM Sucrose, 0.1 mM EDTA, 0.5% Nonidet P-40, 5 mM $MgCl_2$, containing protease inhibitors (SIGMA). Nuclear pellets were washed twice with the same buffer, and nuclear proteins were extracted by high salt buffer (20 mM HEPES pH 7.9, 420 mM NaCl, 25% glycerol, 0.2 mM EDTA, 1.5 mM $MgCl_2$, containing protease inhibitors (SIGMA)). Protein concentration was measured by Bradford assay and 40 μg of nuclear extracts were resolved by SDS PAGE and

electrophoretically transferred on a Nytrocellulose (Millipore) membrane. Immunoreactive bands were visualized by the Pierce West Dura Signal ECL system. The following antibodies were employed: anti HIF-1α monoclonal antibody (BD biosciences); anti lamin B1 polyclonal antibody (Santa Cruz) was used to asses equal loading of nuclear proteins.

Cell proliferation

Growth rate was measured by seeding $2x10^5$ cell / 60 mm dishes in triplicates, and counting cell number after 48 h. Convenient dilution was used for successive rounds of seedings. Cell proliferation was also measured with the CellTiter 96® AQ_{ueous} One Solution Cell Proliferation Assay (Promega Corporation) according to the manufacturer's instructions. To measure the relative proliferation index of wtTB10 and siHIF-TB10 cells in coculture, 10^5 wtTB10#8 GFP cells and 10^5 siHIF-TB10#12 RED cells were seeded per 60 mm dish. Every 72 hrs the cells were collected and one fourth of the population was re-seeded and the remaining cells were used for DNA preparation. Genomic DNA was digested with the restriction enzyme EcoRI and 10 μg used for quantification by real time PCR with probes specific for GFP, DsRed and an hTERT DNA sequence in an intron-less region. The relative proliferation of wtTB10 and siHIF-TB10 cells was calculated by comparing the RQs of GFP and DsRed with respect to hTERT in DNA preparations from cells at different passages of cocolture to the RQs in a DNA preparation from equal number of wtTB10 and siHIF-TB10 cells.

Measurement of cellular ATP

Measurement of cellular ATP was performed using the ATPlite assay (Perkin Elmer-Cetus, Norwalk, CY) according to the manufacturer's instructions. In brief, cells seeded in 96-well

microplates were resuspended in 50 µl lysis buffer, and after 5 min, 40 µl of substrate solution (Luciferase/Luciferin) was added to each sample. The luminescence was measured using a luminescence plate reader (Victor2 1420 multilabel counter; Wallac Oy, Turku, Finland). The ATP concentration was standardized using the total cellular protein concentration estimated by using Bradford protein assay (Bio-Rad). To confirm results, the experiments have been repeated by normalizing the ATP content to the number of cells.

Determination of Glutathione Content

Determination of intracellular glutathione was performed in HPLC as described in Ciriolo et al., 1997. In brief, cell pellets were resuspended in 1:1 solution of PBS and HCl 0.01M. Then, the cells were lysated by "freeze and thaw" method. By adding of metaphosphoric acid (MPA), protein content was precipitated. NaHCO3 and Iodacetic Acid (AIA) were added to the supernatant, for buffering solution and to block thiol groups, respectively. Then, 1:1 ratio of Sanger reactive (Dinitrofluorobenzene, $((NO_2)_2C_6H_3F)$) was added to the solution. The samples were separated by chromatographic column (Bondpack NH_2 model).

Glioblastoma Cells Xenografting in Immunodeficient Mice

Four-week-old male nude mice (Harlan, Udine, Italy) were used as hosts for the *in vivo* models of tumorigenesis. The experiments on animals were approved by the Ethical Committee of the Catholic University School of Medicine, Rome. TB10 cells were harvested, washed twice, and resuspended in cold PBS at the concentration of 1×10^4/ µl. Then, 100 µl of cells were mixed with 100 µl of Matrigel (BD Bioscience, Bedford, MA) on ice, and the mixture was implanted by subcutaneous injection using a 25-gauge needle.

Only one injection was performed on a single mouse. The animals were kept under pathogen-free conditions in positive-pressure cabinets (Tecniplast Gazzada, Varese, Italy).

Histology, Immunohistochemistry, and Fluorescence Microscopy

The Matrigel implants were removed by one to 8 weeks after grafting. The mice were deeply anesthetized and transcardially perfused with 0.1 M PBS (pH 7.4), followed by 4% paraformaldehyde in 0.1 M PBS. The implants were surgically removed, stored in 30% sucrose buffer overnight at 4°C, and either embedded in paraffin or cryotomed. In paraffinized sections (5 μm thick), a previous step of heat-induced antigen retrieval technique by microwave oven processing (2 cycles of 5 minutes, 750W) in citrate buffer was used. The sections were then incubated with anti-GFP (BD Biosciences Clontech, Palo Alto, CA). After incubation with the primary antibody, immunodetection was performed using the avidin biotin complex peroxidase method (ABC-px method) (LSAB-Dako, Golstrup, Denmark) using freshly made diaminobenzidine as a chromogen. Alternate sections were stained with H&E for morphological analysis. The material was studied under light field illumination and images were captured with a Leitz microscope equipped with a Nikon Coolpix 995 camera and connected to a PC. For fluorescence microscopy, cryotomed sections (20 μm thick) were collected in distilled water, mounted on slides, and cover-slipped with Eukitt. Images were obtained with a Laser Scanning Confocal Microscope (IX81, Olympus Inc, Melville, NY). Representative images from each slide were acquired using the confocal microscope with fixed optical parameters, light intensity, filter settings, and magnification. Acquired images were stored as TIFF files and evaluated using Adobe Photoshop 6.

Statistical Analyses

Results are expressed as the mean ± standard deviation (SD). The significance of differences was assessed by the unpaired two-tail Student-*t* test. Significance was set at $p < 0.05$.

RESULTS- Part 2

Production of GBM clones with reduced HIF-1a expression

In order to obtain a polyclonal population of TB10 cell line in which HIF-1a was inhibited, we used RNA interference technique, by retroviral mediated delivery of shRNA. To vehicle shRNA into the cells we used the pRETRO-Super vector (see mat & met section). Infected cells were selected by puromycin and the resulting polyclonal population was named siHIF-TB10. Control populations were obtained by infecting TB10 cells with empty pRETRO-Super (wtTB10) or with a pRETRO-Super encoding for a shRNA of random sequence that has no homology with any human transcript (siR5-TB10). Since in every condition used, and for every parameter measured, siR5-TB10 and wtTB10 cells were indistinguishable only the data obtained with wtTB10 will be shown.
In addition, we isolated from the siHIF-TB10 polyclonal population a number of independent clones.
Expression of HIF-1a RNA, as measured by real time RT-PCR, was significantly reduced both in the in the polyclonal population and in the single siHIF-TB10 cells (Figure 20). In order to asses if the decrease in HIF-1a mRNA was paralleled by a similar reduction in HIF-1a protein, nuclear extracts prepared from wt and siHIF-TB10 cells were examined by western blot using anti HIF-1a antibodies. Nuclear proteins were extracted also from cells treated overnight with 100 nM deferoxamine, a widely used hypoxia-mimetic drug that inhibits PHDs. As shown in Figure 21, deferoxamine treatment of wtTB10 cells resulted in the induction of HIF-1a protein from an undetectable band to a strong signal. This increase in HIF-1a protein content was substantially reduced in extracts of siHIF-TB10 cells and even more so in the single clones.

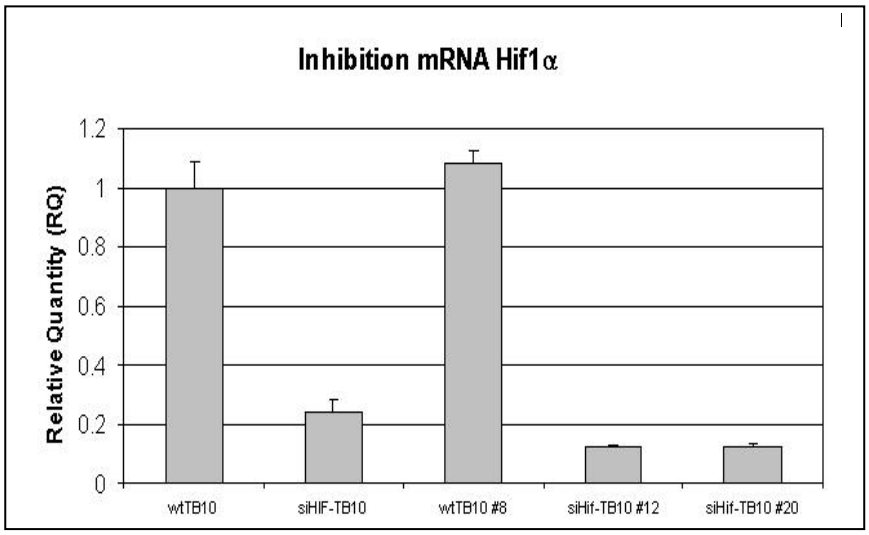

Figure 20: HIF-1a mRNA expression was measured by real time RT-PCR in wtTB10 cells, siHIF-TB10 cells and in selected clones. Stable expression of shRNA against HIF-1a significantly reduced HIF-1a mRNA levels.

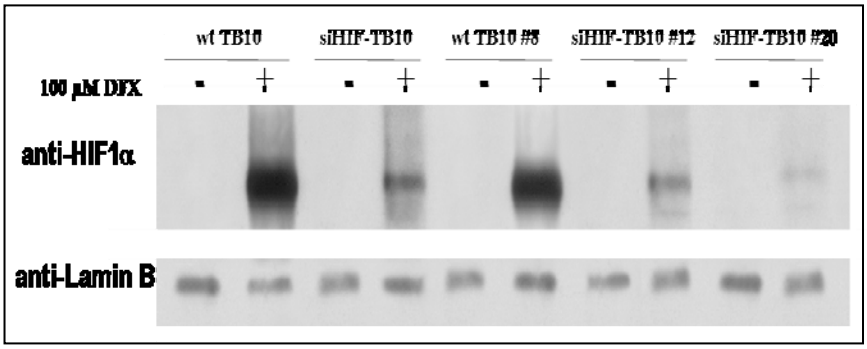

Figure 21: HIF-1a protein levels were measured by Western blot analysis of nuclear extracts of cells cultured for 12 hrs in the absence (odd lanes) or in the presence (even lanes) of the hypoxia-mimetic deferoxamine. The amount of lamin B, a nuclear protein, is shown as loading control.

Finally we measured to which extent the transcription of HIF-1-regulated genes was affected by HIF-1a silencing. RNA was extracted from wtTB10 and siHIF-TB10 cells cultured in the absence or in the presence of deferoxamine, and the level of HIF-1 target genes mRNAs was measured by real time RT-PCR. HIF-1 target genes that we chose for this analysis were: Carbonic Anydrase-9 (CA9), Vascular Endothelial Growth Factor (VEGF), Phosphoglycerate Kinase-1 (PGK-1), and Glucose Transporter-1 (GLUT-1). As shown in figure 22, deferoxamine treatment induced, although to a different extent, all these transcripts in wild type cells. Such a transcriptional response was blunted in siHIF-TB10 cells. Of note the amount of CA9 and VEGF transcripts was significantly lower in siHIF-TB10 cells with respect to wtTB10 cells, even in normoxia. Single clones displayed different degrees of inhibition in the expression of hypoxia-responsive genes ranging from 40% to 90%.

For all the following experiments we used two independent clones, named siHIF-TB10#12 and siHIF-TB10#20, which showed the strongest inhibition of HIF-1a protein expression and activity (Figures 21 and 22). Single clones isolated from the wtTB10 cell population had comparable expression of HIF-1α mRNA (less than 10% difference among distinct clones).

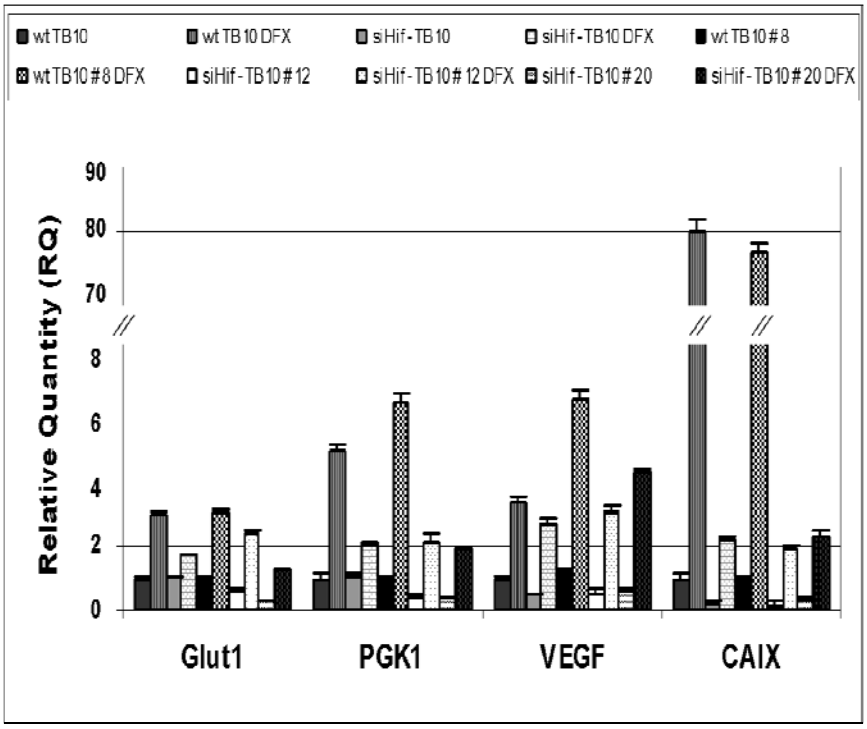

Figure 22: Expression of hypoxia-regulated transcripts was measured by real time RT-PCR on total RNA extracted from cells cultured for 12 hrs in the absence (empty lanes) or in the presence (black lanes) of the hypoxia-mimetic deferoxamine. For each gene examined the RQ in wtTB10 cells grown in the absence of deferoxamine was set equal to 1.

HIF-1a suppression does not alter ATP concentration, redox status and cell proliferation

As described in introduction section (see Warburg effect paragraph), under hypoxic conditions cells shift their metabolism from oxygen-dependent Krebs cycle to oxygen-

independent glycolysis. This metabolic profile is a characteristic feature of tumor cell even in normoxic conditions. One consequence of the impairment of mitochondrial respiratory chain is the reduction of mitochondrial mass. HIF-1 regulates the metabolic switch by transcriptional increase of glycolytic enzymes (as well as GLUT-1 and PGK-1). Therefore, in tumor cells the presence of active HIF-1, even in normoxia, resulted in a reduction of mitochondrial mass that leads to lower levels of ATP and ROS. We thus characterized our TB10 cell lines *in vitro* for ATP content and redox status. Moreover, we analyzed cell proliferation in order to evaluate if a different metabolic *spectrum* reflects differences in cell growth.

Surprisingly, the total quantity of ATP, Figure 23A, and of reduced glutathione, a measure of oxidative stress, Figure 23B, was to a large extent the same in wtTB10 and siHIF-TB10 cells. For cell proliferation, we measured the growth rate of wtTB10 pool, wtTB10#8 cells, siHIF-TB10 pool, siHIF-TB10#12 and siHIFTB10#20 cells. As shown in Table1, the rate of population doubling of TB10 cells was unaffected by the level of expression of HIF-1a. This probably reflects the fact that in GBM cells mitogenic responses to growth factors are quite altered with respect to normal cells and proliferation may loose feedback control by the metabolic state of the cell.

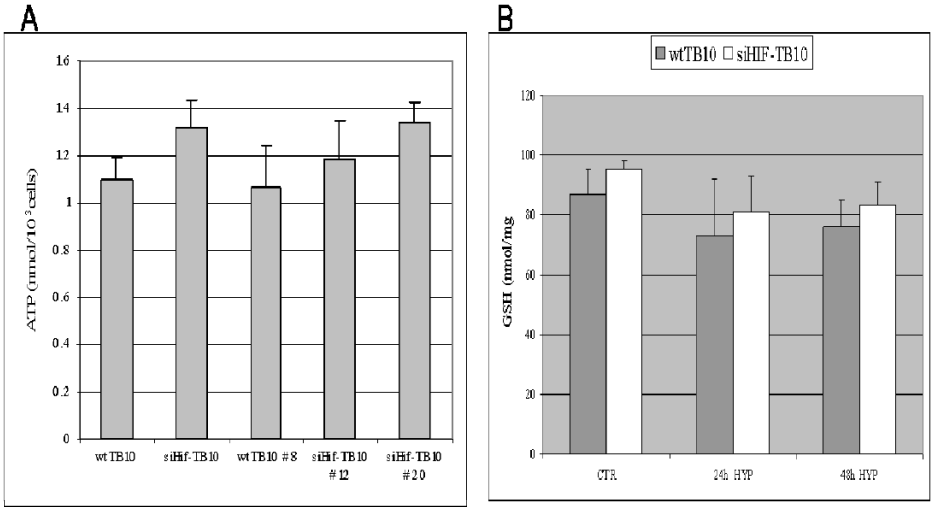

Figure 23: A: Intracellular ATP concentration was measured in wild type and HIF-1a-inhibited TB10 cells cultured in normoxia or in hypoxic conditions. B: Intracellular content of reduced glutathione.

TABLE 1	
Rate of population doubling (PD)	
wtTB10	28.98± 5.49
wtTB10#8	28.01± 4.86
siHif-TB10	32.55± 3.25
siHif-TB10#12	33.54± 5.31

Table 1. Proliferation rate of experimental groups.

wtTB10 cells out compete siHIF-TB10 cells in mixed culture

We decided to examine if the growth rate of each cell population was affected by the presence of the other cell type. Indeed, although wtTB10 and siHIF-TB10 cells showed comparable proliferation rate in standard conditions, they may show differences in sub-optimal conditions. Moreover, wtTB10 and siHIF-TB10 cells may differently utilize limiting resources due to their metabolic profiles. For this purpose we mixed at 1:1 ratio the two cell populations and co-cultured them under standard and limiting conditions, i.e. glucose limiting concentrations. It is well established that tumor cells require high flux of glucose for the fast synthesis of ATP through the glycolytic pathway and at the same time for production of anabolites necessary for cell growth and cell duplication. Since HIF-1 is a major regulator of glucose uptake, we reasoned that siHIF-TB10 cells may be outcompeted by wtTB10 cells when glucose in the medium becomes limiting. To distinguish the two cell types in mixed co-cultures, we generated wtTB10#8 cells expressing the enhanced green fluorescent protein (EGFP) and siHIF-TB10#12 cells expressing the red fluorescent protein DsRed, by retroviral infection (plasmid map in mat & met). In a preliminary experiment we showed that the expression of the fluorescent proteins did not modify the proliferation rate of the cells. The co-culture was split 1:4 every three days and at day 0, 2, 8, 11, 14 and 16 genomic DNA was extracted. The relative abundance of wtTB10 and siHIFTB10 cells was measured by quantifying, through real time PCR, the amount of DNA encoding for EGFP and DsRed protein respectively. The data were normalized using an exon of the telomerase catalytic subunit hTERT as an internal standard. As shown in Figure 24, wtTB10 cells increased in relative abundance with respect to siHIF-TB10 cells in long term co-cultures. Moreover, wtTB10 cells outgrew siHIF-TB10 cells much faster when glucose concentration was reduced (Figure 24B). It was previously described that one hundredfold reduction in glucose concentration in the medium strongly promotes apoptosis of

cultured GBM cells, however in our experimental setting, i.e. a fivefold reduction in glucose concentration, there was no induction of apoptosis neither in wt nor in siHIF-TB10 cells (not shown).

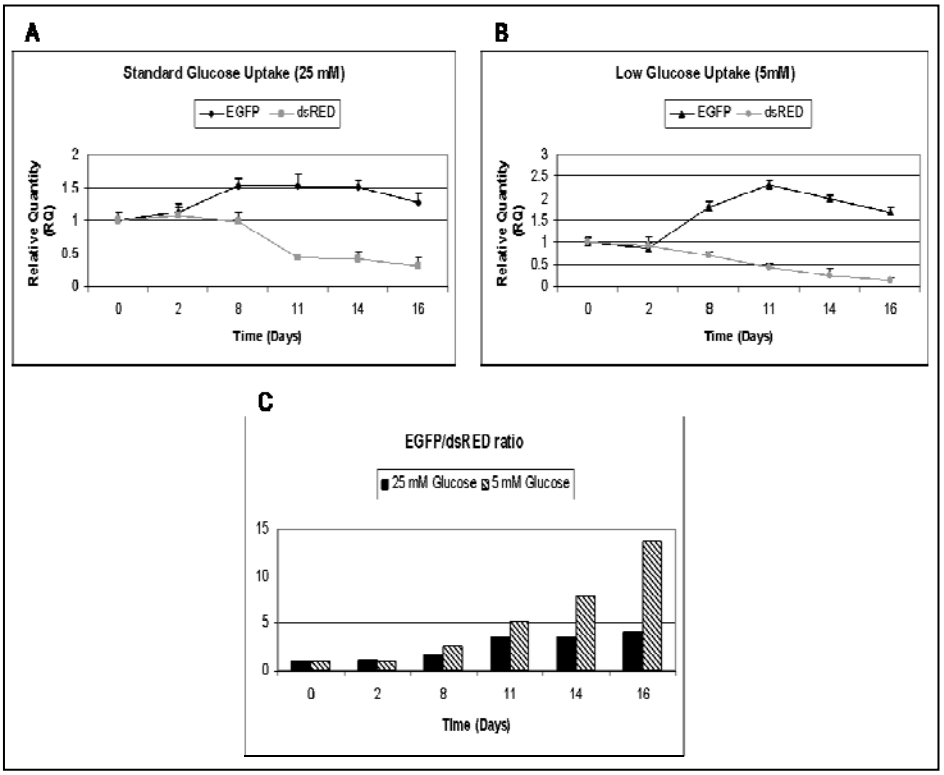

Figure 24: The relative number of wtTB10 # 8 and siHIF-TB10 # 12 in co-colture was assesed at the indicated time points by measuring the ratio of EGFP and DS-Red –encoding DNA as measured by real time PCR. The values are expressed setting the ratio at time 0 equal to 1. A: Cells were grown in standard (25 mM). B: Cells were grown in reduced (5 mM) glucose concentration. C: Ratio of EFGP and DsRED protein RQ.

Xenografts of mixed population of wtTB10 and siHIF-TB10 cells grow faster than xenografts of either wtTB10 or siHIF-TB10 cells

We next assessed whether the inhibition of HIF-1 signaling may affect the growth of TB10 GBM cells *in vivo*.

We therefore set up an *in vivo* model of tumor xenografts in immunocompromised mice. The EGFP-labeled control TB10#8 and the DsRed-labeled siHIF-TB10#12 cell populations were subcutaneously implanted either as single cell populations and as mixed 1:1 co-cultures. This approach allowed us to study not only if HIF inhibition results in a reduced tumorigenicity *in vivo*, but, most interestingly, to observe possible cooperation between the two groups. The following parameters were analysed to evaluate tumorigenicity: rate of tumor appearance, volume of tumor xenografts and number of cells *per* histological section.

Tumor growth was monitored over an 8 week period. After 4 weeks, the rate of tumour appearance was 37% (*n*, 3/8), 37% (*n*, 3/8), and 75% (*n*, 6/8) in the wtTB10 group, siHIF-TB10 group, and wtTB10/ siHIF-TB10 group, respectively (Figure 25A). Moreover, after 8 weeks, the mean diameter of the tumour xenografts was significantly greater in the wtTB10/ siHIF-TB10 grafted mice as compared both with the wtTB10 and with the siHIF-TB10 grafted mice ($p<0.05$, Student's *t*-test; Figure 25B). On histological examination, the xenografts showed the typical morphology of GBM tumours, without substantial differences of the tumour cyto-architecture and vasculature among the different experimental groups (Not shown).

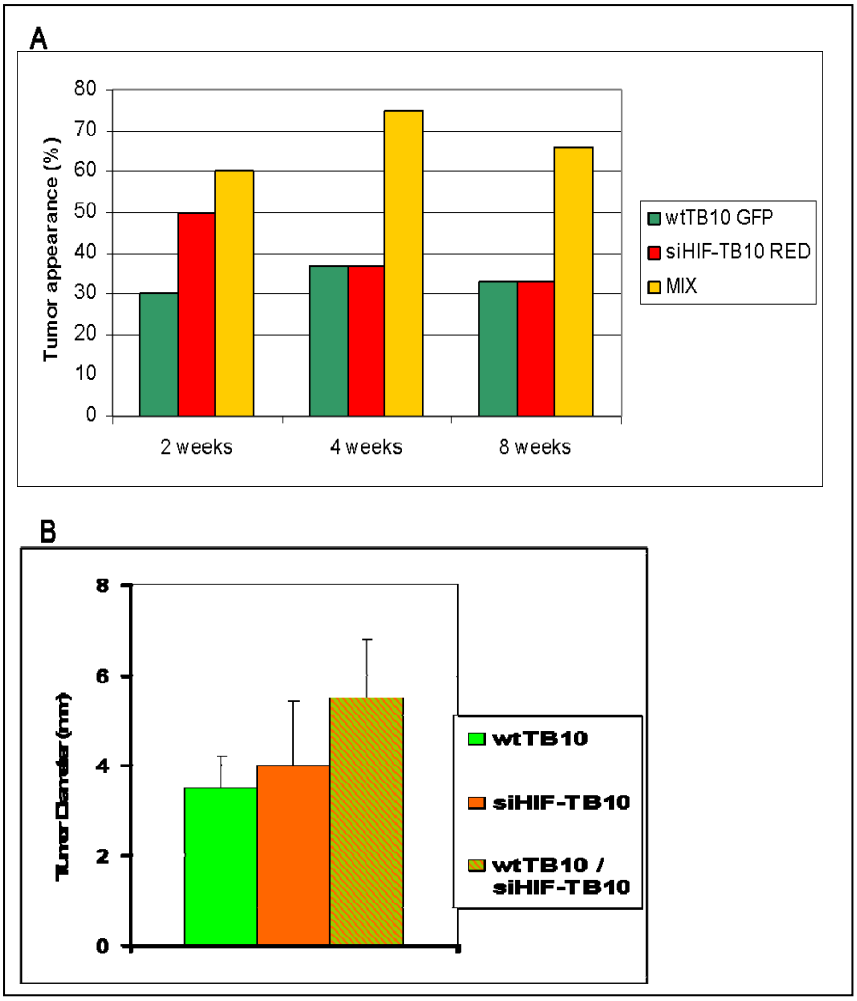

Figure 25: Rate of tumor appearance and volume of tumor xenografts. A: Rate of tumour appearance in single and mixed grafts. Percent of tumorigenicity in experimental groups show an increase of this parameters in mixed tumours. B: Diameters of tumours obtained by injections. After 8 weeks, the mean diameter of the tumour xenografts was significantly greater in the wtTB10/ siHIF-TB10 grafted mice as compared both with the wtTB10 and with the siHIF-TB10 grafted mice ($p<0.05$, Student's *t*-test).

By analysis of tumour sections under fluorescent microscopy, we observed the organization and distribution of the two cell types into the tumour. As mentioned before, each cell group was marked with two different fluorescent proteins. Analysis of the sections obtained by single graft did not evidence differences between the two groups (Figures 26 and 27). In fact, the images showed a homogeneous dissemination of cells into the tumour sections, with no differences in the number of cells *per* section. When we analysed the mixed wtTB10/ siHIF-TB10 xenografts by 2 weeks after grafting, we did not find major differences in the topographical distribution of the EGFP-expressing wtTB10 and the DsRed-expressing siHIF-TB10 cells (Figure 26). By 4 weeks after grafting, however, the central region of the mixed wtTB10/ siHIF-TB10 tumour xenografts was mostly populated by DsRed-expressing siHIF-TB10 (Figure 27). Therefore, our *in vivo* study unexpectedly showed that cografting GBM cells with different levels of HIF-1α expression gives origin to more aggressive tumors as compared to grafting tumor cells with homogeneously high or low HIF-1α expression. In the mixed wtTB10/ siHIF-TB10 cell grafts, the siHIF-TB10 GBM cells not only are rescued but even exhibit a growth advantage in the central region of the tumor.

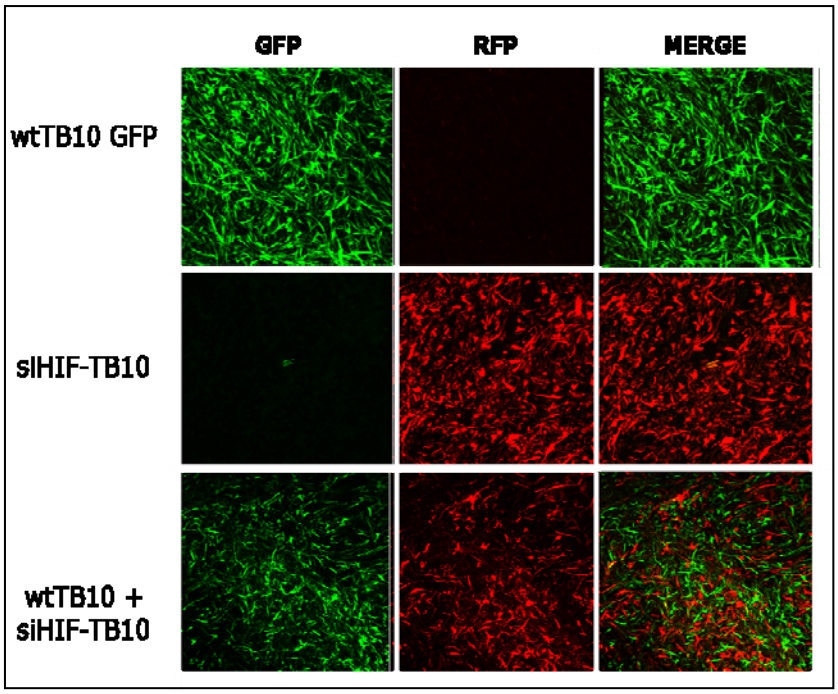

Figure 26: Analysis of tumour sections obtained at two weeks post-injection, by fluorescent microscopy. The images showed a homogeneous dissemination of cells into the tumour sections.

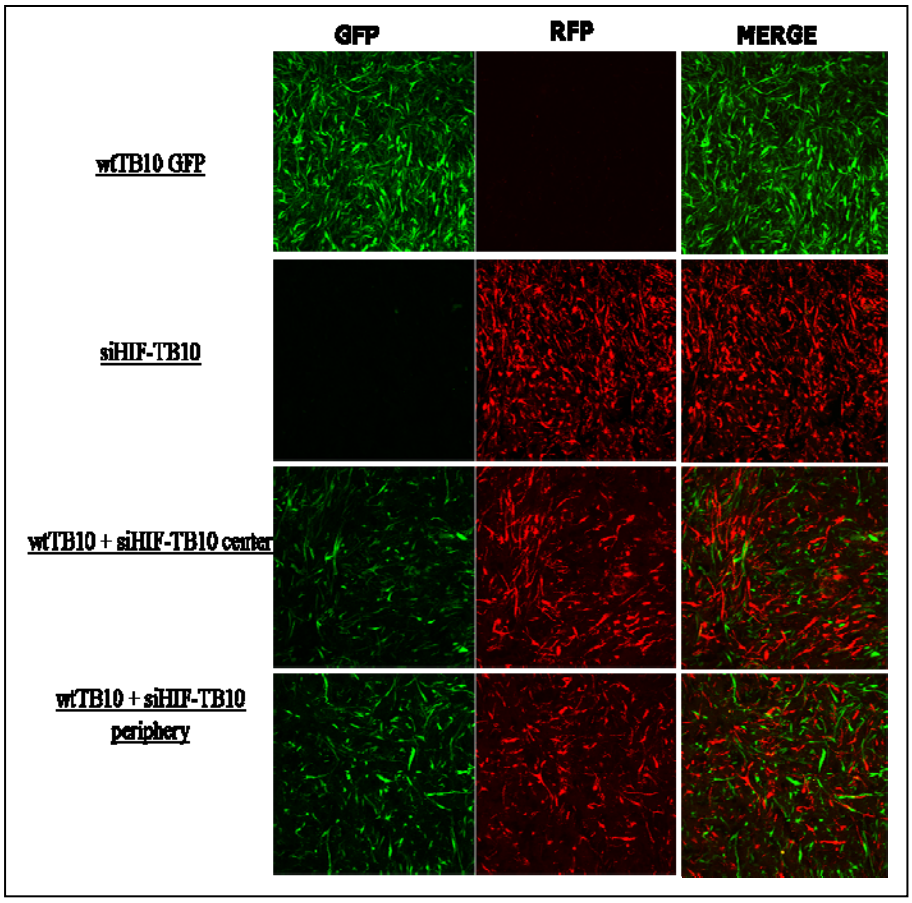

Figure 27: Analysis of tumour sections obtained at four weeks post-injection, by fluorescent microscopy. By 4 weeks after grafting, however, the central region of the mixed wtTB10/ siHIF-TB10 tumour xenografts was mostly populated by DsRed-expressing siHIF-TB10.

DISCUSSION- Part 2

In this study we employed siRNA-mediated down regulation of HIF-1α to produce human GBM cells with an altered response to hypoxia. HIF-1 appears to be the major regulator of TB10 cell transcriptional response to lowered O2 tension while HIF-2 plays only a marginal role. In fact inhibition of HIF-1α is sufficient to prevent transcriptional induction by hypoxia and PHD inhibitors of all the hypoxia-responsive genes that we examined. Furthermore HIF-1α inhibition reduced the basal expression of the same genes in normoxia. Recent work has enlightened a more pervasive function of HIF-1 in cells kept in normoxia than previously thought. In particular, ablation of HIF-1α in primary fibroblasts *in vitro* was shown to promote cellular senescence via a p53 mediated pathway (Welford et al., 2006). Secondly HIF-1 was shown to be an essential regulator of growth factor-stimulated glucose metabolism in normoxia (Lum et al., 2007). We anticipated that HIF-1 would play even a more crucial role inTB10 cells that, in accordance to Warburg's hypothesis, may take profit from a "hypoxic phenotype". Surprisingly a number of metabolic parameters were relatively unaffected by RNAi-mediated down regulation of HIF-1α in spite of the fact that a decrease of HIF-1α expression by about 70%, as in siHIF-TB10 pool, or by about 90%, as in siHIF-TB10 clones #12 and #20, resulted in a congruent reduction in hypoxia-regulated gene expression, both in normoxia and in hypoxia. Thus, there were only minor variations in ATP content (Fig) and reduced glutathione level (Fig). Recent work enlightened an essential role of HIF-1 in promoting cell proliferation via metabolic reprogramming. In particular, suppression of HIF-1α by cre-mediated recombination or by RNA interference promotes glucose utilization in lipid synthesis with a consequent increase in cell size (Lum et al., 2007). We noticed that when grown in standard conditions wtTB10 and siHIF-TB10 cells proliferate at similar rates. It is noteworthy that the experiments described by Lum and collegues, were performed on immortalized bone marrow derived IL-3 dependent cells, on primary cultures of T cells or on NIH 3T3 cells. All these cell types are essentially

untransformed and do not posses those additional alterations that contribute to the cancerous phenotype of glioblastoma cells and that may uncouple cell growth from cell proliferation. Although wtTB10 and siHIF-TB10 cells have the same replication time when grown separately, wtTB10 outgrew siHIF-TB10 cells when co-cultured. Reduction of glucose concentration in the medium exacerbated this difference in replication rate suggesting that siHIF-TB10 may be more dependent on glucose for growth.

Our *in vivo* experiments failed to show significant differences in tumor growth among subcutaneously grafted wtTB10 or siHIF-TB10 cells. Conflicting results are reported in the literature concerning the consequences of HIF-1 inhibition on tumor growth *in vivo*. In a recent study silencing of HIF-1α by RNAi was demonstrated to attenuate human glioma cell growth in xenograft models (Gillespie et al., 2007). Others, using inducible RNA interference, have reported that HIF-1α inhibition may result in a transient reduction of established tumor growth or no effect on tumor growth depending on the tumor cell line (Li et al., 2005). Finally expression of a dominant negative form of HIF-1α in a rat glioma promoted tumor growth possibly by reducing apoptosis in hypoxia (Acker et al., 2005). While in that experimental setting it was not possible to distinguish the relative contribution of HIF-1 and HIF-2 inhibition, HIF-1α-deficient teratomas were shown to grow faster than HIF-1α-positive teratomas (Carmeliet et al., 1998). Such heterogeneity of behaviors in experimental tumors parallels clinical data, therefore elevated HIF-1 and HIF-2 expression was generally found to correlate with poor prognosis, but patients with HIF-1 α -positive nonsmall cell lung carcinomas had a longer survival than HIF-1 α negative patients and expression of HIF α in surgically treated patients with head and neck squamous cell carcinoma was associated with improved disease-free and overall survival (Volm et al., 2000; Beasley et al., 2002). Possibly the most relevant finding of our work is the significant increase in aggressiveness of tumors derived from xenografts of mixed populations of HIF-1 α -positive and HIF-1 α -negative TB10 cells. In an intriguing paper it was shown that even a small number of HIF-1 α -

positive ES cells was able to rescue the growth defect of HIF-1 α -negative ES cells implanted in nude mice (Hopfl et al., 2002). In that experimental setting, differently from what we observe with TB10 cells, teratocarcinomas derived from HIF-1-negative ES cells grew significantly less than those derived from HIF-1 α -positive ES cells. Interestingly HIF-1 α -positive ES cells did not overgrow HIF-1 α -negative ES cells in the mixed tumors. We propose two, not necessarily contradictory, explanations for the increased growth of tumors from mixed populations of HIF-1 α -positive and HIF-1 α -negative TB10 cells. According to the first hypothesis, these tumors grow faster because the two populations colonize different microenviroments. In protracted and extreme hypoxia, HIF-1 induces the synthesis of pro-apoptotic genes, thus siHIF-TB10 cells may be more resistant to hypoxia-induced apoptosis, may survive in oxygen-poor niches from where wtTB10 cells are excluded. In well vascularized regions, wtTB10 and siHIF-TB10 cells will grow at a similar rate while, at a certain distance from blood vessels where nutrients may become limiting, wild type cells may have a growth advantage. Fluorescence microscopy examination of the tumors at later times appears to corroborate this hypothesis, however, at early times, the two populations of wtTB10 and siHIF-TB10 cells appear well interspersed and homogenously distributed within the tumor mass. According to the second hypothesis, wtTB10 and siHIF-TB10 cells actually cooperate, so that each population gains a growth advantage from the presence of the other one. Koukourakis et al. suggested that cancer cells with an "anaerobic metabolism" (Koukourakis et al., 2006) and tumor associated stroma cells, which display an "aerobic metabolism", functionally cooperate by exchanging metabolites and buffering potentially toxic products. This metabolic cooperation may as well occur between wtTB10 and siHIF-TB10 cells that differ in their glucose utilization because of different HIF-1 activities. Cooperation among tumor cells with different genotypes has been proposed as a major driving force in tumor progression (Axelrod et al., 2006) and suggests that the hallmarks of cancer (Hanahan et al., 2000) are not necessarily cell autonomous mutations that each cell within the tumor must acquire, but may

be a resource of the tumor as a whole. Our findings suggest that caution should be used in evaluating anticancer therapies based on inhibition of HIF functions. Should a hypothetical anti-HIF drug reach only a subpopulation within a tumor mass, it may promote, instead of hamper, cancer growth.

REFERENCES

Akeno N, Czyzyk-Krzeska MF, Gross TS, Clemens TL. Hypoxia induces vascular endothelial growth factor gene transcription in human osteoblast-like cells through the hypoxia-inducible factor-2alpha. *Endocrinology*. (2001) **142**: 959-62

Acker T, Diez-Juan A, Aragones J, Tjwa M, Brusselmans K, Moons L, Fukumura D, Moreno-Murciano MP, Herbert JM, Burger A, Riedel J, Elvert G, Flamme I, Maxwell PH, Collen D, Dewerchin M, Jain RK, Plate KH, and Carmeliet P. Genetic evidence for a tumor suppressor role of HIF-2alpha. *Cancer Cell* (2005) **8**: 131-141

Artandi SE, Alson S, Tietze MK, Sharpless NE, Ye S, Greenberg RA, Castrillon DH, Horner JW, Weiler SR, Carrasco RD, DePinho RA. Constitutive telomerase expression promotes mammary carcinomas in aging mice. *Proc Natl Acad Sci U S A.* (2002) **99**:8191-6

Axelrod R, Axelrod DE, and Pienta KJ. Evolution of cooperation among tumor cells. *Proc.Natl.Acad.Sci.U.S.A* (2006) **103**: 13474-13479

Bardos JI & Ashcroft M. Negative and positive regulation of HIF-1: a complex network. *Biochimica et Biophysica Acta* (2005) **1755**: 107–120

Beasley NJ, Leek R, Alam M, Turley H, Cox GJ, Gatter K, Millard P, Fuggle S, and Harris AL. Hypoxia-inducible factors HIF-1alpha and HIF-2alpha in head and neck cancer: relationship to tumor biology and treatment outcome in surgically resected patients. *Cancer Res* (2002) **62**: 2493-2497

Beliveau A, Bassett E, Lo AT, Garbe J, Rubio MA, Bissell MJ, Campisi J, Yaswen P. p53-dependent integration of telomere and growth factor deprivation signals. *Proc Natl Acad Sci U S A.* (2007) **104**:4431-6

Berra E, Benizri E, Ginouves A, Volmat V, Roux D & Pouyssegur J. HIF prolyl-hydroxylase 2 is the key oxygen sensor setting low steady-state levels of HIF-1alpha in normoxia. *EMBO Journal* (2003) **22**: 4082–4090

Bilaud T, Brun C, Ancelin K, Koering CE, Laroche T, Gilson E. Telomeric localization of TRF2, a novel human telobox protein. *Nat. Genet*. (1997) **17**:236–239

Birlik B, Canda S, Ozer E. Tumour vascularity is of prognostic significance in adult, but not paediatric astrocytomas. *Neuropathol Appl Neurobiol.* (2006) **32**:532-8

Blasco MA, Rizen M, Greider CW, Hanahan D. Differential regulation of telomerase activity and telomerase RNA during multi-stage tumorigenesis. *Nat Genet.* (1996) **12**:200-4

Blum R, Jacob-Hirsch J, Amariglio N, Rechavi G, Kloog Y. Ras inhibition in glioblastoma down-regulates hypoxia-inducible factor-1alpha, causing glycolysis shutdown and cell death. *Cancer Res*. (2005) **65**:999-1006

Bruick RK. Expression of the gene encoding the proapoptotic Nip3 protein is induced by hypoxia. *Proc Natl Acad Sci U S A*. (2000) **97**: 9082-7

Bruick RK & McKnight SL. A conserved family of prolyl-4-hydroxylases that modify HIF. *Science* (2001) **294**: 1337–1340

Canela A, Martín-Caballero J, Flores JM, Blasco MA. Constitutive expression of tert in thymocytes leads to increased incidence and dissemination of T-cell lymphoma in Lck-Tert mice. *Mol Cell Biol.* (2004) **24**:4275-93

Cayuela ML, Flores JM, Blasco MA. The telomerase RNA component Terc is required for the tumour-promoting effects of Tert overexpression. *EMBO Rep.* (2005) **6**:268-74

Carmeliet P, Dor Y, Herbert JM, Fukumura D, Brusselmans K, Dewerchin M, Neeman M, Bono F, Abramovitch R, Maxwell P, Koch CJ, Ratcliffe P, Moons L, Jain RK, Collen D, Keshert E. Role of HIF-1alpha in hypoxia-mediated apoptosis, cell proliferation and tumour angiogenesis. *Nature* (1998) **394**: 485-90

Chen C, Pore N, Behrooz A, Ismail-Beigi F, Maity A. Regulation of glut1 mRNA by hypoxia-inducible factor-1. Interaction between H-ras and hypoxia. *J Biol Chem.* (2001) **276**: 9519-25

Chomczynski, P. and Sacchi, N. Single-step method of RNA isolation by acid guanidinium thiocyanate-phenol-chloroform extraction. *Anal. Biochem.* (1987) **162**: 156-159

Cockman ME, Masson N, Mole DR, Jaakkola P, Chang GW, Clifford SC, Maher ER, Pugh CW, Ratcliffe PJ & Maxwell PH. Hypoxia inducible factor-alpha binding and ubiquitylation by the von Hippel-Lindau tumor suppressor protein. *Journal of Biological Chemistry* (2000) **275**: 25733–25741

Compernolle V, Brusselmans K, Acker T, Hoet P, Tjwa M, Beck H, Plaisance S, Dor Y, Keshet E, Lupu F, Nemery B, Dewerchin M, Van Veldhoven P, Plate K,

Moons L, Collen D, Carmeliet P. Loss of HIF-2alpha and inhibition of VEGF impair fetal lung maturation, whereas treatment with VEGF prevents fatal respiratory distress in premature mice. *Nat Med.* (2002) **8**: 702-10

Cooper GM and Hausman RE. *The Cell* (2007) Chapter 6

Counter CM, Meyerson M, Eaton EN, Weinberg RA. The catalytic subunit of yeast telomerase. *Proc Natl Acad Sci U S A.* (1997) **94**:9202-7

Counter CM, Meyerson M, Eaton EN, Ellisen LW, Caddle SD, Haber DA, Weinberg RA. Telomerase activity is restored in human cells by ectopic expression of hTERT (hEST2), the catalytic subunit of telomerase. *Oncogene.* (1998) **16**:1217-22

Covello KL, Kehler J, Yu H, Gordan JD, Arsham AM, Hu CJ, Labosky PA, Simon MC, Keith B. HIF-2alpha regulates Oct-4: effects of hypoxia on stem cell function, embryonic development, and tumor growth. *Genes Dev.* (2006) **20**: 557-70

Dagarag M, Evazyan T, Rao N, Effros RB. Genetic manipulation of telomerase in HIV-specific CD8+ T cells: enhanced antiviral functions accompany the increased proliferative potential and telomere length stabilization. *J Immunol.* (2004) **173**:6303-11

Dang CV, Semenza GL. Oncogenic alterations of metabolism. *Trends Biochem Sci.* (1999) **24**: 68-72. Review

de Lange. Shelterin: the protein complex that shapes and safeguards human telomeres. *Genes Dev*. (2005) **19**:2100–2110

de Lange T, Shiue L, Myers RM, Cox DR, Naylor SL, Killery AM, Varmus HE. Structure and variability of human chromosome ends. *Mol. Cell. Biol*. (1990) **10**:518–527

Donehower LA. Does p53 affect organismal aging? *J Cell Physiol.* (2002) **192**:23-33. Review

Dull T, Zufferey R, Kelly M, Mandel RJ, Nguyen M, Trono D, Naldini L. A third-generation lentivirus vector with a conditional packaging system.*J Virol* (1998) **72**:8463-71

Elstrom RL, Bauer DE, Buzzai M, Karnauskas R, Harris MH, Plas DR, Zhuang H, Cinalli RM, Alavi A, Rudin CM, Thompson CB. Akt stimulates aerobic glycolysis in cancer cells. *Cancer Res*. (2004) **64**:3892-9

Ema M, Taya S, Yokotani N, Sogawa K, Matsuda Y & Fujii-Kuriyama Y. A novel bHLH-PAS factor with close sequence similarity to hypoxia-inducible factor 1alpha regulates the VEGF expression and is potentially involved in lung and vascular development. *PNAS* (1997) **94**: 4273–4278

Ema M, Hirota K, Mimura J, Abe H, Yodoi J, Sogawa K, Poellinger L & Fujii-Kuriyama Y. Molecular mechanisms of transcription activation by HLF and HIF1alpha in response to hypoxia: their stabilization and redox signal-induced interaction with CBP/p300. *EMBO Journal* (1999) **18**: 1905–1914

Epstein AC, Gleadle JM, McNeill LA, Hewitson KS, O'Rourke J, Mole DR, Mukherji M, Metzen E, Wilson MI, Dhanda A *et al. C. elegans* EGL-9 and mammalian homologs define a family of dioxygenases that regulate HIF by prolyl hydroxylation. *Cell* (2001) **107**: 43–54

Falchetti ML, Levi A, Molinari P, Verna R, D'Ambrosio E**.** Increased sensitivity and reproducibility of TRAP assay by avoiding direct primers interaction. *Nucleic Acids Res.* (1998) **26**: 862-863

Falchetti ML, Falcone G, D'Ambrosio E, Verna R, Alema S, Levi A. Induction of telomerase activity in v-myc-transformed avian cells. *Oncogene*. (1999a) **18**: 1515-9

Falchetti ML, Pallini R, Larocca LM, Verna R, D'Ambrosio E. Telomerase expression in intracranial tumours: prognostic potential for malignant gliomas and meningiomas. *J Clin Pathol*. (1999b) **52**: 234-6

Falchetti ML, Pallini R, D'Ambrosio E, Pierconti F, Martini M, Cimino-Reale G, Verna R, Maira G, Larocca LM. *In situ* detection of telomerase catalytic subunit mRNA in glioblastoma multiforme. *Int. J. Cancer* (2000) **88**: 895-901

Falchetti ML, Pierconti F, Casalbore P, Maggiano N, Levi A, Larocca LM, Pallini R. Glioblastoma induces vascular endothelial cells to express telomerase in vitro. *Cancer Res* (2003) **63**:3750-4

Falchetti ML, Mongiardi MP, Fiorenzo P, Petrucci G, Pierconti F, D'Agnano I, D'Alessandris G, Alessandri G, Gelati M, Ricci-Vitiani L, Maira G, Larocca LM, Levi A and Pallini R. Inhibition of telomerase in the endothelial cells disrupts tumor angiogenesis in glioblastoma xenografts. *Int. J. Cancer* (2008) **122**:1236-42

Fantin VR, St-Pierre J, Leder P. Attenuation of LDH-A expression uncovers a link between glycolysis, mitochondrial physiology, and tumor maintenance. *Cancer Cell* (2006) **9**:425-34

Folkman J. Angiogenesis: an organizing principle for drug discovery? *Nat Rev Drug Discov* (2007) **6**:273-86. Review

Franco S, Segura I, Riese HH, Blasco MA. Decreased B16F10 melanoma growth and impaired vascularization in telomerase-deficient mice with critically short telomeres. *Cancer Res*. (2002) **62**: 552-9

Freedman DA, Folkman J. Maintenance of G1 checkpoint controls in telomerase-immortalized endothelial cells. *Cell Cycle* (2004) **3**: 811-6

Gillespie, D. L., Whang, K., Ragel, B. T., Flynn, J. R., Kelly, D. A., and Jensen, R. L. Silencing of hypoxia inducible factor-1alpha by RNA interference attenuates human glioma cell growth in vivo. *Clin.Cancer Res* (2007) **13**: 2441-2448

Gilley D, Blackburn EH. Specific RNA residue interactions required for enzymatic functions of Tetrahymena telomerase. *Mol Cell Biol*. (1996) **16**:66-75

González-Suárez E, Geserick C, Flores JM, Blasco MA. Antagonistic effects of telomerase on cancer and aging in K5-mTert transgenic mice. *Oncogene*. (2005) **24**:2256-70

Gonzalo S, Jaco I, Fraga MF, Chen T, Li E, Esteller M, Blasco MA. DNA methyltransferases control telomere length and telomere recombination in mammalian cells. *Nat. Cell Biol*. (2006) **8**:416–424

Greider CW, Blackburn EH. A telomeric sequence in the RNA of Tetrahymena telomerase required for telomere repeat synthesis. *Nature* (1989) **337**:331-7

Greider CW, Blackburn EH. Identification of a specific telomere terminal transferase activity in Tetrahymena extracts. *Cell* (1985) **43**:405–413

Griffith J, Bianchi A, de Lange T. TRF1 promotes parallel pairing of telomeric tracts *in vitro*. *J. Mol. Biol*. (1998) **278**:79–88

Griffith JD, Comeau L, Rosenfield S, Stansel RM, Bianchi A, Moss H, de Lange T. Mammalian telomeres end in a large duplex loop. *Cell* (1999) **97**:503–514

Gu YZ, Moran SM, Hogenesch JB, Wartman L & Bradfield CA. Molecular characterization and chromosomal localization of a third alpha-class hypoxia inducible factor subunit, HIF3alpha. *Gene Expression* (1998) **7**: 205–213

Hahn WC, Dessain SK, Brooks MW, King JE, Elenbaas B, Sabatini DM, DeCaprio JA, Weinberg RA. Enumeration of the simian virus 40 early region elements necessary for human cell transformation. *Mol Cell Biol*. (2002) **22**: 2111-23. Erratum in: *Mol Cell Biol* (2002) **22**: 3562

Hanahan D and Weinberg RA. The hallmarks of cancer. *Cell* (2000) **100**: 57-70

Hammond PW, Lively TN, Cech TR. The anchor site of telomerase from Euplotes aediculatus revealed by photo-cross-linking to single- and double-stranded DNA primers. *Mol Cell Biol.* (1997) **17**:296-308

Harley CB, Futcher AB, Greider CW. Telomeres shorten during ageing of human fibroblasts. *Nature* (1990) **345**:458–460

Hopfl G, Wenger RH, Ziegler U, Stallmach T, Gardelle O, Achermann R, Wergin M, Kaser-Hotz B, Saunders HM, Williams KJ, Stratford IJ, Gassmann M, and Desbaillets I. Rescue of hypoxia-inducible factor-1alpha-deficient tumor growth by wild-type cells is independent of vascular endothelial growth factor. *Cancer Res* (2002) **62**: 2962-2970

Horsman MR, Siemann DW. Pathophysiologic effects of vascular-targeting agents and the implications for combination with conventional therapies. *Cancer Res.* (2006) **66**:11520-39. Review

Huang LE, Gu J, Schau M & Bunn HF. Regulation of hypoxia-inducible factor 1alpha is mediated by an O_2-dependent degradation domain via the ubiquitin-proteasome pathway. *PNAS* (1998) **95**: 7987–7992

Iliopoulos O, Levy AP, Jiang C, Kaelin WG Jr, Goldberg MA. Negative regulation of hypoxia-inducible genes by the von Hippel-Lindau protein. *Proc Natl Acad Sci U S A.*(1996) **93**:10595-9

Ivan M, Kondo K, Yang H, Kim W, Valiando J, Ohh M, Salic A, Asara JM, Lane WS & Kaelin WG, Jr. HIFalpha targeted for VHL-mediated destruction by proline hydroxylation: implications for O_2 sensing. *Science* (2001) **292**: 464–468

Iwai K, Yamanaka K, Kamura T, Minato N, Conaway RC, Conaway JW, Klausner RD & Pause A. Identification of the von Hippellindau tumor-suppressor protein as part of an active E3 ubiquitin ligase complex. *PNAS* (1999) **96**: 12436–12441

Jaakkola P, Mole DR, Tian YM, Wilson MI, Gielbert J, Gaskell SJ, Kriegsheim A, Hebestreit HF, Mukherji M, Schofield CJ *et al.* Targeting of HIF-alpha to the von

Hippel-Lindau ubiquitylation complex by O_2-regulated prolyl hydroxylation. *Science* (2001) **292**: 468–472

Jeong JW, Bae MK, Ahn MY, Kim SH, Sohn TK, Bae MH, Yoo MA, Song EJ, Lee KJ & Kim KW. Regulation and destabilization of HIF-1alpha by ARD1-mediated acetylation. *Cell* (2002) **111**: 709–720

Jiang BH, Rue E, Wang GL, Roe R & Semenza GL. Dimerization, DNA binding, and transactivation properties of hypoxia-inducible factor 1. *Journal of Biological Chemistry* (1996) **271**: 17771–17778

Jiang BH, Zheng JZ, Leung SW, Roe R & Semenza GL. Transactivation and inhibitory domains of hypoxia-inducible factor 1alpha. Modulation of transcriptional activity by oxygen tension. *Journal of Biological Chemistry* (1997) **272**: 19253–19260

Kamura T, Sato S, Iwai K, Czyzyk-Krzeska M, Conaway RC & Conaway JW. Activation of HIF1alpha ubiquitination by a reconstituted von Hippel-Lindau (VHL) tumor suppressor complex. *PNAS* (2000) **97**: 10430–10435

Kaur B, Tan C, Brat DJ, Post DE, Van Meir EG. Genetic and hypoxic regulation of angiogenesis in gliomas. *J Neurooncol.* (2004) **70**:229-43 Review

Kivirikko KI & Myllyharju J. Prolyl 4-hydroxylases and their protein disulfide isomerase subunit. *Matrix Biology* (1998) **16**: 357–368

Kohlstaedt LA, Wang J, Friedman JM, Rice PA, Steitz TA. Crystal structure at 3.5 A resolution of HIV-1 reverse transcriptase complexed with an inhibitor. *Science* (1992) **256**:1783-90

Koukourakis MI, Giatromanolaki A, Sivridis E, Gatter KC, Harris AL; Tumor and Angiogenesis Research Group. Pyruvate dehydrogenase and pyruvate dehydrogenase kinase expression in non small cell lung cancer and tumor-associated stroma. *Neoplasia.* (2005) **7**:1-6

Koukourakis MI, Giatromanolaki A, Harris AL, and Sivridis E. Comparison of metabolic pathways between cancer cells and stromal cells in colorectal carcinomas: a metabolic survival role for tumor-associated stroma. *Cancer Res* (2006) **66**: 632-637

Krishnamachary B, Berg-Dixon S, Kelly B, Agani F, Feldser D, Ferreira G, Iyer N, LaRusch J, Pak B, Taghavi P, Semenza GL. Regulation of colon carcinoma cell invasion by hypoxia-inducible factor 1. *Cancer Res.* (2003) **63**: 1138-43

Larder BA, Purifoy DJ, Powell KL, Darby G. Site-specific mutagenesis of AIDS virus reverse transcriptase. *Nature* (1987) **327**:716-7

Laughner E, Taghavi P, Chiles K, Mahon PC, Semenza GL. HER2 (neu) signaling increases the rate of hypoxia-inducible factor 1alpha (HIF-1alpha) synthesis: novel mechanism for HIF-1-mediated vascular endothelial growth factor expression. *Mol Cell Biol* (2001)**21**:3995-4004

Leon SP, Folkerth RD, Black PM. Microvessel density is a prognostic indicator for patients with astroglial brain tumors. *Cancer* (1996) **77**:362-72

Li H, Ko HP & Whitlock JP. Induction of phosphoglycerate kinase 1 gene expression by hypoxia. Roles of Arnt and HIF1alpha. *Journal of Biological Chemistry* (1996) **271**: 21262–21267

Li L, Lin, X, Staver M, Shoemaker A, Semizarov D, Fesik SW, and Shen Y. Evaluating hypoxia-inducible factor-1alpha as a cancer therapeutic target via inducible RNA interference in vivo. *Cancer Res* (2005) **65**: 7249-7258

Li S, Rosenberg JE, Donjacour AA, Botchkina IL, Hom YK, Cunha GR, Blackburn EH. Rapid inhibition of cancer cell growth induced by lentiviral delivery and expression of mutant-template telomerase RNA and anti-telomerase short-interfering RNA. *Canc. Res*. (2004) **64**: 4833-40

Li S, Crothers J, Haqq CM, Blackburn EH. Cellular and gene expression responses involved in the rapid growth inhibition of human cancer cells by RNA interference-mediated depletion of telomerase RNA. *J Biol. Chem*. (2005) **280**:23709-17

Ligon KL, Alberta JA, Kho AT, Weiss J, Kwaan MR, Nutt CL, Louis DN, Stiles CD, Rowitch DH. *J Neuropathol Exp Neurol* (2004) **63**: 499-509

Lingner J, Cech TR. Purification of telomerase from Euplotes aediculatus: requirement of a primer 3' overhang. *Proc Natl Acad Sci U S A*. (1996) **93**:10712-7

Lisztwan J, Imbert G, Wirbelauer C, Gstaiger M & Krek W. The von Hippel-Lindau tumor suppressor protein is a component of an E3 ubiquitin-protein ligase activity. *Genes & Development* (1999) **13**: 1822–1833

Louis DN, Ohgaki H, Wiestler OD, Cavenee WK, Burger PC, Jouvet A, Scheithauer BW, Kleihues P. The 2007 WHO classification of tumors of the central nervous system. *Acta Neuropathol* (2007) **114**:97-109 Review

Lu H, Forbes RA, Verma A. Hypoxia-inducible factor 1 activation by aerobic glycolysis implicates the Warburg effect in carcinogenesis. *J Biol Chem.* (2002) **277**: 23111-5

Lum, J. J., Bui, T., Gruber, M., Gordan, J. D., DeBerardinis, R. J., Covello, K. L., Simon, M. C., and Thompson, C. B. The transcription factor HIF-1alpha plays a critical role in the growth factor-dependent regulation of both aerobic and anaerobic glycolysis. *Genes Dev.* (2007) **21**: 1037-1049

Lundblad V, Szostak JW. A mutant with a defect in telomere elongation leads to senescence in yeast. *Cell* (1989) **57**:633-43

Maher EA, Brennan C, Wen PY, Durso L, Ligon KL, Richardson A, Khatry D, Feng B, Sinha R, Louis DN, Quackenbush J, Black PM, Chin L, DePinho RA. Marked genomic differences characterize primary and secondary glioblastoma subtypes and identify two distinct molecular and clinical secondary glioblastoma entities. *Cancer Res.* (2006) **66**:11502-13

Makarov VL, Hirose Y, Langmore JP. Long G tails at both ends of human chromosomes suggest a C strand degradation mechanism for telomere shortening. *Cell* (1997) **88**:657–666

Makino Y, Kanopka A, Wilson WJ, Tanaka H & Poellinger L. Inhibitory PAS domain protein (IPAS) is a hypoxia-inducible splicing variant of the hypoxia-inducible factor-3alpha locus. *Journal of Biological Chemistry* (2002) **277**: 32405–32408

Manalo DJ, Rowan A, Lavoie T, Natarajan L, Kelly BD, Ye SQ, Garcia JG, Semenza GL. Transcriptional

regulation of vascular endothelial cell responses to hypoxia by HIF-1. *Blood* (2005) **105**:659-69

Masson N, Willam C, Maxwell PH, Pugh CW & Ratcliffe PJ. Independent function of two destruction domains in hypoxia-inducible factor-alpha chains activated by prolyl hydroxylation. *EMBO Journal* (2001) **20**: 5197–5206

Masutomi K, Yu EY, Khurts S, Ben-Porath I, et al. Telomerase maintains telomere structure in normal human cells. *Cell* (2003) **114**: 241-253

Masutomi K, Possemato R, Wong JM, Currier JL,Tothova Z, Manola JB, Ganesan S, Lansdorp P, Collins K e Hahn WC. The telomerase riverse transcriptase regulates chromatin state and DNA damage responses. *PNAS* (2005) **102**:8222-8227

Metzen E, Berchner-Pfannschmidt U, Stengel P, Marxsen JH, Stolze I, Klinger M, Huang WQ, Wotzlaw C, Hellwig-Burgel T, Jelkmann W *et al.* Intracellular localisation of human HIF-1 alpha hydroxylases: implications for oxygen sensing. *Journal of Cell Science* (2003) **116**: 1319–1326

Morin GB. The human telomere terminal transferase enzyme is a ribonucleoprotein that synthesizes TTAGGG repeats. *Cell* (1989) **59**:521-9

Morin GB. Recognition of a chromosome truncation site associated with alpha-thalassaemia by human telomerase. *Nature* (1991) **353**:454-6

Moyzis RK, Buckingham JM, Cram LS, Dani M, Deaven LL, Jones MD, Meyne J, Ratliff RL, Wu JR A highly conserved repetitive DNA sequence, (TTAGGG) n, present at the telomeres of human chromosomes. *Proc. Natl. Acad. Sci. USA* (1988) **85**:6622–6626

Murasawa S, Llevadot J, Silver M, Isner JM, Losordo DW, Asahara T. Constitutive human telomerase reverse transcriptase expression enhances regenerative properties of endothelial progenitor cells. *Circulation* (2002) **106**:1133-9

Murray-Rust TA, Oldham NJ, Hewitson KS & Schofield CJ. Purified recombinant hARD1 does not catalyse acetylation of Lys532 of HIF-1alpha fragments *in vitro. FEBS Letters* (2006) **580**: 1911–1918

Nakamura TM, Morin GB, Chapman KB, Weinrich SL, Andrews WH, Lingner J, Harley CB, Cech TR. Telomerase catalytic subunit homologs from fission yeast and human. *Science* (1997) **277**:955-9

Nikitina T, Woodcock CL. Closed chromatin loops at the ends of chromosomes. *J. Cell Biol*. (2004) **166**:161–165

Oh H, Taffet GE, Youker KA, Entman ML, Overbeek PA, Michael LH, Schneider MD Telomerase reverse transcriptase promotes cardiac muscle cell proliferation, hypertrophy, and survival. *Proc Natl Acad Sci U S A* (2001) **98**:10308-13

Ohh M, Park CW, Ivan M, Hoffman MA, Kim TY, Huang LE, Pavletich N, Chau V & Kaelin WG. Ubiquitination of hypoxia-inducible factor requires direct binding to the beta-domain of the von Hippel-Lindau protein. *Nature Cell Biology* (2000) **2**: 423–427

Olovnikov AM. A theory of marginotomy. The incomplete copying of template margin in enzymic synthesis of polynucleotides and biological significance of the phenomenon. *J. Theor. Biol*. (1973) **41**:181–190

Pallini R, Pierconti F, Falchetti ML, D'Arcangelo D, Fernandez E, Maira G, D'Ambrosio E, Larocca LM.

Evidence for telomerase involvement in the angiogenesis of astrocytic tumors: expression of human telomerase reverse transcriptase messenger RNA by vascular endothelial cells. *J Neurosurg*. (2001) **94**: 961-71

Papandreou I, Cairns RA, Fontana L, Lim AL, Denko NC.HIF-1 mediates adaptation to hypoxia by actively downregulating mitochondrial oxygen consumption. *Cell Metab.* (2006) **3**:187-97

Phung TL, Ziv K, Dabydeen D, Eyiah-Mensah G, Riveros M, Perruzzi C, Sun J, Monahan-Earley RA, Shiojima I, Nagy JA, Lin MI, Walsh K, Dvorak AM, Briscoe DM, Neeman M, Sessa WC, Dvorak HF, Benjamin LE. Pathological angiogenesis is induced by sustained Akt signaling and inhibited by rapamycin. *Cancer Cell* (2006) **10**:159-70

Pugh CW, O'Rourke JF, Nagao M, Gleadle JM & Ratcliffe PJ. Activation of hypoxia-inducible factor-1; definition of regulatory domains within the alpha subunit. *Journal of Biological Chemistry* (1997) **272**: 11205–11214

Ravi R, Mookerjee B, Bhujwalla ZM, Sutter CH, Artemov D, Zeng Q, Dillehay LE, Madan A, Semenza GL, Bedi A. Regulation of tumor angiogenesis by p53-induced degradation of hypoxia-inducible factor 1alpha. *Genes Dev* (2000) **14**:34-44

Riethman H, Ambrosini A, Paul S. Human subtelomere structure and variation. *Chromosome Res*. (2005) **13**:505–515

Rolfs A, Kvietikova I, Gassmann M, Wenger RH. Oxygen-regulated transferrin expression is mediated by hypoxia-inducible factor-1. *J Biol Chem.* (1997) **272**:20055-62

Röth A, Baerlocher GM, Schertzer M, Chavez E, Dührsen U, Lansdorp PM. Telomere loss, senescence, and genetic instability in CD4+ T lymphocytes overexpressing hTERT. *Blood* (2005) **106**:43-50

Rubelj I, Vondracek Z. Stochastic mechanism of cellular aging – abrupt telomere shortening as a model for stochastic nature of cellular aging. *J. Theor. Biol*. (1999) **197**:425–438

Sarin KY, Cheung P, Gilison D, Lee E, Tennen RI, Wang E, Artandi MK, Oro AE, Artandi SE. Conditional telomerase induction causes proliferation of hair follicle stem cells. *Nature* (2005) **436**:1048-52

Seagroves TN, Ryan HE, Lu H, Wouters BG, Knapp M, Thibault P, Laderoute K, Johnson RS. Transcription factor HIF-1 is a necessary mediator of the pasteur effect in mammalian cells. *Mol Cell Biol.* (2001) **21**: 3436-44

Semenza GL, Nejfelt MK, Chi SM, Antonarakis SE. Hypoxia-inducible nuclear factors bind to an enhancer element located 3' to the human erythropoietin gene. *Proc Natl Acad Sci U S A.* (1991) **88**:5680-4

Semenza GL. Targeting HIF-1 for cancer therapy. *Nat Rev Cancer.* (2003) **3**: 721-32. Review

Shchors K, Shchors E, Rostker F, Lawlor ER, Brown-Swigart L, Evan GI. The Myc-dependent angiogenic switch in tumors is mediated by interleukin 1beta. *Genes Dev*. (2006) **20**:2527-38

Smith LL, Coller HA, Roberts JM. Telomerase modulates expression of growth-controlling genes and enhances cell proliferation. *Nat Cell Biol.* (2003) **5**: 474-9

Stewart SA, Ben-Porath I, Carey VJ, O'Connor BF, Hahn WC, Weinberg RA. Erosion of the telomeric single-strand overhang at replicative senescence. *Nat Genet*. (2003) **33**: 492-6.

Stiver SI, Tan X, Brown LF, Hedley-Whyte ET, Dvorak HF. VEGF-A angiogenesis induces a stable neovasculature in adult murine brain. *J Neuropathol Exp Neurol.* (2004) **63**:841-55

Tabori U, Nanda S, Druker H, Lees J, Malkin D. Younger age of cancer initiation is associated with shorter telomere length in Li-Fraumeni syndrome. *Cancer Res.* (2007) **67**:1415-8

Talks KL, Turley H, Gatter KC, Maxwell PH, Pugh CW, Ratcliffe PJ, Harris AL. The expression and distribution of the hypoxia-inducible factors HIF-1alpha and HIF-2alpha in normal human tissues, cancers, and tumor-associated macrophages. *Am J Pathol.* (2000) **157**: 411-21

Tanimoto K, Makino Y, Pereira T & Poellinger L. Mechanism of regulation of the hypoxia-inducible factor-1 alpha by the von Hippel-Lindau tumor suppressor protein. *EMBO Journal* (2000) **19**: 4298–4309

Tian H, McKnight SL & Russell DW. Endothelial PAS domain protein 1 (EPAS1), a transcription factor selectively expressed in endothelial cells. *Genes & Development* (1997) **11**: 72–82

Vogel J, Gehrig M, Kuschinsky W, Marti HH. Massive inborn angiogenesis in the brain scarcely raises cerebral blood flow. *J Cereb Blood Flow Metab.* (2004) **24**:849-59

Volm M, Koomägi R. Hypoxia-inducible factor (HIF-1) and its relationship to apoptosis and proliferation in lung cancer. *Anticancer Res.* (2000) **20**: 1527-33

Wang GL, Jiang BH, Rue EA & Semenza GL. Hypoxia-inducible factor 1 is a basic-helix-loop-helix-PAS heterodimer regulated by cellular O_2 tension. *PNAS* (1995) **92**: 5510–5514

Warburg O. On respiratory impairment in cancer cells. *Science*. (1956) **124**:269-70

Watnick RS, Cheng YN, Rangarajan A, Ince TA, Weinberg RA. Ras modulates Myc activity to repress thrombospondin-1 expression and increase tumor angiogenesis. *Cancer Cell* (2003) **3**:219-31

Welford, S. M., Bedogni, B., Gradin, K., Poellinger, L., Broome, P. M., and Giaccia, A. J. HIF1alpha delays premature senescence through the activation of MIF. *Genes Dev* (2006)**20**: 3366-3371

Weinrich SL, Pruzan R, Ma L, Ouellette M, Tesmer VM, Holt SE, Bodnar AG, Lichtsteiner S, Kim NW, Trager JB, Taylor RD, Carlos R, Andrews WH, Wright WE, Shay JW, Harley CB, Morin GB. Reconstitution of human telomerase with the template RNA component hTR and the catalytic protein subunit hTRT. *Nat Genet.* (1997) **17**:498-502

Welsh SJ, Bellamy WT, Briehl MM & Powis G. The redox protein thioredoxin-1 (Trx-1) increases hypoxia-inducible factor 1alpha protein expression: Trx-1 over-expression results in increased vascular endothelial growth factor production and enhanced tumor angiogenesis. *Cancer Research* (2002) **62**: 5089–5095

Wenger RH.Cellular adaptation to hypoxia: O2-sensing protein hydroxylases, hypoxia-inducible transcription factors, and O2-regulated gene expression. *FASEB J.* (2002) **16**: 1151-62. Review

Wu KJ, Grandori C, Amacker M, Simon-Vermot N, Polack A, Lingner J, Dalla-Favera R. Direct activation of TERT transcription by c-MYC. *Nat Genet.* (1999) **21**: 220-4

Yang J, Nagavarapu U, Relloma K, Sjaastad MD, Moss WC, Passaniti A, Herron GS. Telomerized human microvasculature is functional in vivo. *Nat Biotechnol.* (2001) **19**: 219-24

Yu GL, Bradley JD, Attardi LD, Blackburn EH. In vivo alteration of telomere sequences and senescence caused by mutated Tetrahymena telomerase RNAs. *Nature* (1990) **344**:126-32

Zhong Z, Shiue L, Kaplan S, de Lange T. A mammalian factor that binds telomeric TTAGGG repeats *in vitro*. *Mol. Cell. Biol*. (1992) **12**:4834–4843

Zundel W, Schindler C, Haas-Kogan D, Koong A, Kaper F, Chen E, Gottschalk AR, Ryan HE, Johnson RS, Jefferson AB, Stokoe D, Giaccia AJ. Loss of PTEN facilitates HIF-1-mediated gene expression. *Genes Dev* (2000) **14**:391-6

Appendix A

p-BABE-puro-hTERT and p-BABE-puro-DN-hTERT

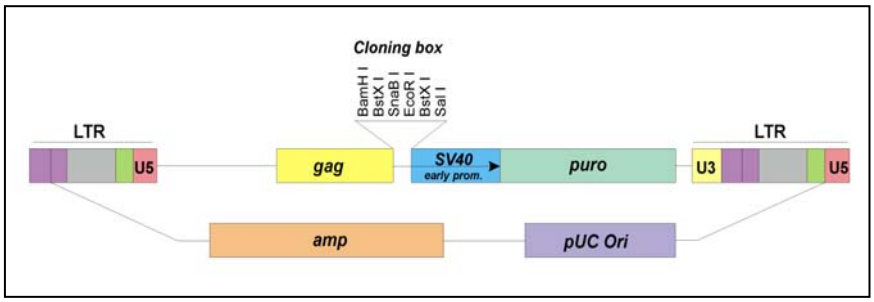

pBabe-puro is a retroviral vector. The pBabe vectors are based on the Moloney Murine Leukemia Virus (MoMuLV). The vector provides the viral package signal, transcription and processing elements, and a target gene. The viral *env* gene, produced by the package cell line, encodes the envelop protein, which determines the viral infectivity range. The vector contains the bacterial origin of replication, ampicillin-resistance gene, and puromicin resistance gene for the growth of infected mammalian cells to select stable cell lines.

pRETROSUPER

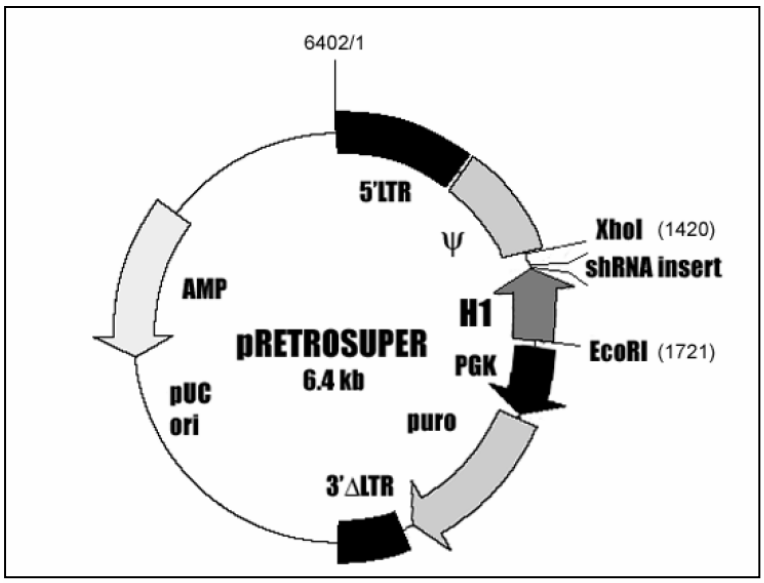

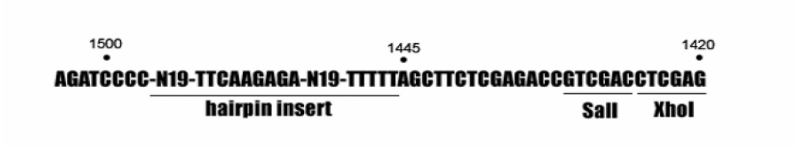

The pRETROSUPER vector is derived from the Murine Embryonic Stem Cell virus (pMSCV). It contains the pSUPER shRNA expression cassette.The hairpin oligonucleotides for the RNAi are cloned downstream of the polymerase III Histone H1-RNA promoter (H1). The pRETROSUPER has a specifically designed 3'LTR that has a deletion in the LTR promoter elements. This deletion results in inactivation of the LTR mediated transcription upon retroviral integration. The phosphoglyceratekinase promoter (PGK) drives the expression of the puromycin resistance gene (puro) for selection in eukaryotic cells. The pRETROSUPER plasmid can be propagated in E.Coli under ampicillin (AMP) selection.

pCCLsin.PPT.hPGK.GFPpre

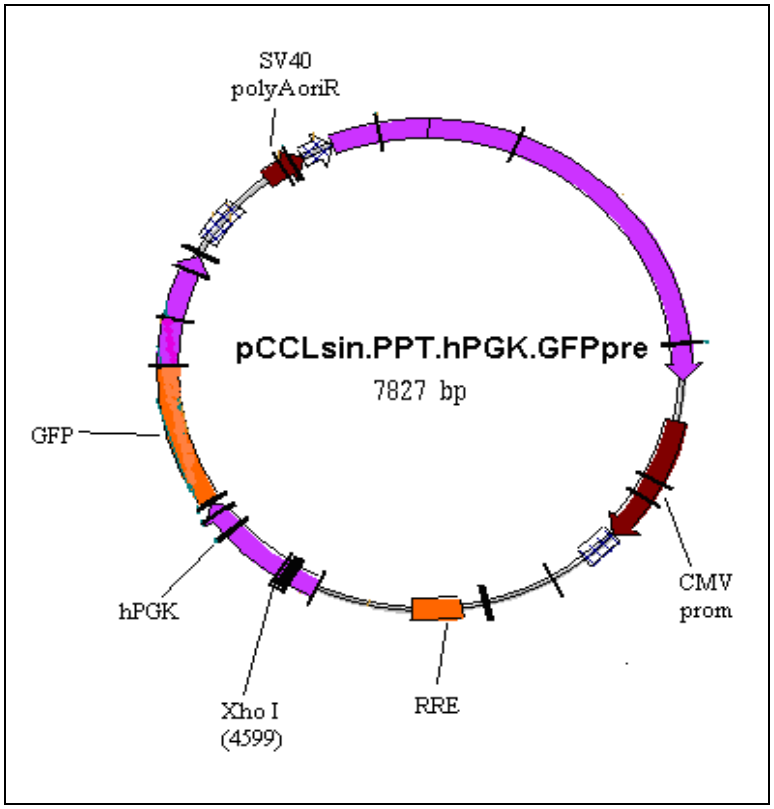

pCCLsin.PPT.hPGK.GFPpre lentivirus vector contains the enhanced Green Fluorescent Protein (eGFP) (750-bp *Bam*HI-*Not*I fragment from pEGFP-1) coding region, under the control of the human PGK promoter.

pEGFP-C1

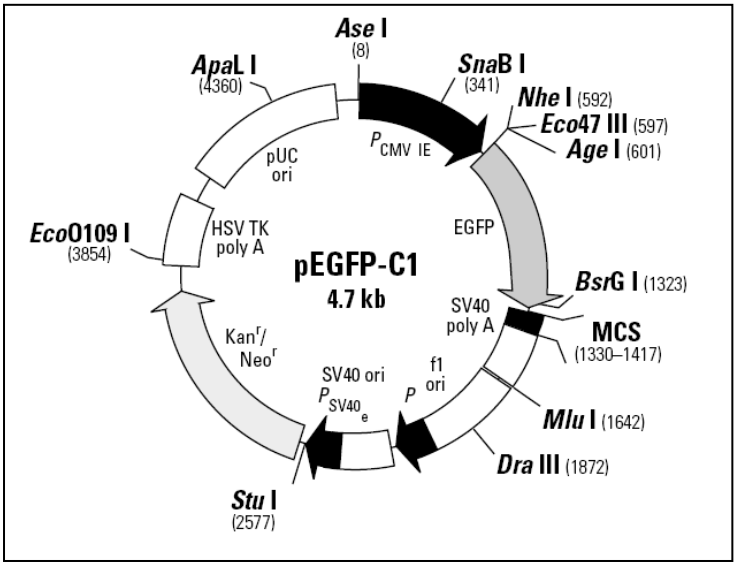

pEGFP-C1 encodes a red-shifted variant of wild type GFP which has been optimized for brighter fluorescence and higher expression in mammalian cells. pEFGP-C1 encodes the GFPmut1 variant which contains the double aminoacid substitution of Phe-64 to Leu and Ser-65 to Thr. Genes cloned in to the MCS will be expressed as fusions to the C- terminus of EGFP. The vector backbone also contains an SV40 origin for replication in mammalian cells expressing the SV40 T antigen. A neomycin resistance cassette allows stably transfected eukaryotic cells to be selected using G418.

pRetroQ-DsRed Monomer-C1

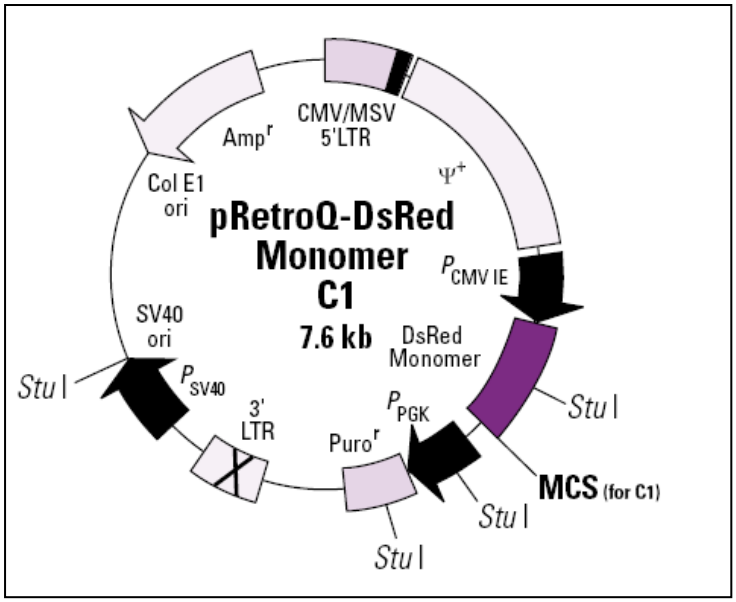

pRetroQ-DsRed Monomer-C1 is a high titer, self inactivating retroviral vector that facilitates delivery and expression of DsRed monomer as well as C-terminal fusions of DsRed monomer to target cells. DsRed.M1 is a monomeric mutant derived from the tetrameric *Dicosoma* sp Red fluorescent protein DsRed.